Finite Element Study Of The Post-Buckling Behaviour Of Plate Girder Panels Under Shear Load

Wafik M. A. Ajam

A Thesis

In

Center for Building

Studies

Presented in Partial Fulfillment of the Requirements
for the Degree of Doctor of Philosophy at
Concordia University
Montréal, Québec, Canada

September 1986

ABSTRACT

Finite Element Study Of The Post-Buckling Behaviour Of Plate Girder Panels Under Shear Load

Wafik M. A. Ajam, Ph.D.
Concordia University, 1986

This study used the finite element method to analyse a single panel with stiffeners along all four edges subjected to imposed shear displacements.

The analysis clarifies the stress distribution from initial buckling until the failure load, and shows that although the theories used in the design of plate girders under shear loading may give satisfactory values, the model used is very far from the real behaviour. For plate girders used in structural engineering the capacity is reached when first yield in shear in the tension corners occurs, without any of the diagonal tension assumed in most of the theories.

The ultimate load capacity of shear webs in a plate girder is modelled as the sum of the shear strength of the web and the bending strength of the flanges. After initial buckling the web provides an increasing shear resistance, without any contribution from flange bending until the first shear yielding occurs in the tension corners. After this yielding occurs, the flanges bend and the capacity of the web may be further increased as a result of the normal force at the boundary created by the bending rigidity in the

flange.

In this study a new simple equation is developed to predict the ultimate shear force for rectangular panels.

ACKNOWLEDGMENTS

The author wishes to express his sincere gratitude to his supervisor, Prof. Cedric Marsh, for his help, valuable guidance and useful suggestions.

The author wishes to thank his co-supervisor, Dr. Kinh Ha for his suggestions, guidance and his continuous encouragement throughout the course of this work.

Last, but not least, the author would like to thank his wife, Sahar and his children Sara, Hajar and Israa for their encouragement and long waiting.

TABLE OF CONTENTS

LIST OF FIGURES

LIST OF TABLES

NOTATION

a	half width of square plate
b	clear width of web panel between stiffeners
b_f	breadth of flange
c	position of plastic hinge from tension corner
c_1	extent of diagonal tension zone
d	clear depth of web plate between flanges
E	elastic modulus
$T+\Delta T_F$	vector of nodal point forces equivalent to the internal element stresses, evaluated at time $T+\Delta T$
F.E.M.	Finite element method
G	elastic shear modulus
i	aspect ratio b/d
(i)	iteration number
$T\ (i-1)$ K	rigidity matrix, coefficient includes linear and non-linear effects for iteration (i-1)
M_p	plastic moment of the flange plate
M'	plastic moment reduced due to axial force
Mx	bending moment about X axis
My	bending moment about Y axis
Mxy	torsion moment about X and Y axis
$\bar{M}$	$\hat{M}x^2 + \hat{M}y^2 - Mx\ My + 3\ \hat{M}xy^2$
Nx	membrane force per unit length along X axis
Ny	membrane force per unit length along Y axis
Nxy	shear force per unit length along X and Y axis

NOTATION

$\bar{N}$	$N_x^2 + N_y^2 - N_x N_y + 3 N_{xy}^2$
$\overline{MN}$	$M_x N_x + M_y N_y - 0.5(M_x N_x + M_y N_y) + 3 M_{xy} N_{xy}$
P.D.P.	Proposed design procedure
P	yield force in the flange
P'	axial force in the flange
q	uniformly lateral load per unit area
Q	$q\ b^4 / E\ t^4$
S	concentrated force
s	$\overline{MN} / \lvert\overline{MN}\rvert$
t	thickness of web panel
t_f	thickness of flange plate
T	time
$T+\Delta T_R$	vector of externally applied nodal points forces, at time $T+\Delta T$
$U^{(i)}$	increment to the current displacement vector for iteration (i)
V_{ex}	shear force in experimental tests
V_f	shear force resisted by the contribution of bending rigidity, suported by flange and web
V_u	ultimate shear capacity
V_w	shear force up to first yield suported by web
V_y	$d\ (\tau y)\ t$
X,Y	axes
x_s	distance along boundary
w	central deflection
β	$(8\ t_f^2\ b_f\ \sigma_{yf})/(b^2\ t\ \sigma_y)$

NOTATION

ν	Poisson's ratio
σ_y	yield stress of web material
σ_{yf}	yield stress of flange material
τ_{cr}	critical shear stress of web material
τ_y	shear yield stress of web material
δ	imposed displacement of the flange
δ_{cr}	displacement at critical stress
δ_y	calculated nominal displacement at first yield
Δ	δ / δ_y
ΔT	time increment
ϕ	rotation angle at the plastic moment
θ	inclination of diagonal tension field
θ_d	angle of the panel diagonal

CHAPTER 1

INTRODUCTION

The linear elastic stability theory for thin flat plates subjected to in-plane shear loading does not provide a valid basis for determining the ultimate load-bearing capacity of slender webs, which can be much greater than the critical load.

Most of the models developed to predict the ultimate shear web capacity are based on the assumption of a tension field in the web panel, but such an assumption only has limited validity.

Rockey and Skaloud [4], in the discusion of the test results for a typical girder having flanges with a small bending strength, stated " It is also of interest to note that at an applied load of 20 tons, which is 83.5 % of the failure load, the diagonal membrane stresses are still elastic ". In the discussion of girders formed from two rectangular panels theoretically under the same loading, they observed " Although one panel has failed the other panel has remained relatively undistorted. This indicates that the final developement of the plastic diagonal zone in the web together with the final developement of the plastic hinges in the flanges is a rather quick phenomenon; this being particularly true in the case of those girders having relatively flexible flanges ". These two points suggest

that the theories of the tension field used in the design of plates girders under shear loading may be far from the real behaviour of plate girders, specially for girders of civil engineering proportions which normaly have thin flanges.

Most of the theories and models predicting the ultimate shear web capacity are based on the assumption that after buckling in shear the web has no ability to carry additional compressive loading. Marsh [7] presented a theoretical model in which the compressive principal stress has values exceeding the initial critical stress.

This study uses the finite element method to clarify the behaviour of the plate girder under shear loading.

1.1 LITERATURE SURVEY

The behaviour of thin flat plates subjected to in-plane shear loading which causes buckling requires large deflection theory of plate behaviour for the post-buckling regime.

A number of researchers have proposed stress models for predicting the ultimate strength of shear webs, most of which are semi-empirical.

A total diagonal tension field, was proposed by Wagner in 1929. Wagner used a complete, uniform tension field to determine the strength of a panel in pure shear. The flanges are assumed to be rigid and the web very thin. This model

has been found to be quite satisfactory for riveted aircraft structures, but is an inappropriate model for the post-buckled behaviour of stiffened shear webs in girders normally used in civil engineering.

Basler [2] in 1960 recognised that, for welded plate girders, the flanges were too flexible to be capable of withstanding forces normal to them, and he proposed a partial tension field anchored against the vertical edges of the panel only. The inclination and width of the yield band are defined by the angle θ, which is chosen so as to maximize the shear strength. Many variations based on the post-buckling tension field have been developed since Basler solution was published (see Fig. 1).

Takeuchi [18] in 1964 appears to have been the first to make an allowance for the effect of flange stiffness on the yield zone in the web. He located the boundaries of the tension field at the distances c1 and c2 from diagonally opposite corners of the panel. These distances are assumed to be proportional to the respective flange stiffnesses, If1 and If2, and were chosen to maximize the shear strength. However, shear strengths determined in this way were not in good agreement with test results.

Fujii [6] in 1968 assumes a tension field encompassing the whole panel, with an interior hinge at midpanel. The web compression in the direction perpendicular to the principal tension is assumed equal to the compression in that

direction at the initiation of buckling. If the flanges can resist the web stress in the yield condition, the web yields uniformly over the panel, but if they cannot, there is a central band of yielding with a smaller tension equal to that which the flange can support in the outer triangular portions.

Komatsu [18] in 1971 gives formulas for four modes of failure. Failure in the first mode occurs where the inner band yields under the combined action of the buckling stress and the post-buckling tension field, while the smaller tension in the outer bands is the value that can be supported by the girder flange. As a beam mechanism with the interior hinge at the distance, c, determined by an empirical formula based on tests. The inclination of the yield band is determined so as to maximize the shear, the optimum inclination must be determined by trial. In the second mode, which is a limiting case of the first mode, the interior hinge develops at midpanel, and the web yields uniformly throughout the panel. In the third mode of failure the flanges are assumed to remain elastic while allowing complete yielding in the web. An optimum value of the diagonal tension inclination must also be found by trial for this case. The fourth case is a limiting case in which a Wagner field develops along with a panel mechanism of the flanges.

Chern and Ostapenko [18] in 1969 proposed a tension

field where the principal band is determined by yielding, taking into account the stress that exists at buckling. A panel mechanism is assumed to develop in the flanges.

Hoglund [25] in 1971 has developed a theory for girders without intermediate transverse stiffeners which was later extended for girders with intermediate stiffeners (see section 4.3 in CHAPTER 4).

Herzog [18] in 1974 takes the boundary of the tension field from the mid-depth of the panel at the stiffeners to the plastic hinges in the flanges, the distance c is based on an average, and a chart, developed from a study of various test results.

Rockey and Skaloud [3] in 1968 showed that for plate girders with heavy flanges the flange rigidity was significant and had an influence on the ultimate load. Failure occurs when a certain region of the web yields as a result of the combined effect of the inclined tensile membrane stress field and the web buckling stress, and when plastic hinges are formed in the flanges due to the diagonal tension in the web.

Calladine [23] in 1973 establish a more rational version of Rockey and Skaloud model.

Porter, Rockey, and Evans [5] in 1975 represented the behaviour of a plate girder, under an increasing applied shear loading, by the following three phases.

- Prebuckled behaviour:

Prior to buckling, if a uniform shear stress, τ, is applied to the web, the principal tensile or compressive stresses of magnitude $\sigma_t = \sigma_c = \tau$ occur at an inclination of 45^c to the flange. This stress system will exist until the applied shear stress τ reaches the critical value τ_{cr} at which the panel buckles. In practice, the value of the critical shear stress is based on the assumption that all the boundaries of the web panel are simply supported, and carry a uniformly distributed stress.

- Post-buckled behaviour:

It is then postulated that once the critical shear stress τ_{cr} is reached and the panel buckles, the panel cannot sustain any increase in compressive stress. Any additional load is assumed to be supported by a tensile membrane field, which anchors against the top and bottom flanges and against the adjacent members on either side of the web. The magnitude of the tensile membrane stress is indicated by σ_t and the angle of inclination of the membrane stress field is denoted by θ.

- Collapse behaviour:

Upon further increase of the applied loading, the tensile membrane stress σ_t developed in the web, increases and exerts an increasing force normal to the flanges. Failure of the girder occurs when the web yields and plastic

hinges are formed in the flanges.

Each of the models adopted, however, fails in some way to satisfy the essential requirements of the stress systems, either normal to the boundaries, where the tension stress is not balanced, or in the distribution of the stress along the boundaries.

Marsh [7] in 1982 proposed a model, the most important aspect of which is that the web is capable of providing a shear resistance well in excess of that causing initial web buckling, without the need for any bending strength in the boundary stiffeners. Only after the shear yielding occurs in the corners do the boundary stiffeners bend and begin to contribute to the shear resistance of the panel.

Up to now no rigorous analysis for the distribution of shear stress in the post-buckling condition has been developed. Classical formulation of this problem leads to a set of partial differential equations which are characterized by a coupling of the variables describing the in-plane and out-of plane behavior of the plate. These equations are difficult to solve.

Another means of obtaining a solution is by the use of the finite element method. This approach yields a numerical solution and can be formulated in terms of simple physical concepts, without recourse to complex differential equations.

This study is focused on:

1- The distribution of the stress along the boundaries after buckling in shear, and the prediction of the ultimate shear force.

2- The membrane stresses, under shear loading, in webs taking account large deflections.

3- The influence of flange strength on the ultimate shear resistance.

To carry out the analyses the computer program ADINA (Automatic Dynamic Incremental Non Linear Analysis) was used.

● plastic hinge
c_1 extent of diagonal tension zone

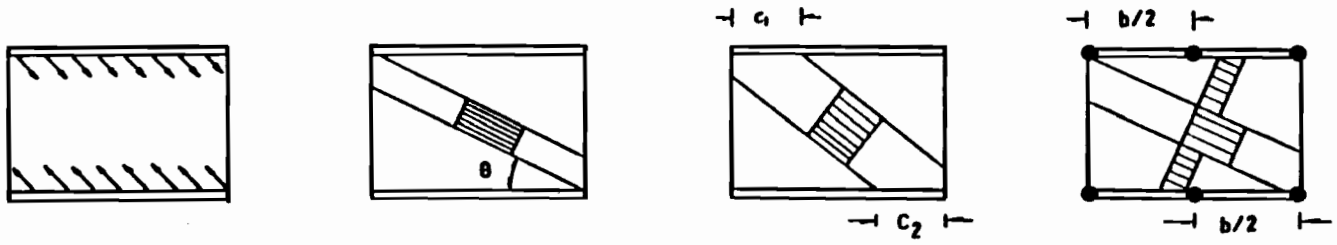

WAGNER BASLER TAKEUCHI FUJII

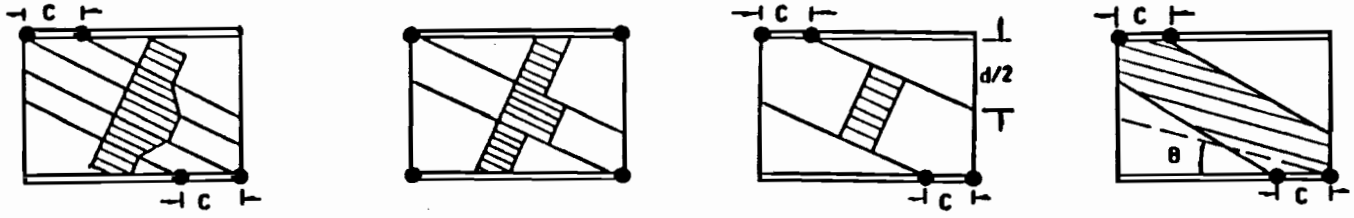

KOMATSU CHERN & OSTAPENKO HERZOG ROCKEY

Fig. 1 THE DISTRIBUTION OF THE TENSION FIELD ACCORDING TO A NUMBER OF RESEARCHERS

CHAPTER 2

NONLINEAR FINITE ELEMENT PROCEDURE

2.1- INTRODUCTION

For nonlinear analysis when displacements are large and strains are small, a step-by-step solution is used to solve the problem [20]. In the analysis for imposed displacements, a transformation from displacement increments to load increments is used [17] to get the solution of the equilibrium equations. Assuming that the externally applied loads are described as a function of time, the basic approach in a step-by-step solution is to assume that the solution for discrete time T is known, and that the solution for discrete $T+\Delta T$ is required, where ΔT is a suitable time increment. The equilibrium condition for a system of finite elements representing the body under consideration can be expressed as:

$$ {}^{T+\Delta T}R - {}^{T+\Delta T}F = 0 \qquad \text{eq. 2.1} $$

where ${}^{T+\Delta T}R$ is a vector of externally applied nodal point forces and ${}^{T+\Delta T}F$ is a vector of nodal point forces equivalent (in the virtual work sense) to the internal element stresses, both being evaluated at time $T+\Delta T$.

The incremental solution of eq. 2.1 results in the following iterative scheme:

$$ {}^{T}K^{(i-1)}\,\Delta U^{(i)} = {}^{T+\Delta T}R - {}^{T+\Delta T}F^{(i-1)} \qquad \text{eq. 2.2} $$

where $^{T}K^{(i-1)}$ is a coefficient matrix include linear and non-linear effects for iteration (i-1) and $U^{(i)}$ is an increment to the current displacement vector for iteration (i):

$$U^{T+\Delta T\,(i)} = U^{T+\Delta T\,(i-1)} + U^{(i)} \qquad \text{eq. 2.3}$$

The essential work in geometric nonlinearity is that the equilibrium equation must be written with respect to the deformed geometry. This is an important difference from linear analysis in which it is assumed that the displacements are infinitesimally small and the equilibrium equations can refer to the initial configuration.

A large-displacement problem can be analysed in Lagrangian coordinates or in Eulerian coordinates [20], [21]. In the Lagrangian approach, called Total Lagrangian (T. L.), the original reference frame remains stationary, and everything is referred to it, i.e. displacements, differentiations and integrations are all with respect to the original frame. As displacements become larger and larger, more and more terms must be added to the strain displacement relations in order to account for nonlinearities.

The use of Eulerian coordinates is called Updated Lagrangian (U. L.). Differentiations and integrations are done with respect to local coordinates. The current deformed state is used as the reference state prior to the next

incremental step of the solution, then the local coordinates are updated to produce a new reference state. In the ADINA program U. L. is used for the triangular plate and shell elements and T. L. is used for the isoparametric elements.

Small prescribed displacement increments make the solution expensive, while displacement increments that are too large, result in convergence difficulties during the equilibrium iterations. The most effective solution is obtained when variable displacement step sizes are used. The best size of displacement increments will be relative to the experience of the program user. It is of significant advantage to employ large displacement steps initially and smaller displacement steps as the critical displacement is approached. The displacement level can then be increased to solve for the post-collapse range.

In the ADINA program the number of equilibrium iteration is limited to 15, if the iteration limit is reached with no convergence the analysis will stop. The convergence of the iteration is reached when the value of the energy convergence tolerance (relative displacement tolerance times the relative force tolerance) is less 10^{-2}.

2.2- CHOICE OF ELEMENT TYPE AND MESH SIZE

The ADINA program was used to solve some large deflection plate problems for lateral and in plane loading. The objective was to establish confidence in the use of the

program and to select the optimum element type and mesh size for the shear web problem.

2.2.1- Lateral Loading

The solution of Von Karman equations in terms of trigonometric series for a simply supported rectangular plate under lateral loading was solved by Samuel Levy for the case of no in plane displacement at the boundaries [12].

Two different elements were used in the analysis to make comparisons with the Levy solutions, with load increments. The first analysis of a quarter plate has 32 triangular elements, U.L. formulation is used, each node has 5 degrees of freedom; 12 incremental steps were performed. The second, with a single isoparametric element, has 16 nodes, T.L. formulation is used, each node has 5 degrees of freedom; 22 incremental steps were performed.

The result of the Adina programm agreed well with the Levy result, (see Fig. 2 and Fig. 3).

2.2.2- In-Plane Compression Loading

For the plate compressed uniformly i.e. subjected to a uniform shortening in the Y direction, using displacement increments, with lateral expansion in the X direction prevented. Timoshenko gives a solution for the stress distribution [19], using only the first term of the Fourier series representing the deflected plate.

With the same boundary conditions, using quarter of the plate with 32 triangular elements and 5 degrees of freedom at each node, uniform equal incremental end displacements of, δ , were applied. The centre deflection ratio after each increment is shown in Fig. 4, up to 10 increments.

The final stresses at the edges of the plate are shown in Fig. 5. It is seen that for larger end displacements the distribution of compressive stresses is no longer uniform and a large part of the load is taken by the plate near the edges.

Using 4 isoparametric elements with 9 nodes per element and 5 degrees of freedom per node and uniform equal incremental end displacements, the result for the deflection and the stress are shown in Fig. 6 and Fig. 7.

Both the triangular elements and the isoparametric elements give satisfactory results.

2.3- ELEMENT CHOICE

The isoparametric element is a high-order element based on regenerating three-dimensional stress conditions. This element is quite effective, but can be costly in use. The element stiffness matrix is relatively large in size and a high integration order must be used. Another disadvantage is that each node is limited at 5 degrees of freedom.

The triangular element is simple, and is basically

obtained by superimposing plate bending and membrane stresses. The element is flat, has 3 nodes with up to 6 degrees of freedom per node. The time required to analyse the Timoshenko problem using a triangular element mesh, with 5 degrees of freedom per node, is one fifth of that required using isoparametric element mesh has the same number of nodes. Another advantage is that the output, in the form of stress resultants (moments, membrane forces), facilitates the interpretation of the results. For these reasons the triangular element is used for the analysis of the shear panels.

2.4- ACCURACY VERSUS ELEMENT NUMBER

Linear analysis, using three different triangular meshes, for a quarter plate under uniform compression in the Y direction, gave the membrane stress distribution shown in Fig. 9. Fig. 11 shows the moments for a square plate subjected to uniform lateral loading.

In both types of problem, the results from the 8 elements mesh are judged to be poor in comparison with the more accurate results obtained from the mesh of 72 elements. The results from the 32 element mesh are comparable in accuracy with the 72 element mesh. A similar analysis should be made for any new problem to select a reasonable mesh.

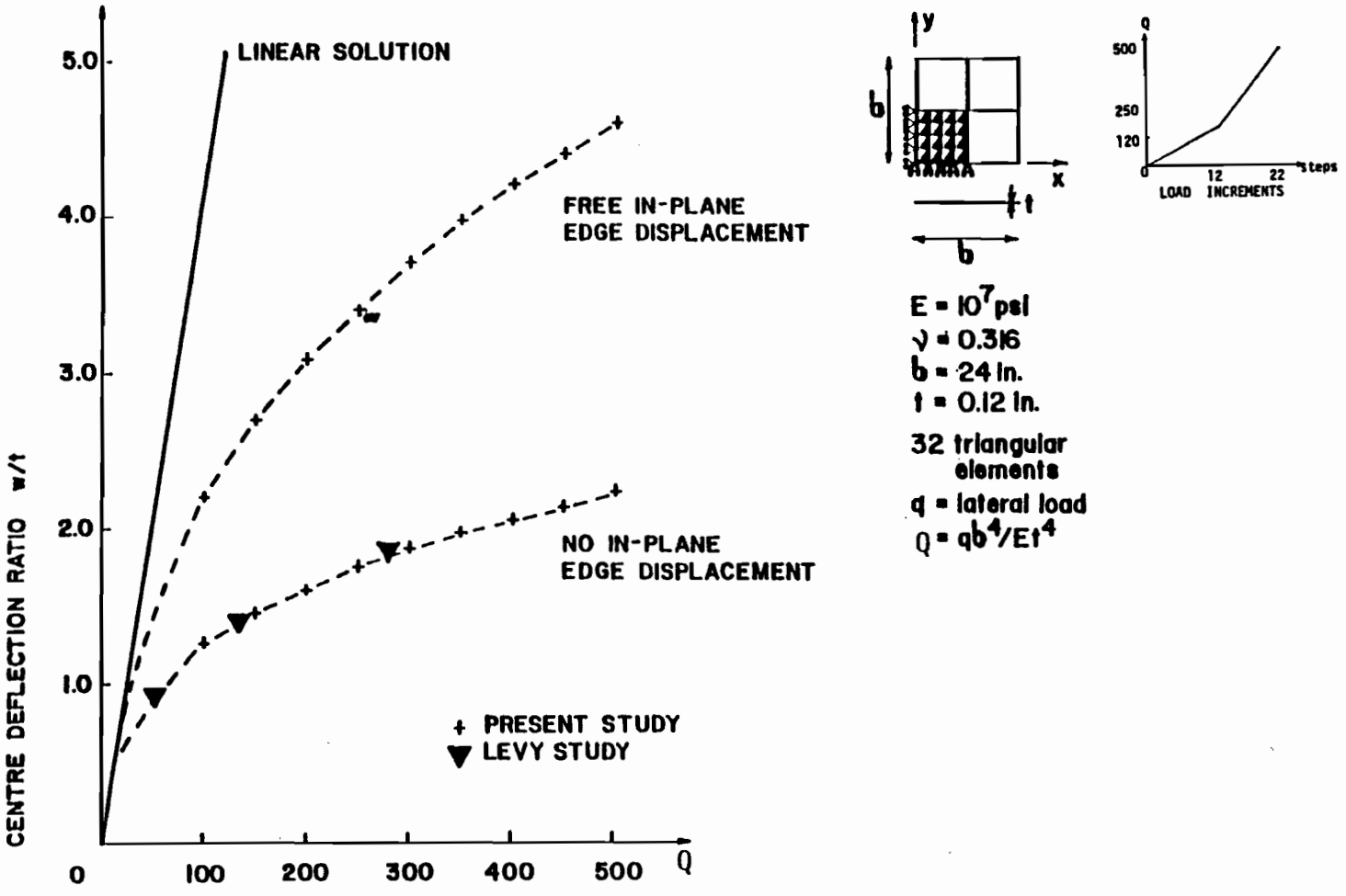

Fig. 2 CENTRAL DEFLECTION OF LATERALLY LOADED SIMPLY SUPPORTED PLATE USING TRANGULAR ELEMENTS

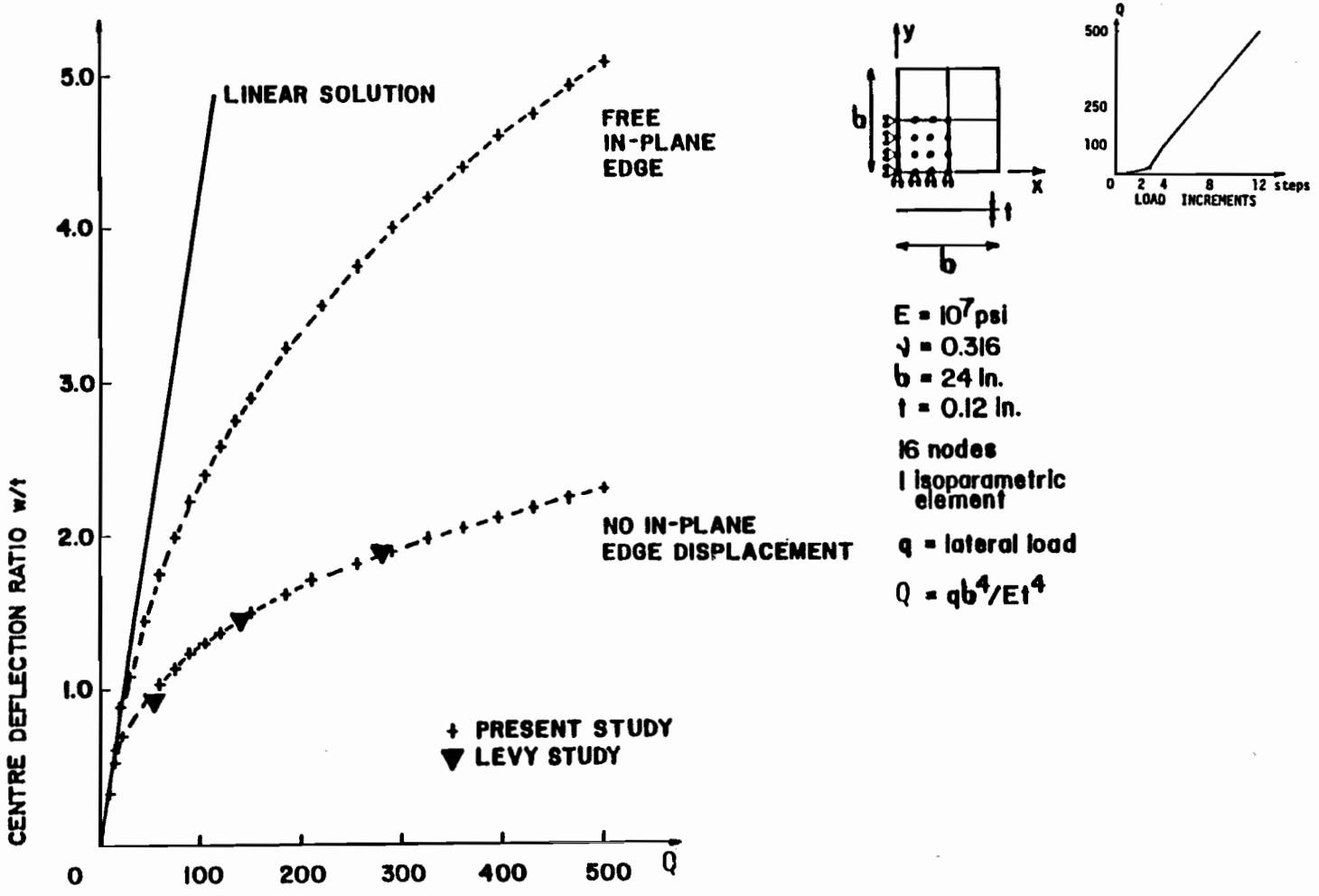

Fig. 3 CENTRAL DEFLECTION OF A LATERALLY LOADED SIMPLY SUPPORTED PLATE USING ISOPARAMETRIC ELEMENT

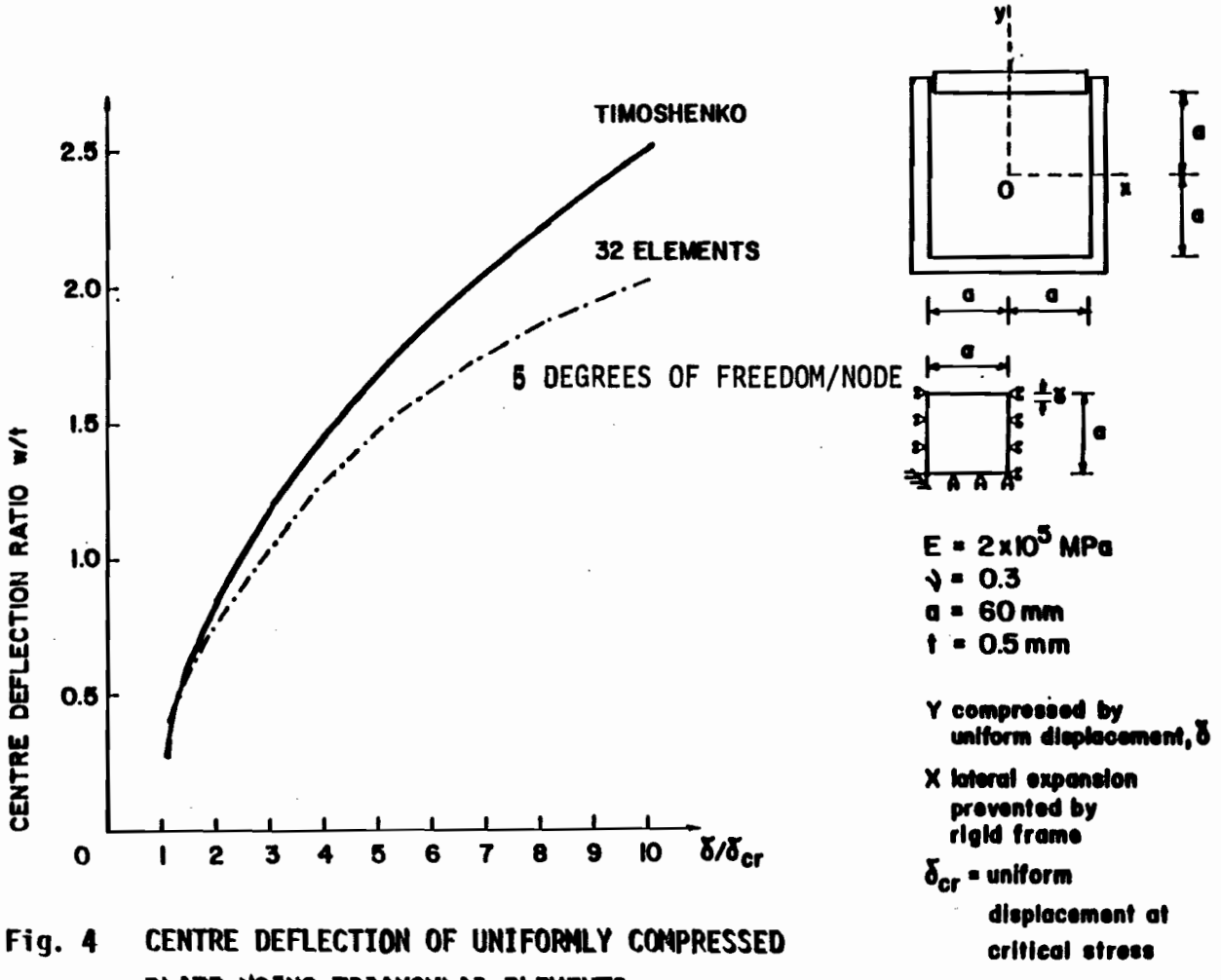

Fig. 4 CENTRE DEFLECTION OF UNIFORMLY COMPRESSED PLATE USING TRIANGULAR ELEMENTS

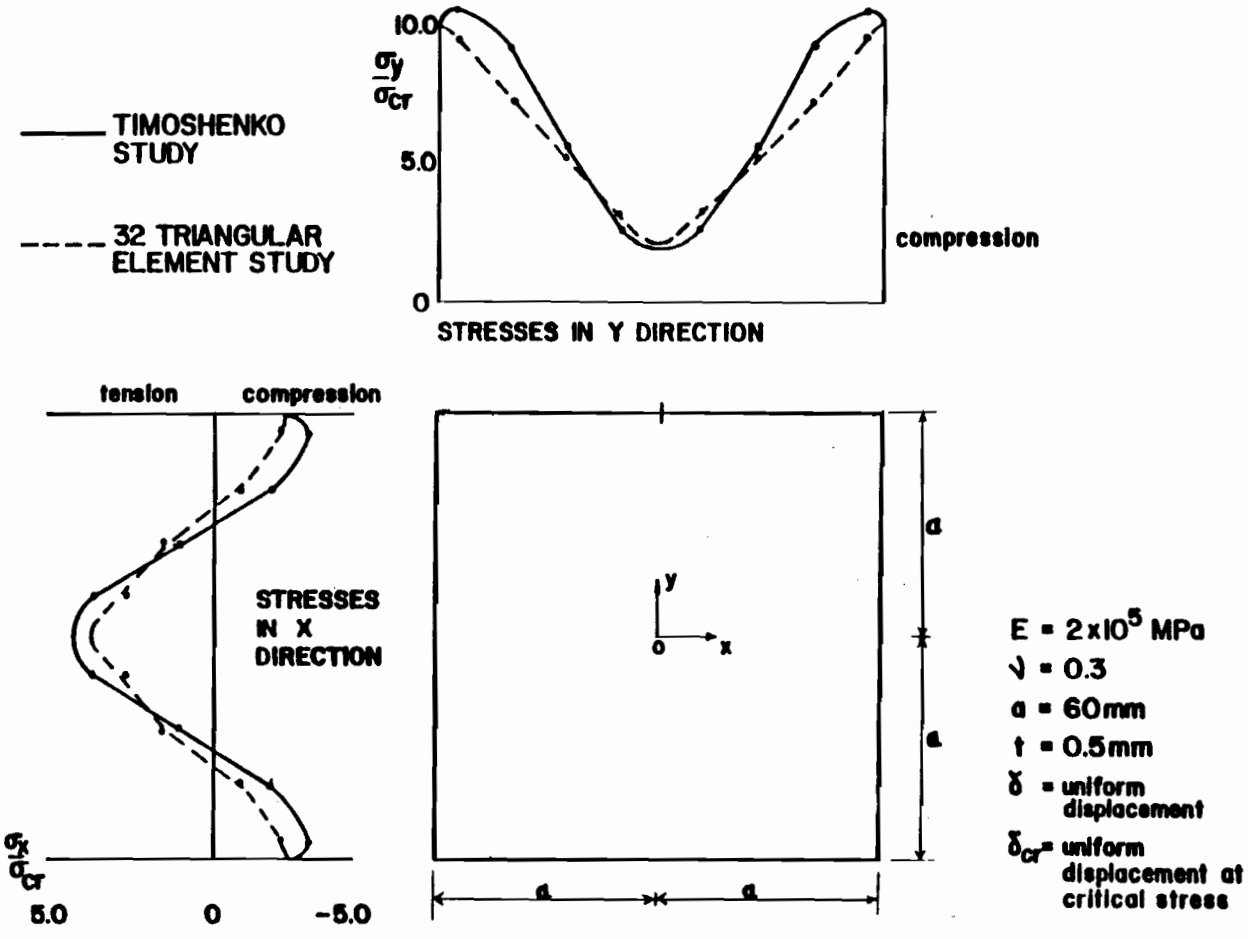

Fig. 5 BOUNDARIES STRESSES FOR A UNIFORMLY COMPRESSED SQUARE PLATE

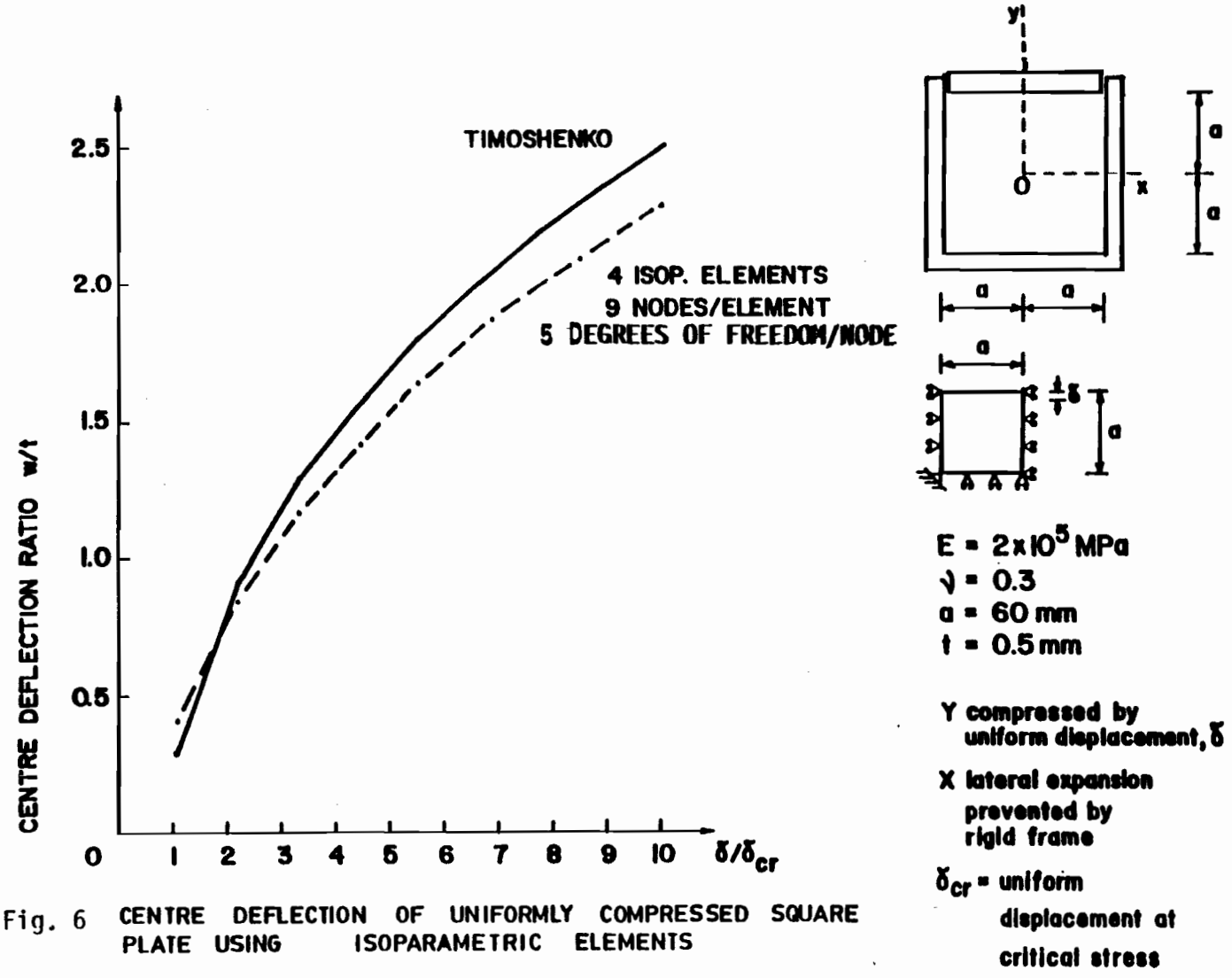

Fig. 6 CENTRE DEFLECTION OF UNIFORMLY COMPRESSED SQUARE PLATE USING ISOPARAMETRIC ELEMENTS

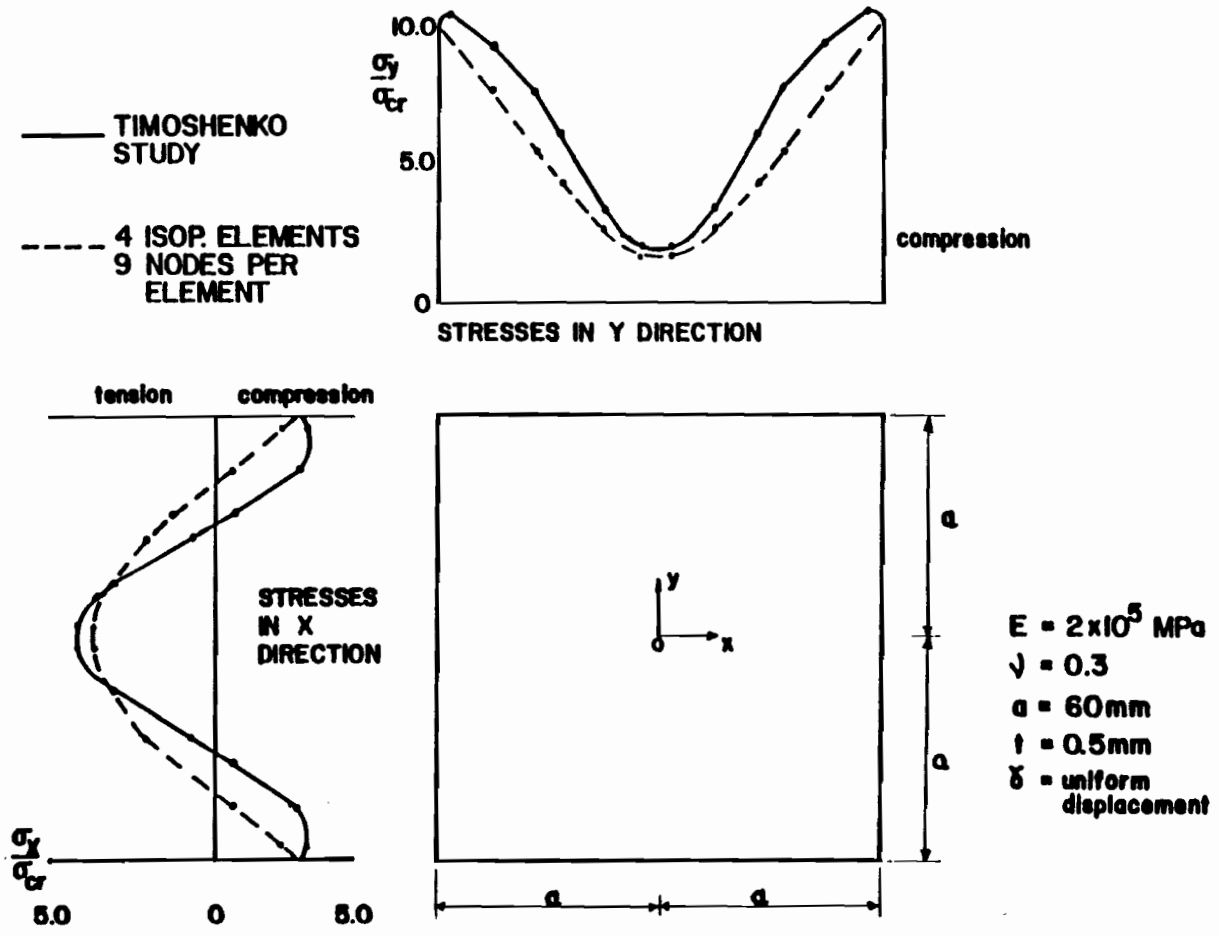

Fig. 7 BOUNDARY STRESSES IN A UNIFORMLY COMPRESSED SQUARE PLATE

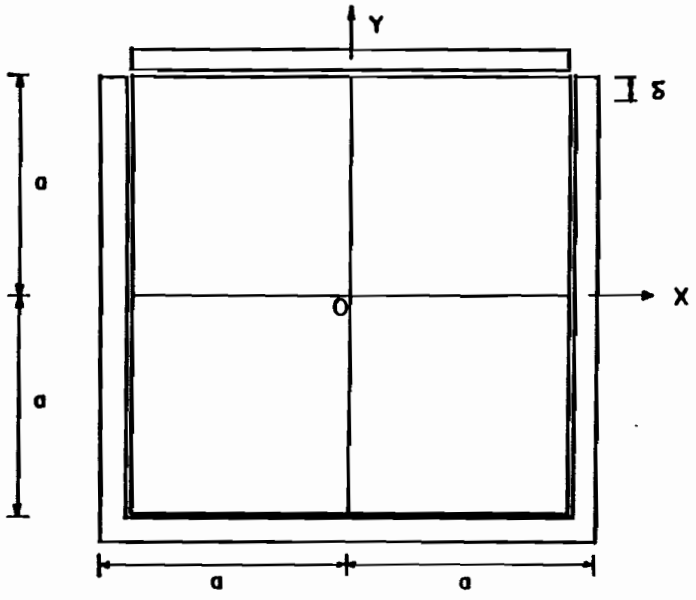

FRAME PREVENTS DISPLACEMENT IN X-DIRECTION

UNIFORM DISPLACEMENT IN Y-DIRECTION = δ

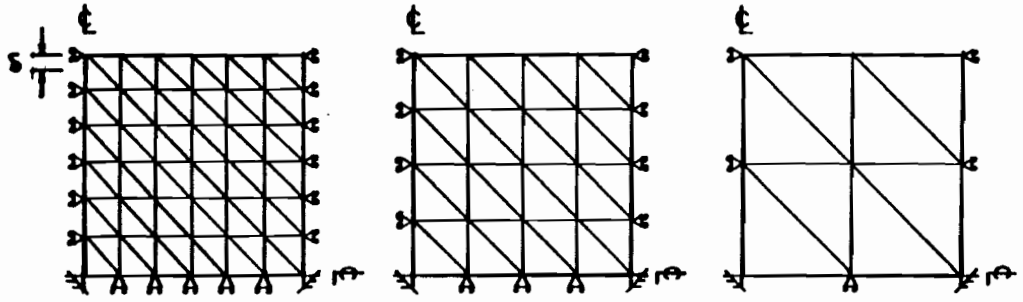

Fig. 8 DIFFERENT MESHES USED TO ANALYSE A UNIFORMLY COMPRESSED PLATE

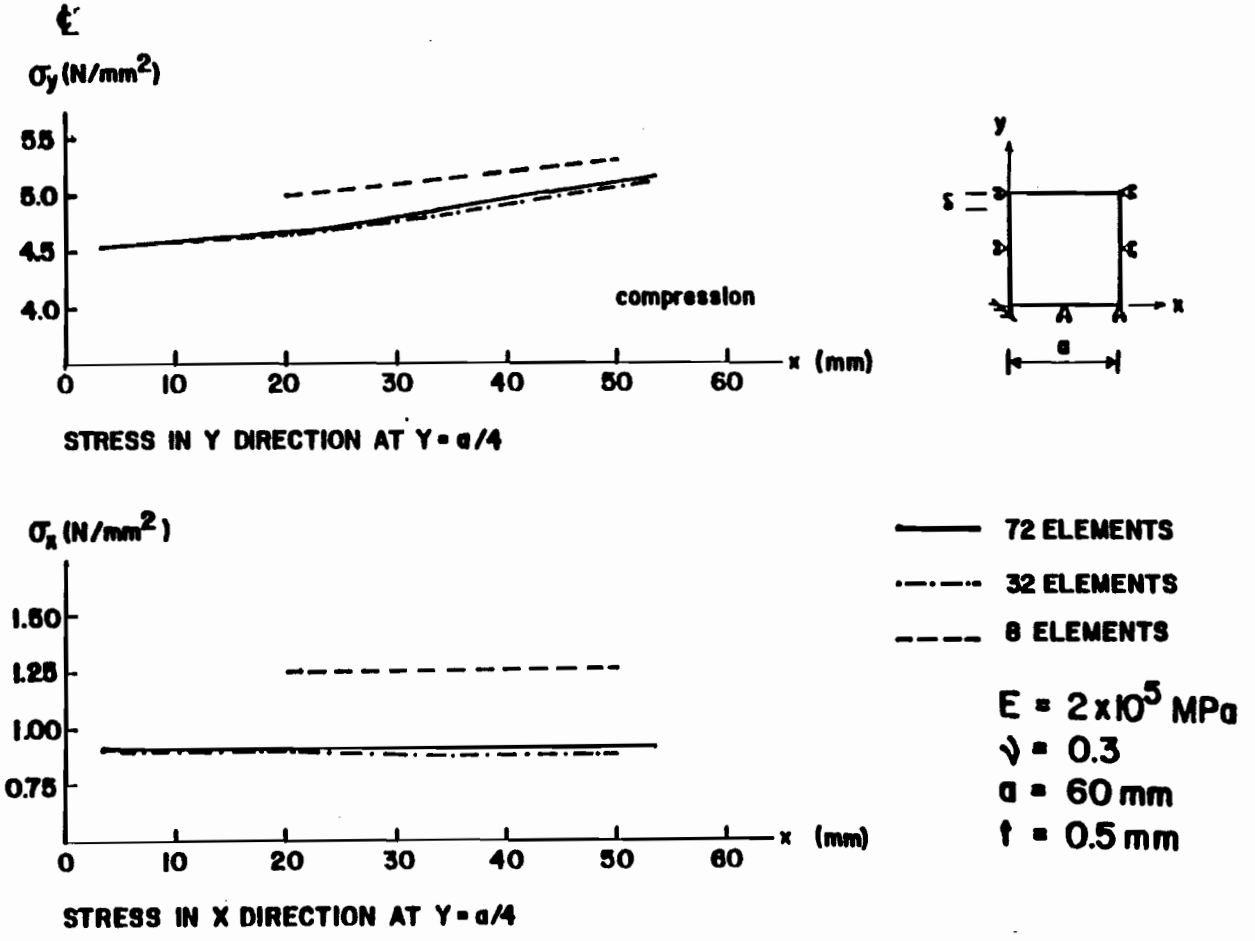

Fig. 9 COMPARISON BETWEEN STRESSES FOR DIFFERENT NUMBERS OF ELEMENTS FOR UNIFORMLY COMPRESSED SQUARE PLATE

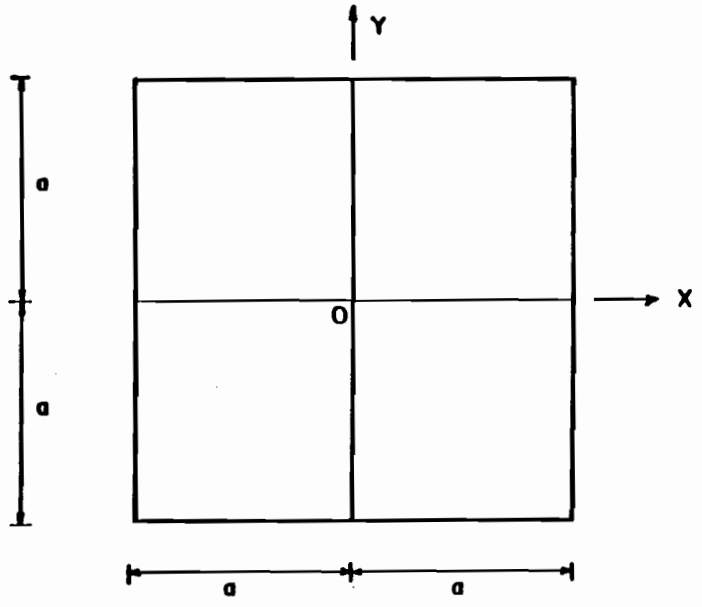

UNIFORM LATERAL LOADING

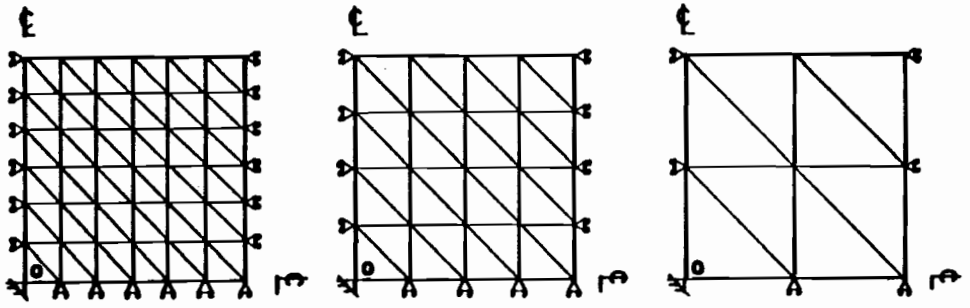

Fig. 10 DIFFERENT MESHES USED TO ANALYSE A SQUARE PLATE SUBJECTED TO LATERAL LOAD

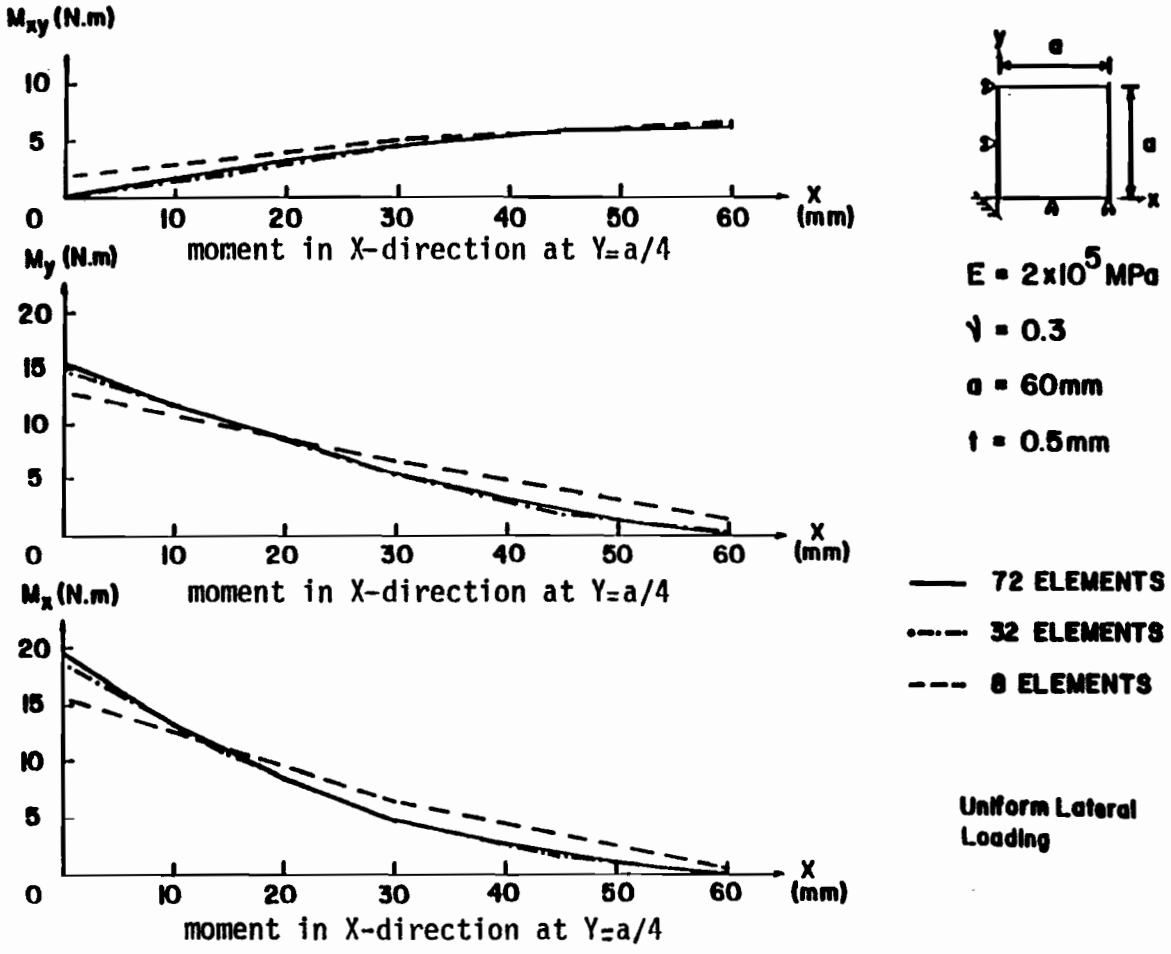

Fig. 11 COMPARISON BETWEEN MOMENTS FOR DIFFERENT NUMBERS OF ELEMENTS FOR A LATERALLY LOADED PLATE

CHAPTER 3

PANEL SUBJECTED TO SHEAR DISPLACEMENTS

3.1- SQUARE PANEL

3.1.1- Web Capacity

The initial analysis is for a single square panel with stiffeners along all four edges, the stiffeners having an area, and hence axial stiffness, but no flexural rigidity. When this panel is subjected to a shear force, it is evident that there can be no normal stress at the boundaries and only shear stress can exist there.

For the analysis, imposed displacements of the stiffeners are used rather than loading. In Fig. 12, the distance OA' is reduced, and distance OB increased, by an amount δ , to cause a shear displacement along the boundary, creating a shear stress distribution which will be determined by the analysis.

For a square panel, of depth d and thickness t, subjected to a uniform shear distribution the elastic buckling stress, τ_{cr}, [19] is given by:

$$\tau_{cr} = 9.34 \ \pi \ E \ t^2 / (\ 12(1- \nu \ ) \ d^2) \qquad \text{eq. 3.1}$$

where ν is Poisson's ratio, E elastic modulus. The total shear force at initial elastic buckling is equal to:

$$V_{cr} = \tau_{cr} \ d \ t \qquad \text{eq. 3.2}$$

After buckling, as the applied displacement increases,

the shear stress is no longer uniform but increases in value towards the tension corner. This process is continued until the web yields in shear at the corner.

The total shear force, V, is given by the integration of the shear flux at the boundary. For more displacement of the flanges the extent of the yield zone increases, but, for the case with flanges having no flexural stiffness, the actual total shear force along the boundary has been shown to decrease, due to a change in the stress distribution.

A finite element model of one quarter of the square panel, with an assumed initial deflection in the plane perpendicular to the web is analysed, using 36 elements for the quarter plate. Ilyushin's yield criterion, which assumes a sudden plastification through the plate depth [22], is used in the ADINA program. This criterion is expressed by.

$$\frac{\bar{N}}{t^2\ \sigma_y^2} + \frac{4\ s\ \overline{MN}}{\sqrt{3}\ t^3\ \sigma_y^2} + \frac{16\ \bar{M}}{t^4\ \sigma_y^2} \leqslant 1 \qquad \text{eq.3.3}$$

where $\bar{N}$, $\overline{MN}$ and $\bar{M}$ are quadratic stress intensities given by:

$$\bar{N} = N_x^2 + N_y^2 - N_x N_y + 3 N_{xy}^2$$

$$\bar{M} = M_x^2 + M_y^2 - M_x M_y + 3 M_{xy}^2$$

$$\overline{MN} = M_x N_x + M_y N_y - 0.5(M_x N_y + M_y N_x) + 3 M_{xy} N_{xy}$$

and $s = \overline{MN} / |\overline{MN}|$.

Since the program ADINA (version 1931) does not have the capability for automatique buckling analysis, an initial lateral deflection must be imposed at the central node.

Fig. 13. shows the variation of the central deflection w/t with respect to the shear displacements, the initial deflection is equal to (t/1000). Irrespective of the assumed initial central deflection, the central deflection increases only when the imposed shear displacement reaches a certain critical value τ_{cr}. This point is the bifurcation point and it agrees very well with the linear buckling theory. At the bifurcation point the plate deflection is formed by three half-waves in the compression direction and one half-wave in the tension direction. There is an advantage to start with this deformed mode as an initial deflection (with a central amplitude equal to t/10), in order to reduce the time for computation.

For non-dimensional presentation of the results, the value on the abscissa is the ratio $\Delta = \delta / \delta_y$, where δ_y is the nominal displacement when the shearing strain is τ_y / G, given by:

$$\delta_y = (d / 2\sqrt{2})(\tau_y / G) \qquad \text{eq. 3.4}$$

where G is the elastic shear modulus.

The ordinate is V / V_y, where V is the total shear force and $V_y = \tau_y$ d t. Fig. 14 shows the behaviour of a panel with d/t = 316, t = 1 mm,and a flange area $A_f = 5A_w = 5d$ t.

The variation of the shear stress along the boundary is shown in Fig. 15, the abscissa is the ratio x/b, the ordinate is τ / τ_y. Because the Ilyushin criterion includes plate bending, the value of τ / τ_y does not reach unity.

Fig. 16 shows the ratio of the central deflection to the thickness plotted along the compression diagonal, for various displacement values.

3.1.2- Influence of Flanges

If the flange has bending and torsional rigidity, it can contribute to the shear capacity of the panel, by the influence of its torsional rigidity on the buckling stress of the web, by resisting the diagonal tension and by its own shear resistance.

The analysis of the panel, for increasing displacements until plastic hinges are formed in the flanges, requires extensive execution time. As a compromise a mesh with 16 triangular elements was used with only a small loss of accuracy, as seen in Fig. 17 which shows the shear stress distribution along the boundaries when, Δ =0.6, obtained using 16 and 36 elements.

The influence of flange strength (axial, bending and torsional rigidity) on the behaviour of shear panels operating in the post-buckled range has been determined. For the purposes of this study, the specimens tested by Rockey [4] were analysed. Table 1 gives the dimensions and properties of the panels tested. The relative proportions of the flange are expressed by the ratio of flange area to web area, A_f/A_w, which is 0.5 for an optimum beam, and the ratio, β, of the plastic moment strength of the flange

($0.25 b_f t_f^2 \sigma_y$) to that required to resist a tension field encompassing the whole panel, with an interior hinge at the midpoint ($\sigma_y b^2 t/32$), this $\beta = 8 b_f t_f^2 / b^2 t$, which is usually less than 0.1 for practical welded plate girders. In studying the results of the tests by Rockey, the sizes of the flanges should be compare with the values $A_f / A_w = 0.5$ and $\beta = 0.1$, which represent girders of civil engineering proportions.

TABLE 1

Girder	Slenderness Ratio	Web Thickness mm	Flange Dimension mm	$\frac{A_f}{A_w}$	Yield Stress σ_y MPa	σ_{yf} MPa	β
TG14	d/t=316	t=0.965	76.2x3.12	0.8	220	309	0.09
TG17	d/t=316	t=0.965	76.2x9.32	2.4	220	315	0.85
TG19	d/t=316	t=0.965	76.2x15.52	4.0	220	268	2.00

3.1.3- Analysis of Test Panels [4]

- Panel TG14

In this panel the flange area is equal to 0.8 dt where d is the depth and t the thickness of the panel. A 16 elements mesh was used. The shear force increases up to first yielding when Δ is thus approximately unity and the ratio V/V_y=0.55. Because the flange has little bending rigidity, the maximum shear force is obtained at the first yielding in shear of the web, shown in Fig. 18. As the displacement increases, the force remains almost constant up to the formation of the first plastic hinge at the tension

corner; at this point Δ = 17. The contribution by the flange was obtained from the shear force across the flange.

Fig. 19 shows the shear stress distribution along the boundary for different values of Δ . Fig. 20 shows the deflection along the compressive diagonal for different values of Δ.

The analysis for this test girder shows that the flange has almost no effect on the web capacity, and that the maximum shear capacity is reached at first shear yielding in the web, when the shear force is some 4 times the theoretical value to cause initial buckling.

- Panel TG17

This panel has a heavy flange area equal to 2.4 dt, β = 0.85. First shear yielding in the web again occurs when Δ is approximately unity, at which point V/V_y=0.60. As the displacement increases beyond this point the shear force increases, due to the development of stresses normal to the boundary resisted by the strength of the flanges. The capacity of the web itself is increased by the development of the diagonal tension, as shown by the lower line in Fig. 21. The additional capacity represented by the distance from the lower line to the upper line is the shear force resisted by the action of the flanges.

The first plastic hinge is developed at the tension corner when Δ = 27. At this point V/V_y = 1.02 when the total

shear force is 70 percent more than the capacity of the web at first yield.

Fig. 22 shows the shear stress distribution along the boundary for different values of Δ. Fig. 23 shows the variation of the deflection along the compressive diagonal for different values of Δ.

- Panel TG19

This panel has a very heavy flange, that would be impractical in civil engineering construction, of area equal to 4.0 dt, β = 2.0. The model proposed by Wagner is clear in this panel. At first yielding, when Δ is approximately unity, the ratio V/V_y=0.68. As the displacement increases the web resistance increases. Fig. 24 shows how the large flange is sufficient to cause the web to yield in shear along the full length of the boundary. The web reaches a total capacity in shear when Δ = 12, beyond this point additional shear resistance is taken by the frame action. The ratio V/V_y at the development of the first plastic hinge is equal to 1.38. The gain in shear force is more than 100 percent of the value obtained at the first yield in the web.

Fig. 25 shows the variation of the shear stress along the boundary for different values of Δ.

Fig. 26 shows how the number of half wave increase from 3 to 5 when Δ= 7.6, due to the development of the diagonal tension.

3.1.4- Deflection Of The Web

After yielding in shear at the tension corner of the web the centre deflection grows more rapidly with light flanges than with heavy ones, due to the influence of the torsional stiffness of the flanges on the initial critical stress, and due to the creation of diagonal tension. Fig. 27 shows the curves obtained from the analysis of three specimens tested by Rockey.

3.1.5- Plate Behaviour

The principal stress resultants for panels TG14 and TG19 at first yield are illustrated, in Figs. 28, 29, which show the inclination of the principal stress at the boundary are shown equal to 45°, Figs. 30, 31 show that after the first yields the angle does not change at the boundaries but it change slightly in the centre of the plate.

For panel TG14, at the compression corners σc decreases but σt does not increase because the band of diagonal tension is narrow and is concentrated along the central diagonal. On the other hand, for panel TG19, σt increases because the band of diagonal tension encompasses the whole panel. This explains why the shear stress near the compression corners decreases in panel TG14 and increases in panel TG19.

It is concluded that the inclination of the tension developed in the square panel with heavy or light flanges

stays at 45^{o}. The varying angle θ used by the different theories to model the inclination of the diagonal tension is inappropriate and does not represent the real behaviour.

3.1.6- Normal Force At The Boundaries

Up to first yield there is no normal force at the boundaries. This means that the flange has no effect. After yielding in the tension corner, the flange begins to contribute. By increasing the displacement, the magnitude of the normal stresses increases up to the maximum value of ($\sigma_y/2$). From Fig. 32 for TG14, where $A_f = 0.8\ A_w$, there is almost no normal stresses near the compression corner.

For panel TG19 with $A_f = 4.0\ A_w$, Fig. 33 shows the distribution of the normal forces. After yielding, the normal forces increase between the two corners due to the bending rigidity. At failure the normal forces are uniformly distributed along the edges.

3.1.7- Comparison Between Tests And FEM Results

The finite element study was compared with the result of experimental tests (see Table 2 for properties of the panels). Table 3 shows the value from experimental tests and the finite element study. The total shear force in the panel, given by the finite element analysis, is the sum of the shear force resisted by the flange and the shear force resisted by the web. The mean value of V_u/V_{ex} is 0.936 and the standard deviation equal to 0.11.

TABLE 2- Properties of square panels analysed by F.E.M.

Ref.	Girder	t	d	A_w	t_f	b_f	A_f/A_w	b/t	β
4	TG1	2.72	609.8	1658.0	4.70	101.6	0.29	224	0.018
4	TG2	2.72	609.8	1658.0	6.55	101.6	0.40	224	0.034
4	TG14	.965	304.8	294.0	3.12	76.2	0.81	316	0.093
4	TG15	.965	304.8	294.0	5.00	76.2	1.30	316	0.224
4	TG16	.965	304.8	294.0	6.45	76.2	1.67	316	0.451
4	TG17	.965	304.8	294.0	9.32	76.2	2.41	316	0.850
4	TG18	.965	304.8	294.0	12.95	76.2	3.36	316	1.593
4	TG19	.965	304.8	294.0	15.52	76.2	4.02	316	2.004
4	TG20	2.03	304.8	619.0	3.25	76.2	0.40	150	0.046
4	TG21	2.03	304.8	619.0	4.88	76.2	0.60	150	0.097
4	TG22	2.03	304.8	619.0	6.48	76.2	0.80	150	0.207
4	TG23	2.03	304.8	619.0	9.22	76.2	1.14	150	0.419
4	TG24	2.03	304.8	619.0	12.95	76.2	1.59	150	0.724
4	TG25	2.03	304.8	619.0	15.54	76.2	1.91	150	0.914
4	G7T1	4.98	1270.0	6325.0	19.50	310.0	0.96	255	0.120
4	G7T2	4.98	1270.0	6325.0	19.50	310.0	0.96	255	0.120

N.B. All the panels are square

TABLE 3- Comparison between test results and F.E.M.

Ref.	Girder	Yield Stress σ_y MPa	σ_{yf} MPa	Finite Element Analysis V_w kN	V_f kN	V_u kN	Exp. Test kN	$\frac{Vu}{Vex}$
4	TG1	253	253	145.0	0.1	145.0	120.0	1.208
4	TG2	238	238	139.0	0.7	140.0	126.0	1.111
4	TG14	219	306	20.2	0.1	20.0	25.0	0.800
4	TG15	219	286	20.2	4.0	24.0	29.0	0.828
4	TG16	219	337	20.7	7.0	28.0	31.0	0.903
4	TG17	219	308	29.3	7.5	37.0	39.0	0.949
4	TG18	219	304	33.4	12.0	45.0	50.0	0.900
4	TG19	219	268	33.5	19.2	53.0	54.0	0.981
4	TG20	229	305	69.5	0.3	70.0	51.0*	
4	TG21	229	286	71.3	0.8	72.0	71.0	1.014
4	TG22	229	337	73.0	1.3	74.0	78.0	0.949
4	TG23	229	308	73.0	2.8	76.0	81.0	0.938
4	TG24	229	304	54.3	23.7	78.0	96.0	0.813
4	TG25	229	268	69.3	25.2	95.0	103.0	0.922
4	G7T1	253	259	539.5	6.6	546.0	623.0	0.876
4	G7T1	253	259	539.5	6.6	546.0	645.0	0.847

The mean value of V_u/V_{ex} is 0.936 and the standard deviation equal to 0.11.

* Flange collapsed because the bending stress exceeded the yield stress in the flange.

3.2- RECTANGULAR PANEL

3.2.1- Web Capacity

For a rectangular panel of width b, depth d and thickness t, subjected to a uniform shear distribution the elastic buckling stress, τ_{cr}, is given by:

$$\tau_{cr} = K \pi E t^2 / (12(1- \nu) d^2) \qquad \text{eq. 3.5}$$

were $K = 5.34 \ (1.0 + 0.75 \ (d/b)^2)$ for $b > d$

ν is Poisson's ratio.

The total shear force at initial elastic buckling is equal to:

$$V_{cr} = \tau_{cr} \ d \ t \qquad \text{eq. 3.2}$$

The analysis was first made for the complete panel using 72 elements, with stiffeners having area but no independent flexural rigidity. The imposed displacements are as shown in Fig. 34, the distance AA' is reduced and distance BB' increased, by an amount 2δ . At first yield in shear in the tension corner the nominal displacement of the flange is taken to be:

$$\delta_y = d/2 (\tau_y / G)(\cos(\text{arctg } d/b)) \qquad \text{eq. 3.6}$$

where G is the elastic shear modulus.

Fig. 35 shows the behaviour of a panel with d/t = 300, t = 0.5 mm, and a flange area of 4 dt. The abscissa is the ratio $\Delta = \delta / \delta_y$, where δ_y is the calculated displacement at the first yield in shear, and the ordinate

is V / V_y, where $V_y = \tau_y d t$. V increases with Δ until, at Δ is approximately unity, shear yielding occurs in the tension corner.

The variation of the shear stress along the boundaries is shown in Fig. 36.

Fig. 37 shows the ratio of deflection over thickness plotted along the compression diagonal.

It should be noted that the aspect ratio of the panel is b/d, which may be more or less than 1.0, and that the summation of the shear stress, to obtain the shear force, is along the depth d.

3.2.2- Influence of Flanges

The influence of flange rigidity on the behaviour of shear panels operating in the post-buckled range has been analysed and compared with the results of the tests by Basler et al. [4] and Rockey et al. [4] Table 4 gives the dimension and properties of the panels tested.

TABLE 4

Girder	Aspect Ratio	d mm	Web Thickness mm	Flange Dimension mm	$\frac{A_f}{A_w}$	Yield σ_y MPa	Stress σ_{yf} MPa	β
G6T1	b/d=1.5	1270	t=4.9	309x19.8	1.0	253	261	0.06
G6T3	b/d=0.5	1270	t=4.9	309x19.8	1.0	253	261	0.51
TG9	b/d=2.0	610	t=2.62	203x9.85	1.3	266	250	0.04

3.2.3- Analysis of Test Panels

- Panel G6T1

In this panel the aspect ratio is 1.5, and the flange area is equal to (d t) where d is the depth and t the thickness of the panel. Fig 38 shows how the shear force increases up to first yielding in shear, when Δ is approximately equal to 1.0 and the ratio V/V_y=0.62, and, because the flange has little bending rigidity, how the maximum shear force is obtained at this point. As the displacement increases, the ratio V/V_y remains almost constant up to formation of the first plastic hinge at the tension corner.

Fig. 39 shows the shear stress distribution along the boundary for different values of Δ.

Fig. 40 shows the deflection profiles along the compressive diagonal for different values of Δ.

From this analysis we can conclude that the flange has almost no effect on the web capacity, and that the maximum shear capacity is reached at first shear yielding in the web, when the shear force is some 4 time the theoretical value to cause initial buckling.

- Panel G6T3

This panel with an aspect ratio of 0.5, has a flange area equal to (dt). First shear yielding in the web occurs

when Δ is approximately equal to 1.0. As the displacement increases beyond this point the shear force decreases. The capacity of the panel is reached approximately at 1.0 see Fig. 41.

Fig. 42. shows the shear stress distribution along the boundary for different values of Δ.

Fig. 43. shows the variation of the deflection along the compressive diagonal for different values of Δ.

- Panel TG9

This panel, with an aspect ratio of 2, has a flange area equal to 1.25 (dt). At first yielding the ratio V/V_y=0.54. Fig. 44 shows how the small flange bending rigidity has little effect on the shear resistance.

Fig. 45 shows the variation of the shear stress along the boundary for different values of Δ.

Fig. 46 shows the deflection profiles along the compressive diagonal for different value of Δ.

3.2.4- Plate Behaviour

The principal in-plane stress resultants for panel TG9 are plotted in Fig. 47, which shows the magnitude and distribution of the principal stress at first yield for the whole panel. Near the compression corners the magnitude of

the stress is much lower than near the tension corners. The inclination of the principal stress along the boundaries is shown to be equal to 45° at first yield. After first yield the angle does not change at the boundary in the area where the diagonal tension is expected to developed, but it changes near the compression corners and in the middle of the plate, where the angle approaches that of the panel diagonal.

3.2.5- Normal Forces at the Boundaries.

Up to first yield there is no normal force at the boundaries i.e. only the capacity of the web itself acts. After yielding a normal force is developed at the boundaries. For the rectangular panel TG5, Fig. 48 shows that the value of the normal force developed along the shorter side is higher than that on the longer side.

3.2.6- Comparison Between Tests and FEM Results

Table 6 shows the finite element study compared with the result of tests made by Basler [4], Rockey [4], Sadao [24] and Fujii [26]. Table 5 shows the properties of the girders. The total shear force obtained by the finite element analysis is equal to the shear force resisted by the frame plus the shear force resisted by the web. From Table 6 we can see the frame resistance in shear decreases, when the flange area is equal to or less than the web area, and when the aspect ratio increases.

The mean value of V_u/V_{ex} in Table 6 is equal to 1.029, and the standard deviation equal to 0.10.

Fig. 49 represents the square and rectangular panels studied by the finite element method compared with the test.

TABLE 5- Properties of rectangular panels analysed by F.E.M.

Ref.	Girder	t mm	d mm	A_w	t_f mm	b_f mm	A_f/A_w	d/t	β	b/d
4	G6T3	4.9	1270	6223	19.8	308	0.98	259	0.504	0.5
4	G6T2	4.9	1270	6223	19.8	308	0.98	259	0.224	0.75
4	G6T1	4.9	1270	6223	19.8	308	0.98	259	0.056	1.5
4	TG5	2.62	610	1598	9.5	203	1.22	233	0.067	1.5
4	TG9	2.62	610	1598	9.9	203	1.25	233	0.041	2.0
24	F10-P1	6.65	1270	8446	32.0	395	1.49	191	0.107	1.5
24	F10-P5	6.53	1270	8293	25.4	408	1.25	194	0.066	1.2
26	G1-2	6.6	1200	7920	36.0	250	1.14	182	0.118	1.5
26	G2-2	6.6	950	6270	32.0	250	1.28	144	0.096	1.5
26	G2	8.0	440	3520	30.0	200	1.70	55	0.131	2.61
26	G6	8.0	560	4480	30.0	250	1.67	70	0.439	1.25
26	G9	8.0	720	5760	30.0	250	1.30	90	0.054	2.78

TABLE 6- Comparison between test results and F.E.M.

Ref.	Girder	Yield Strength		Finte Element			Exp.	$\frac{Vu}{Vex}$
		σ_y MPa	σ_{yf} MPa	V_w kN	V_f kN	V_u kN	kN	
4	G6T3	253	261	779.0	0.0	779.0	787.0	0.990
4	G6T2	253	261	546.5	21.4	568.0	667.0	0.852
4	G6T1	253	261	494.8	3.1	498.0	516.0	0.965
4	TG5	291	291	152.4	1.0	153.0	130.0	1.177
4	TG9	266	266	141.4	0.5	142.0	123.0	1.154
24	F10-P1	236	188	810.0	7.2	817.0	819.0	0.998
24	F10-P2	267	199	815.8	16.8	833.0	846.0	0.985
26	G1-2	486	474	1262.2	19.6	1335.0	1265.0	1.055
26	G2-2	486	485	1032.8	151.2	1184.0	1226.0	0.966
26	G2	430	411	873.0	0.0	873.0	824.0	1.059
26	G6	430	411	1098.0	0.0	1098.0	1177.0	0.933
26	G9	430	411	1408.0	0.0	1408.0	1158.0	1.216

The mean value of V_u/V_{ex} in Table 6 is equal to 1.029, and the standard deviation equal to 0.10.

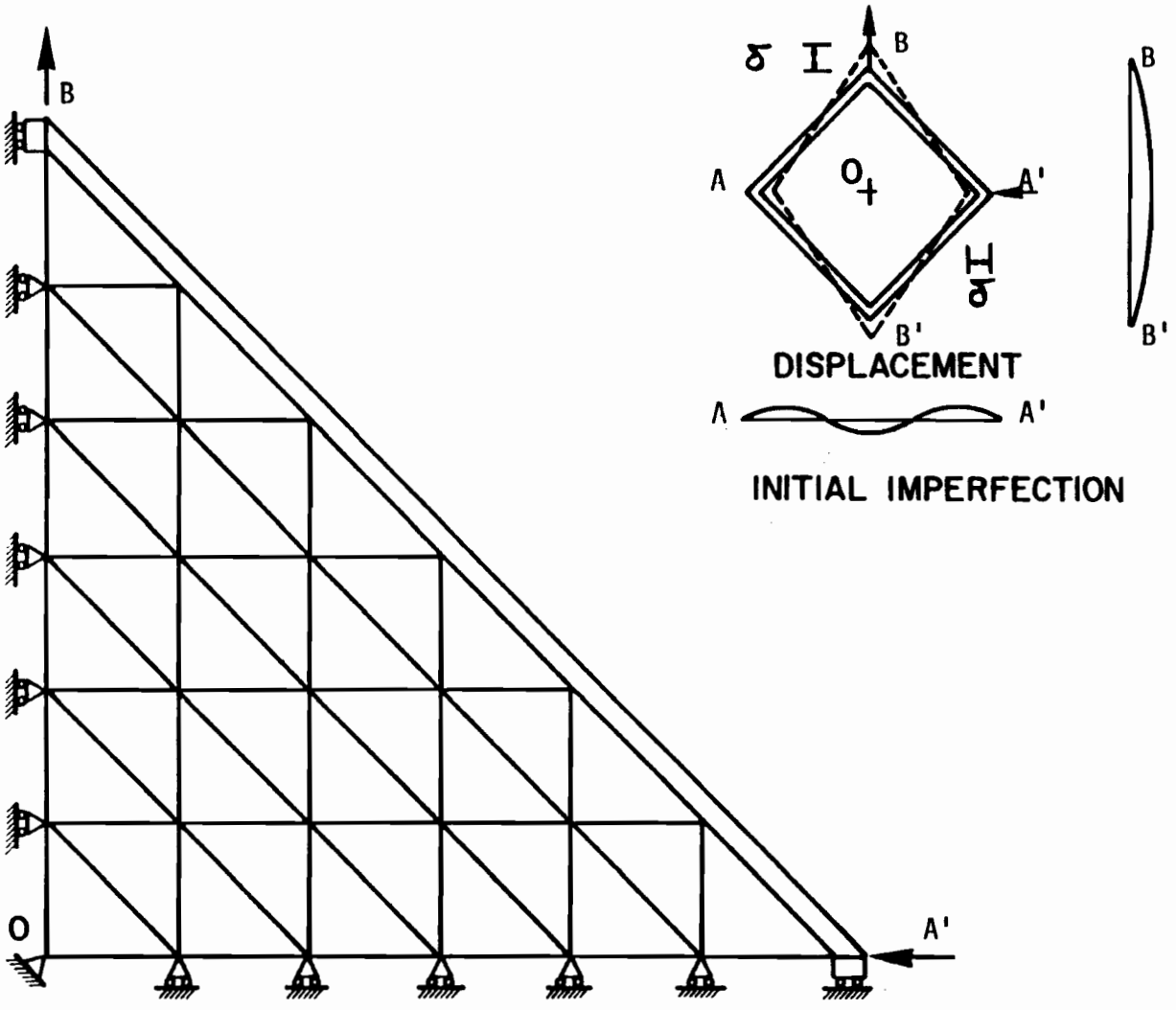

Fig. 12 QUARTER OF A SQUARE PLATE
FINITE ELEMENT GRID, 36 ELEMENTS

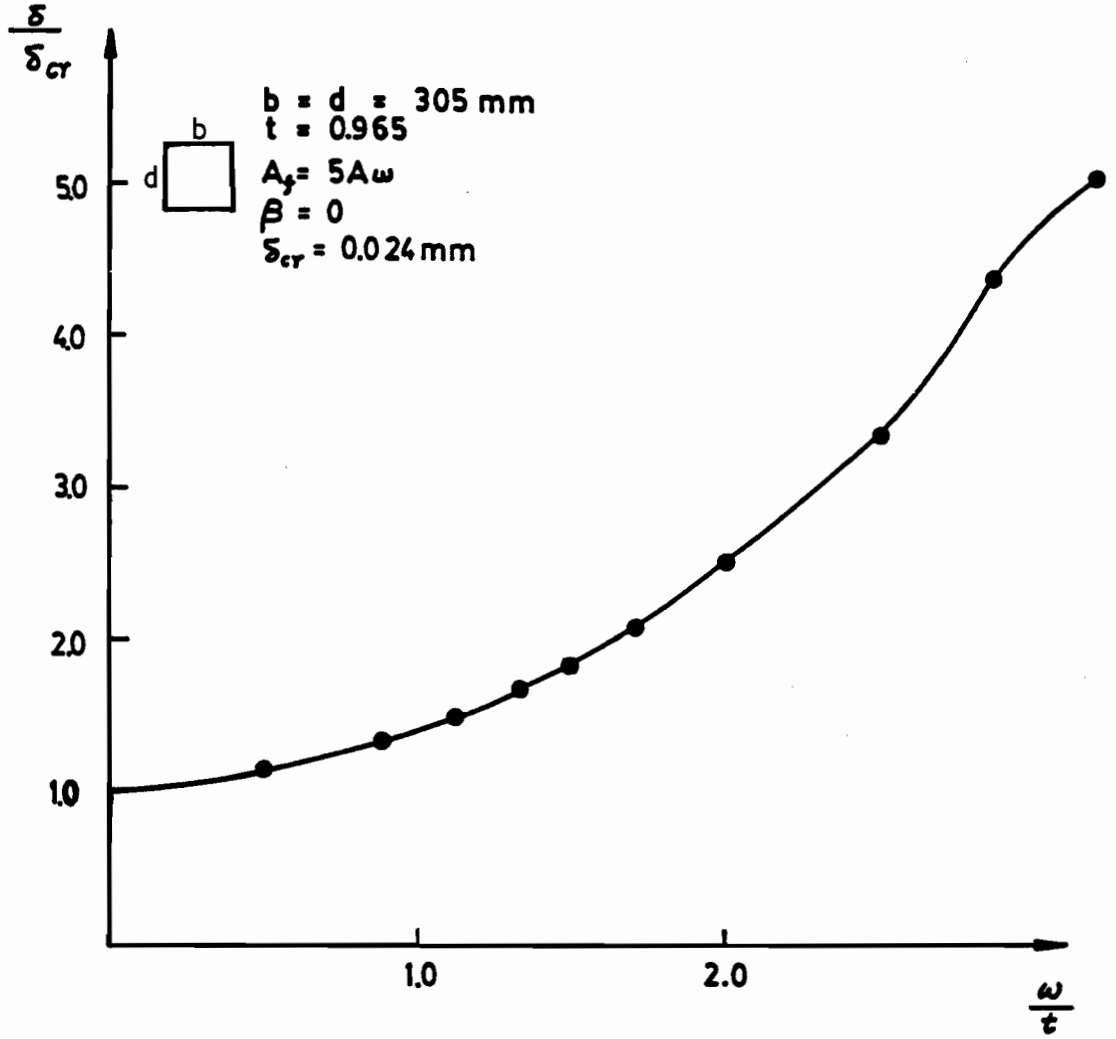

Fig. 13 RELATION BETWEEN SHEAR DISPLACEMENT AND CENTRE DEFLECTION

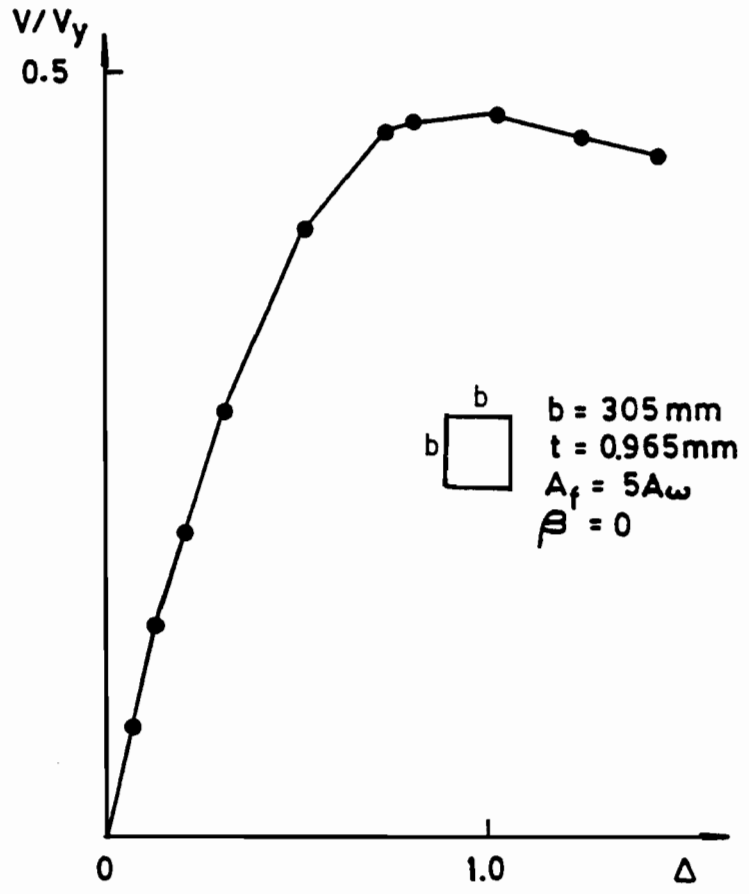

Fig. 14 SHEAR FORCE V DISPLACEMENT

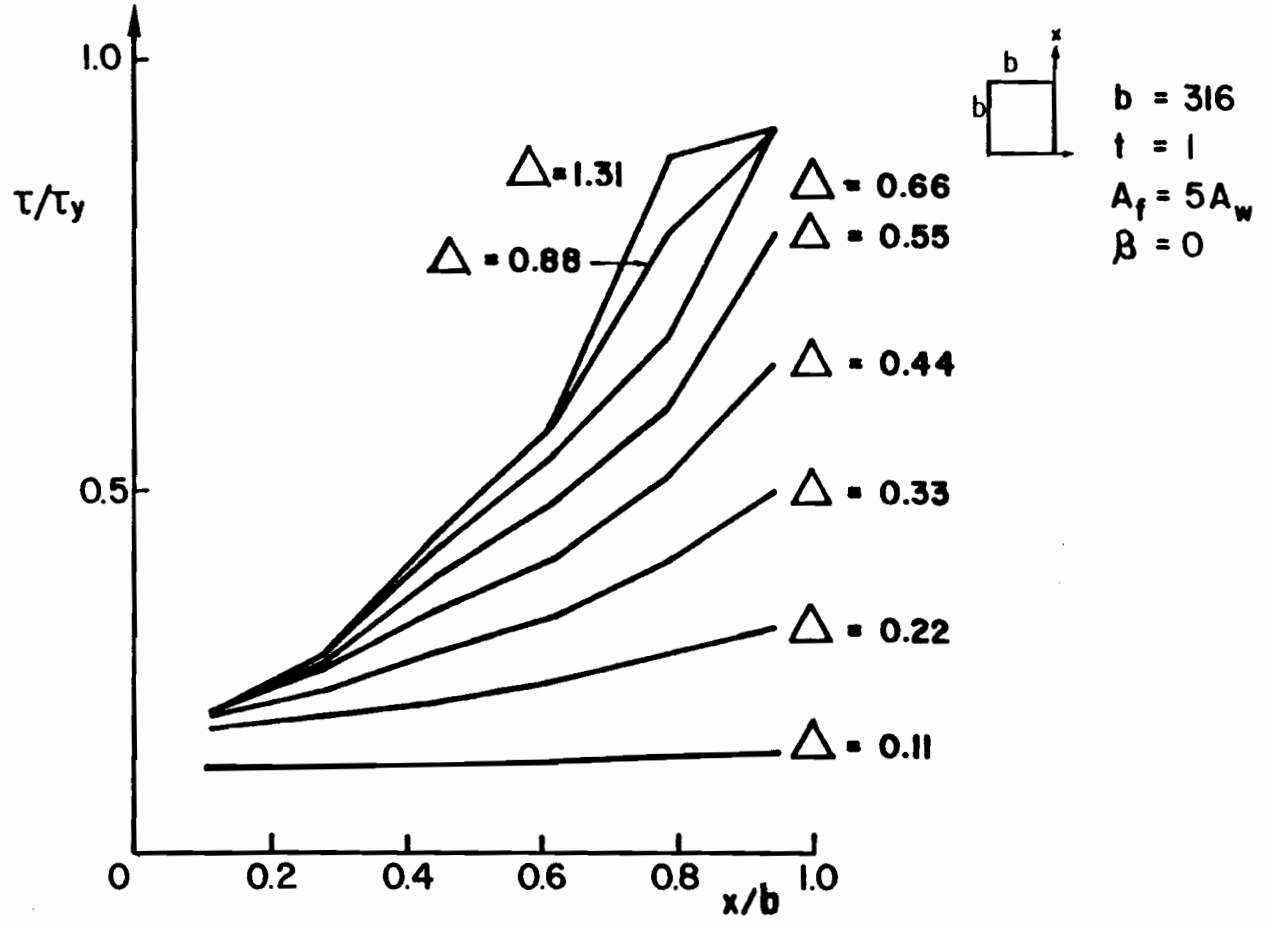

Fig. 15 SHEAR STRESS ALONG BOUNDARY FOR VARYING DISPLACEMENT

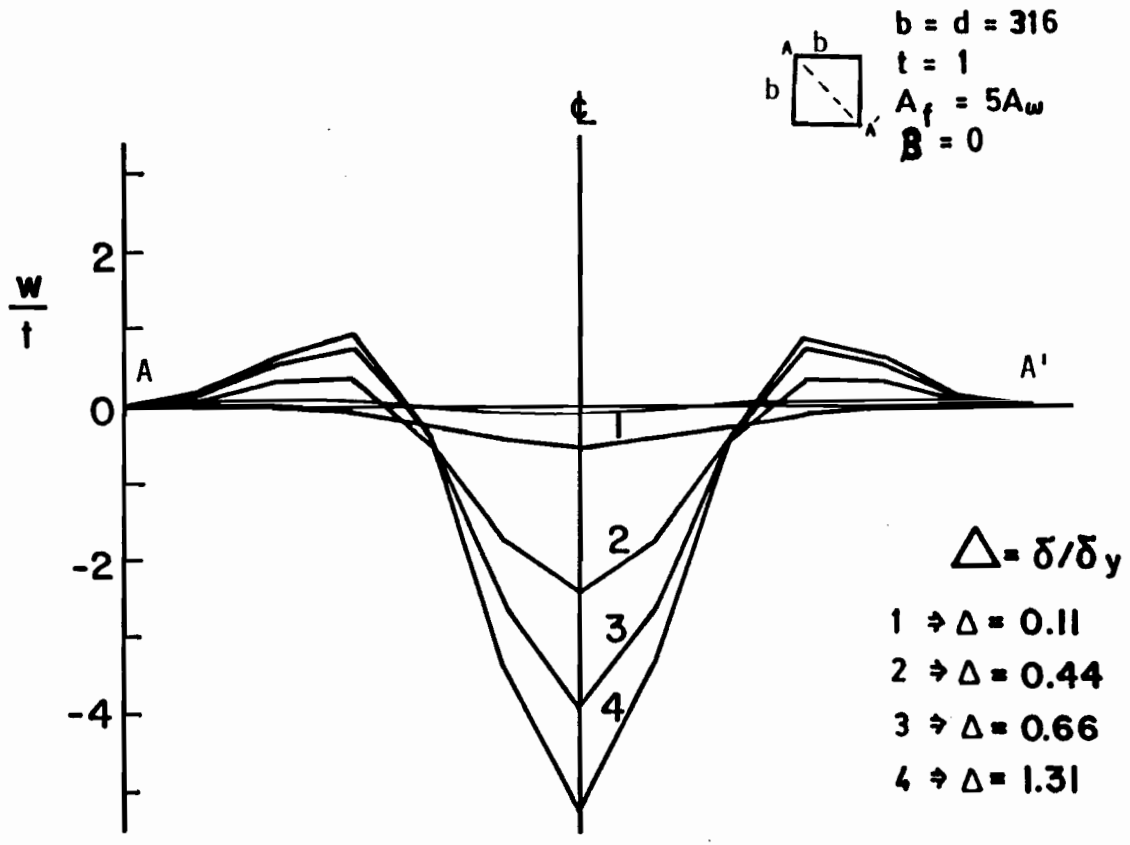

Fig. 16 DEFLECTION ALONG COMPRESSION DIAGONAL

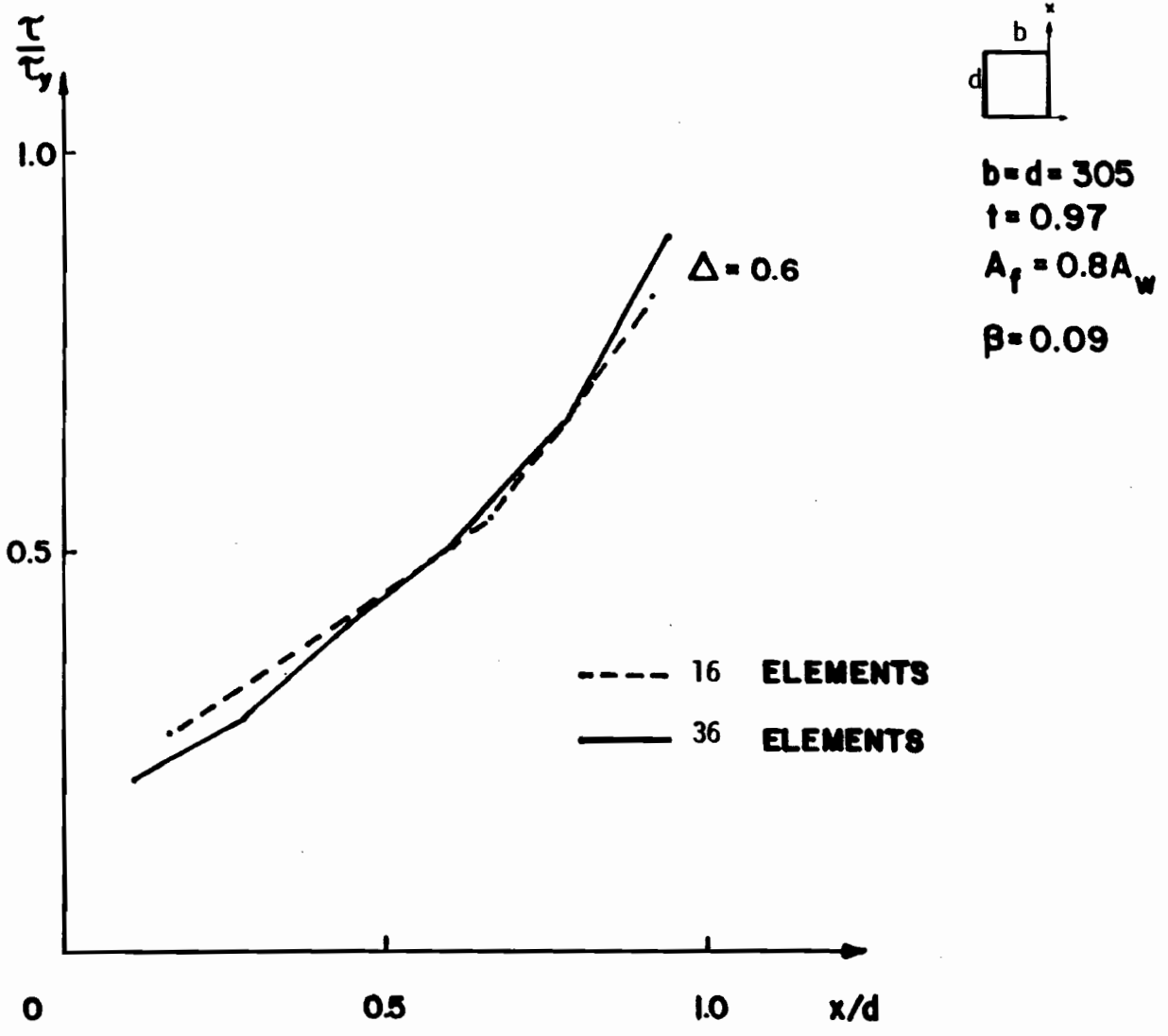

Fig. 17 **BOUNDARY SHEAR STRESS DISTRIBUTION**

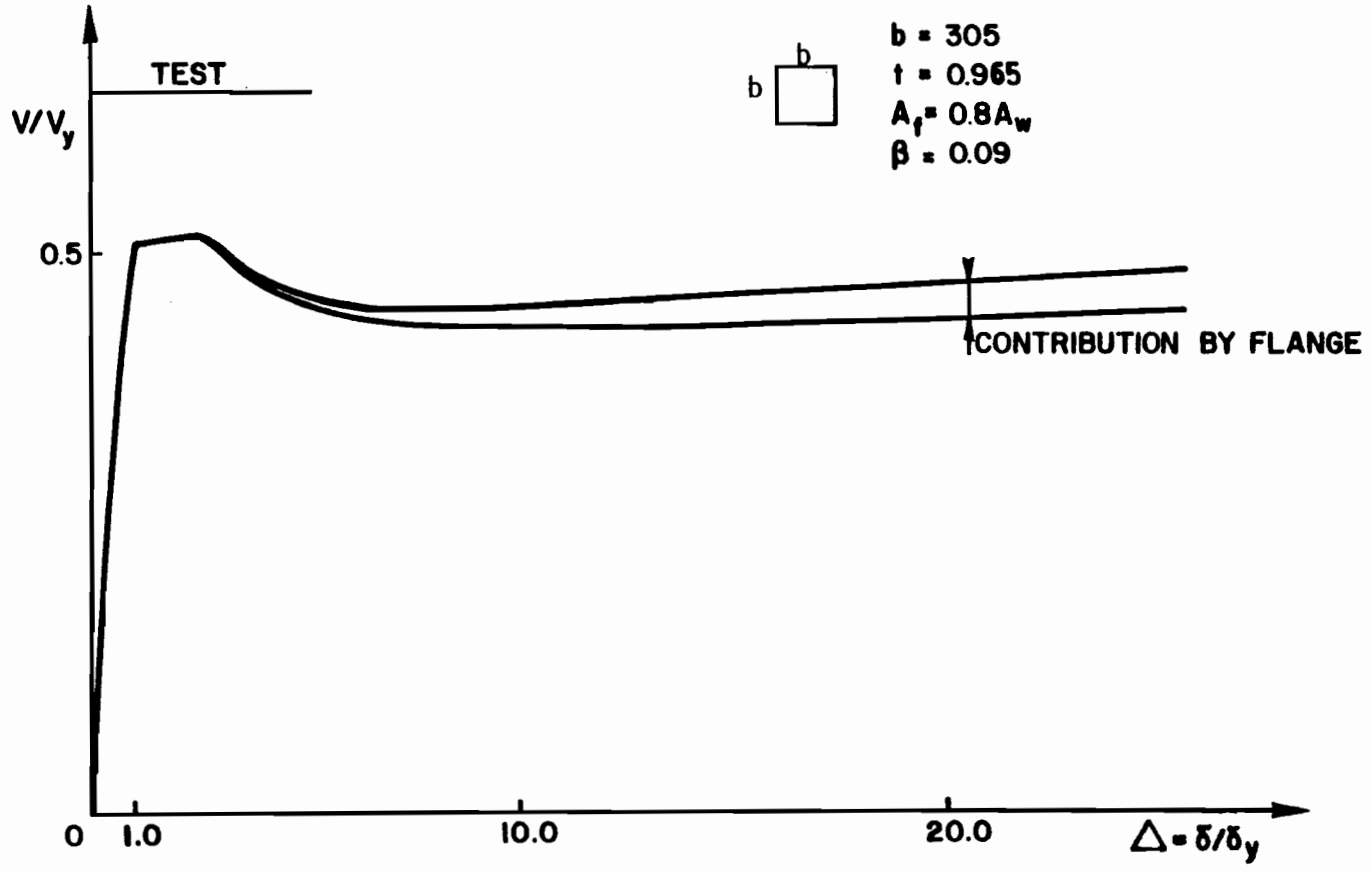

Fig. 18 SHEAR FORCE V DISPLACEMENT, TG 14

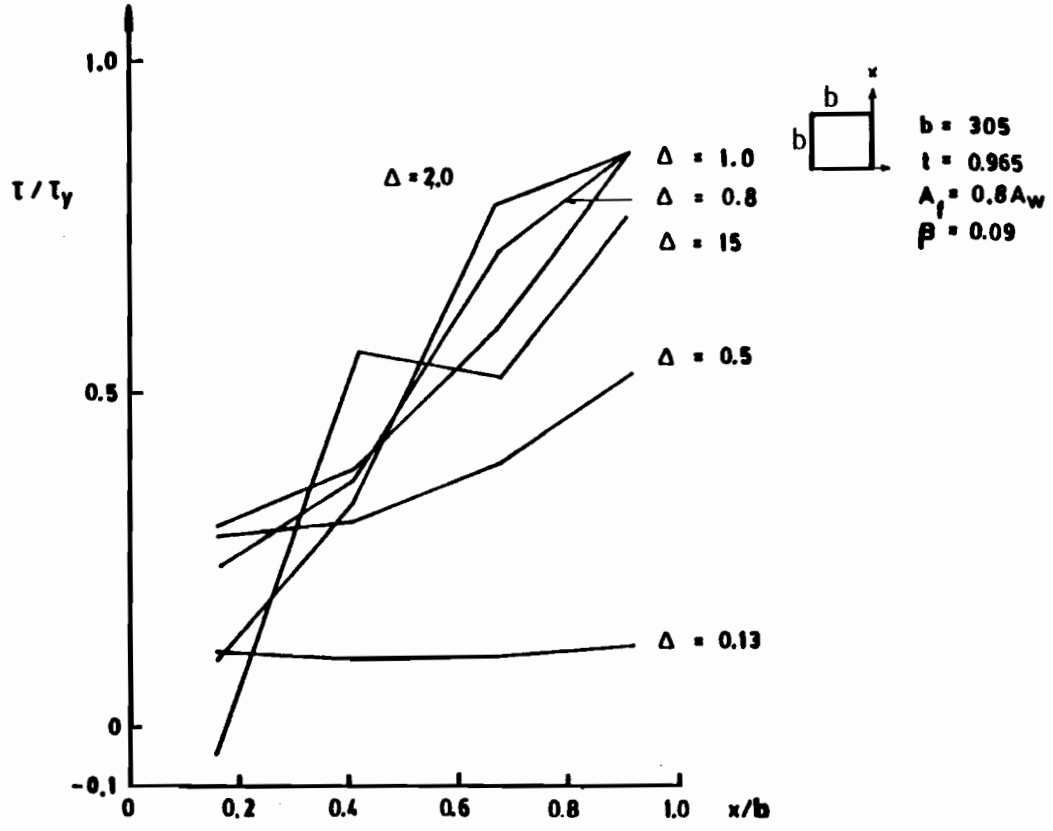

Fig. 19 SHEAR STRESS ALONG BOUNDARY FOR VARYING DISPLACEMENT, TG14

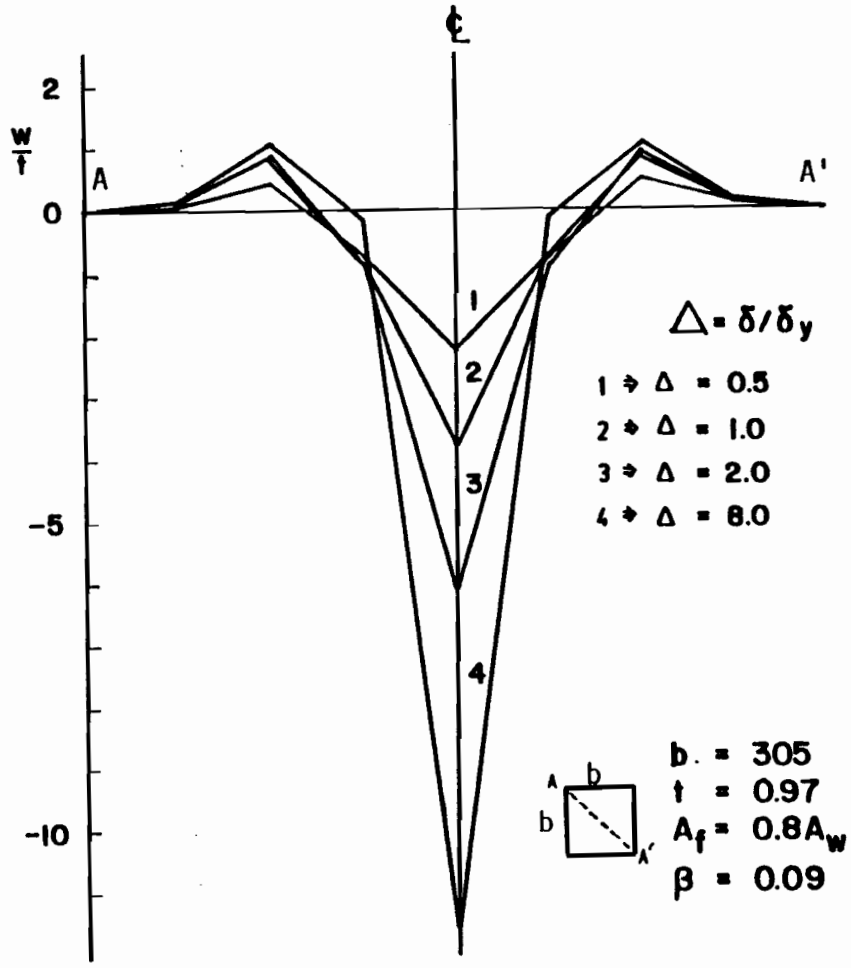

Fig. 20 **DEFLECTION ALONG COMPRESSION DIAGONAL, TG14**

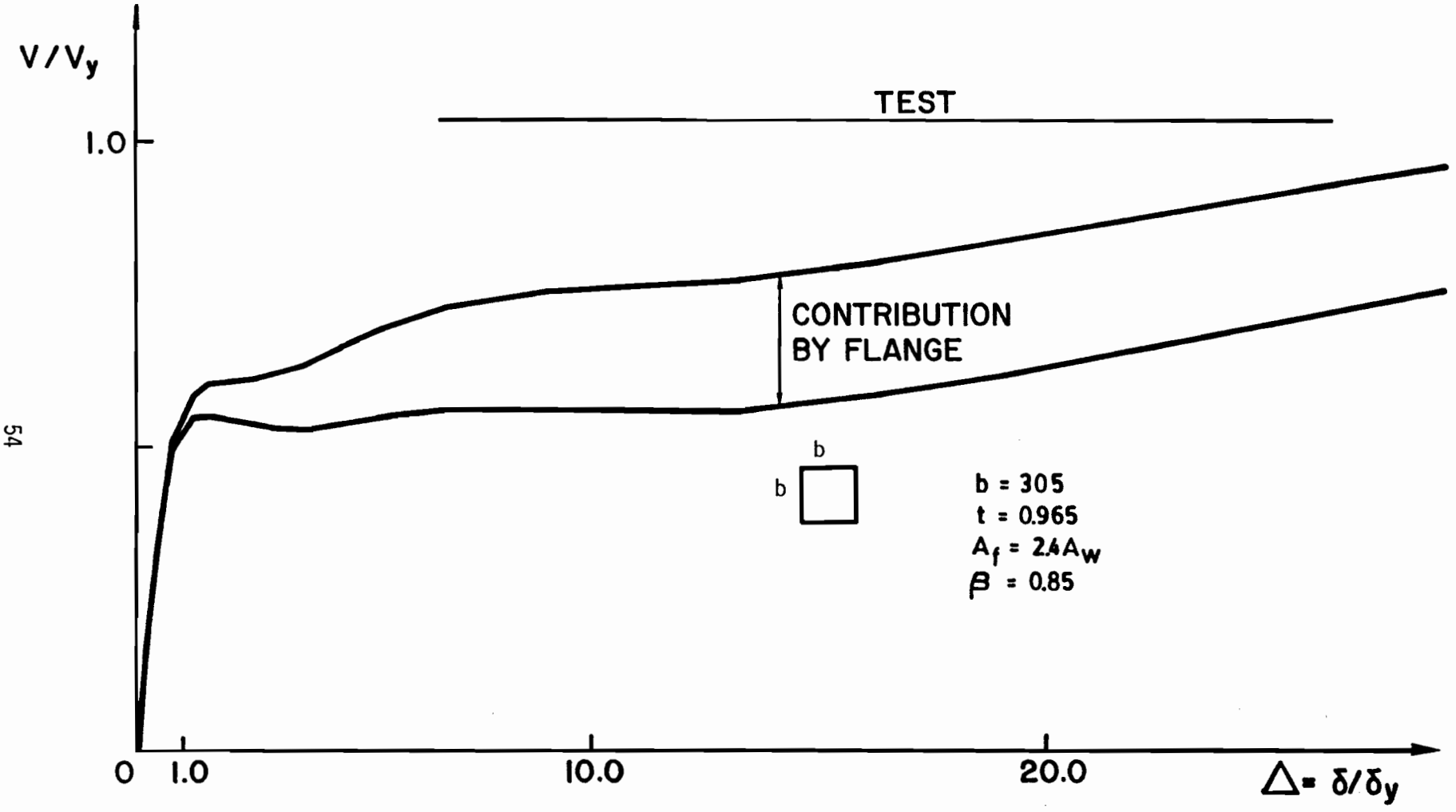

Fig. 21 SHEAR FORCE V DISPLACEMENT, TG17

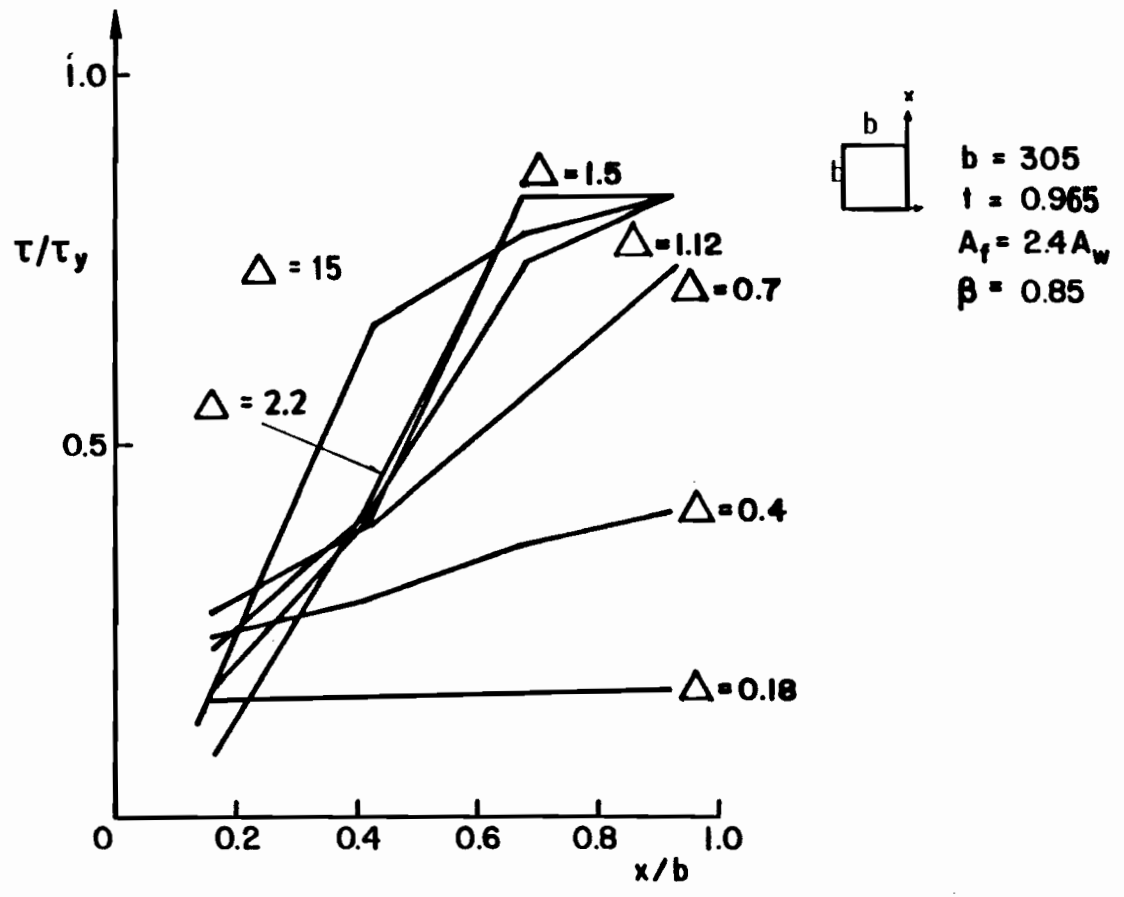

Fig. 22 SHEAR STRESS ALONG BOUNDARY FOR VARYING DISPLACEMENT, TG17

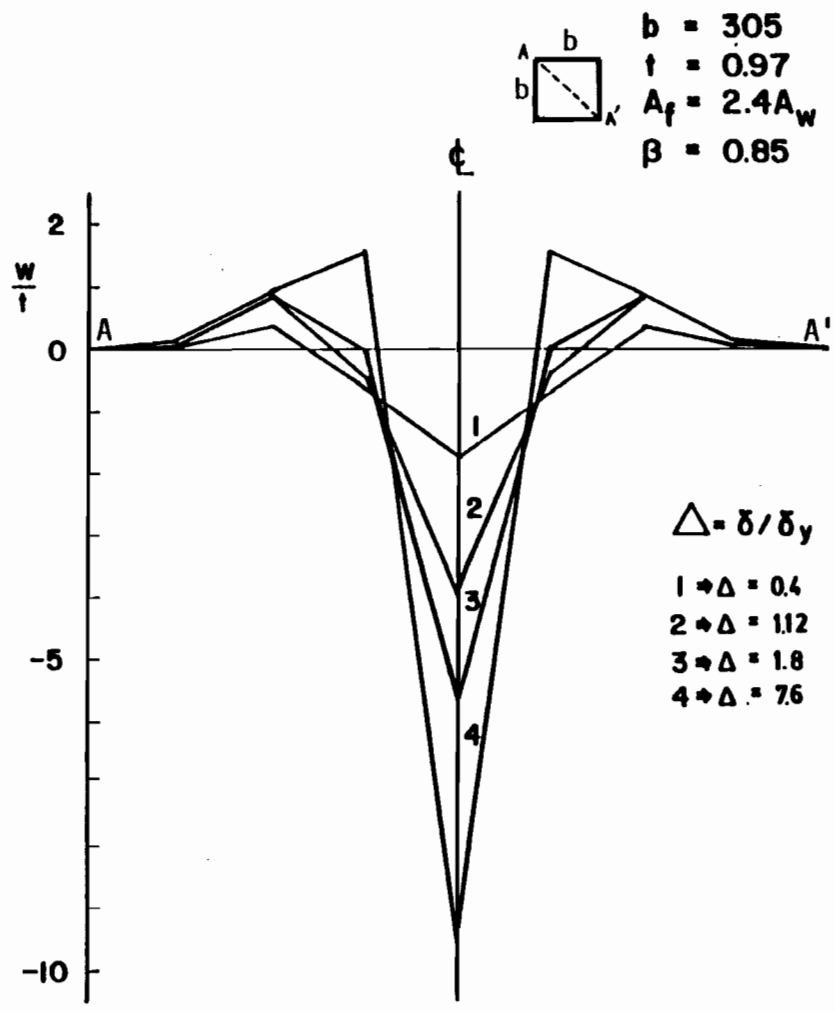

Fig. 23 DEFLECTION ALONG COMPRESSION DIAGONAL, TG17

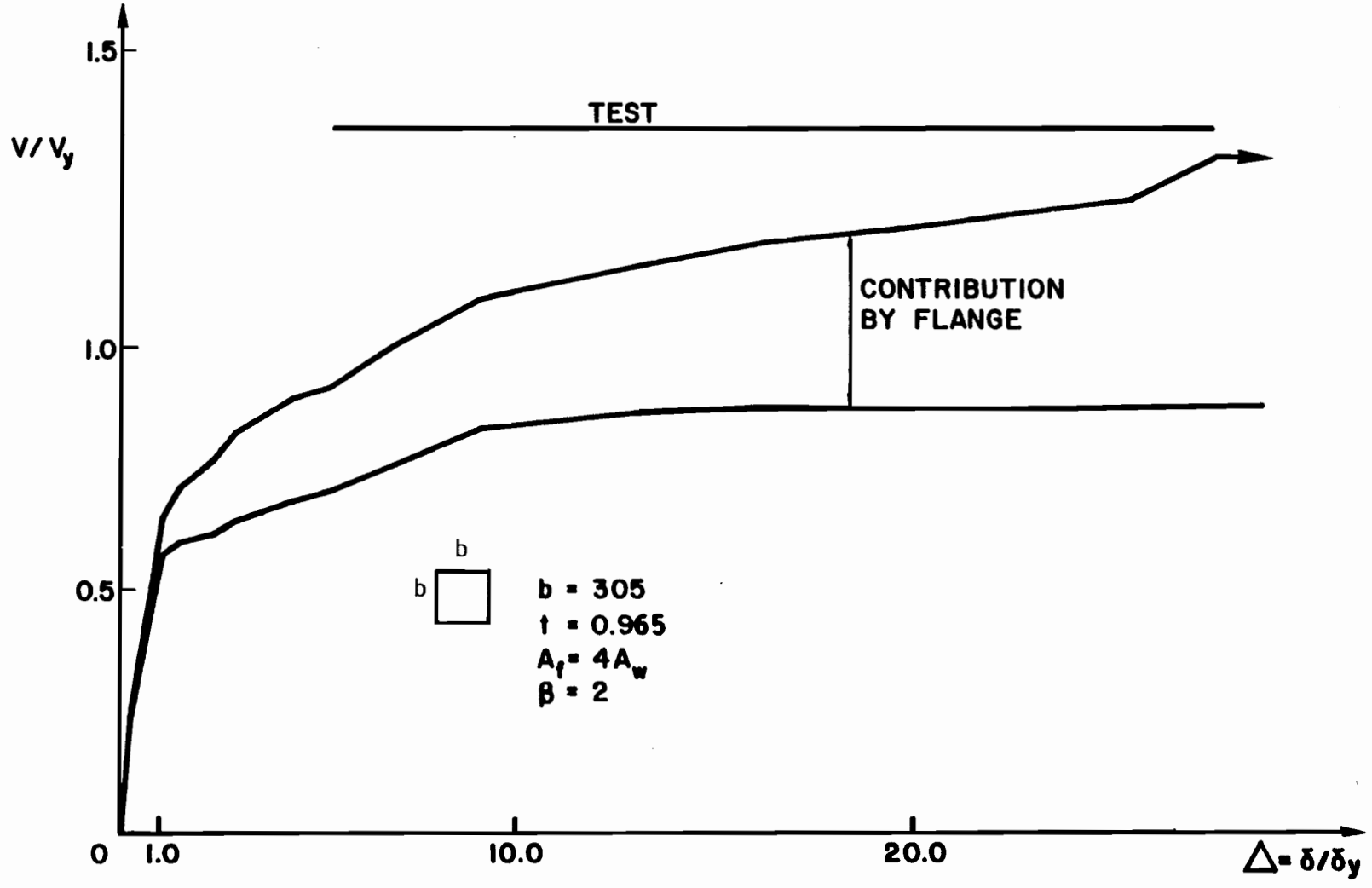

Fig. 24 SHEAR FORCE V DISPLACEMENT, TG19

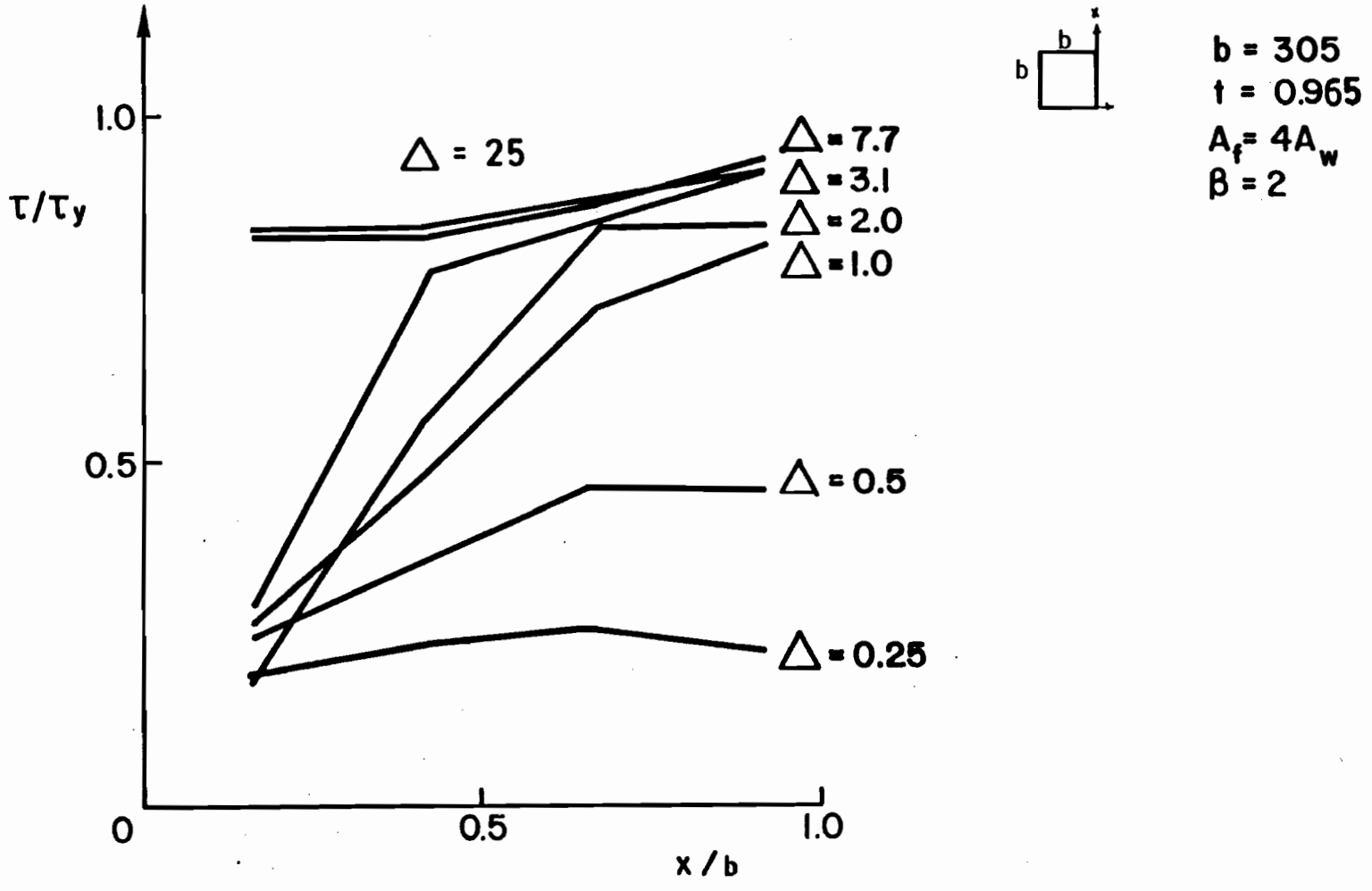

Fig. 25 SHEAR STRESS ALONG THE BOUNDARY FOR VARYING DISPLACEMENT, TG19

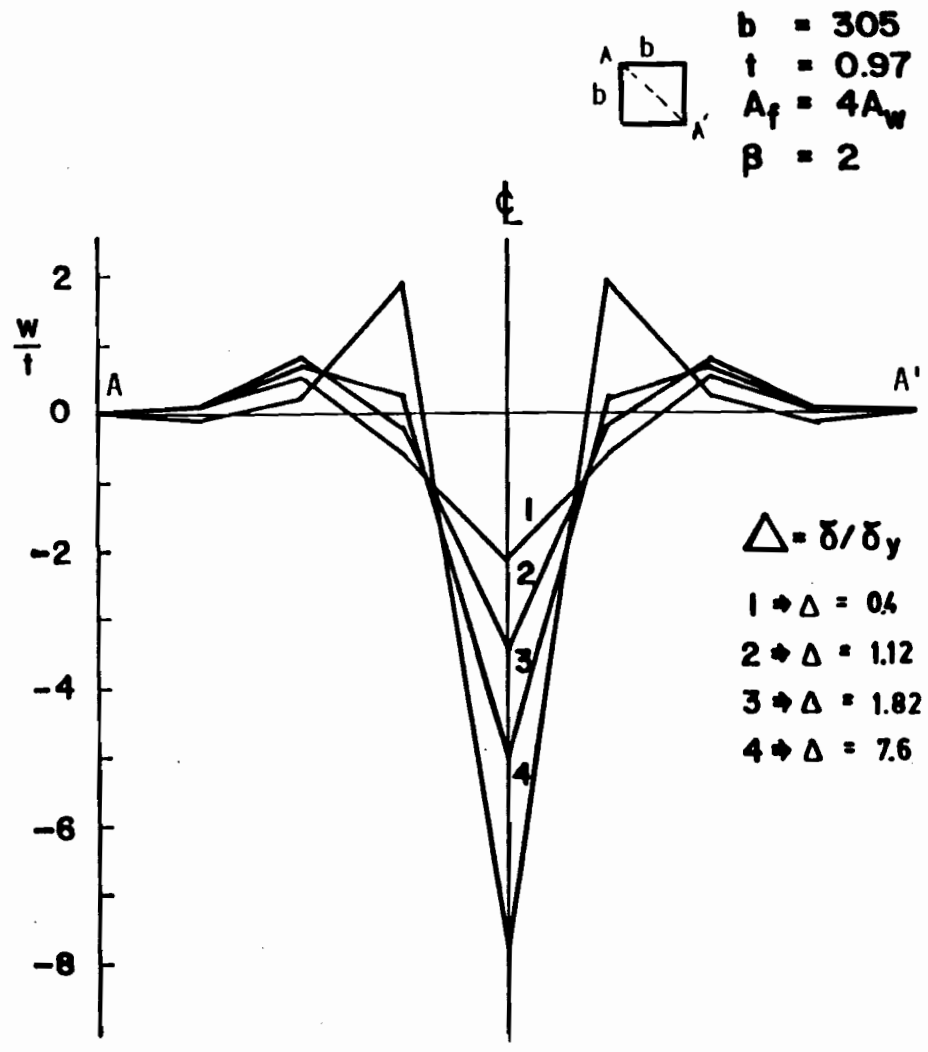

Fig. 26 **DEFLECTION ALONG COMPRESSION DIAGONAL, TG19**

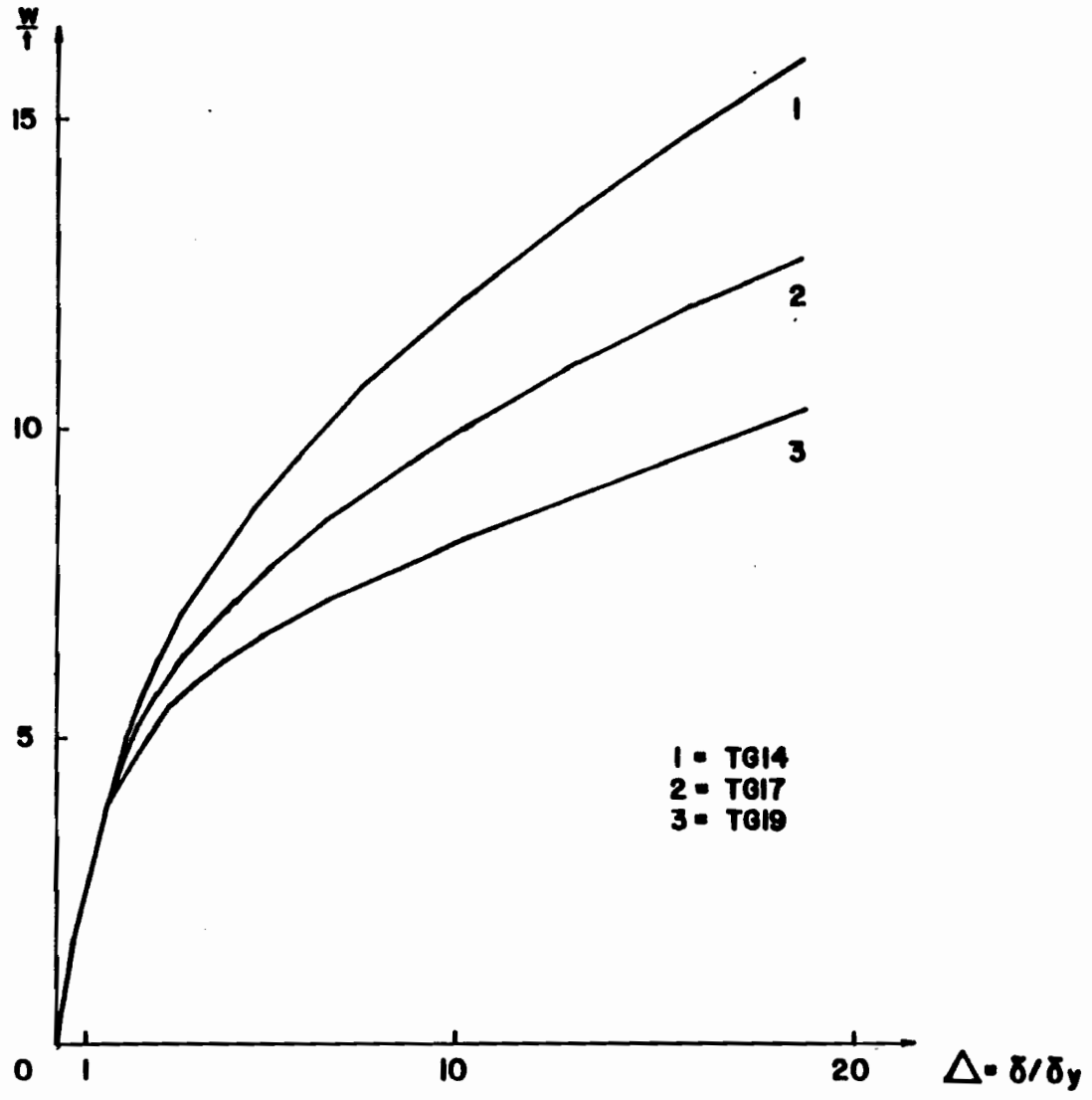

Fig. 27 CENTRE DEFLECTION VARIATIONS, F.E.M.

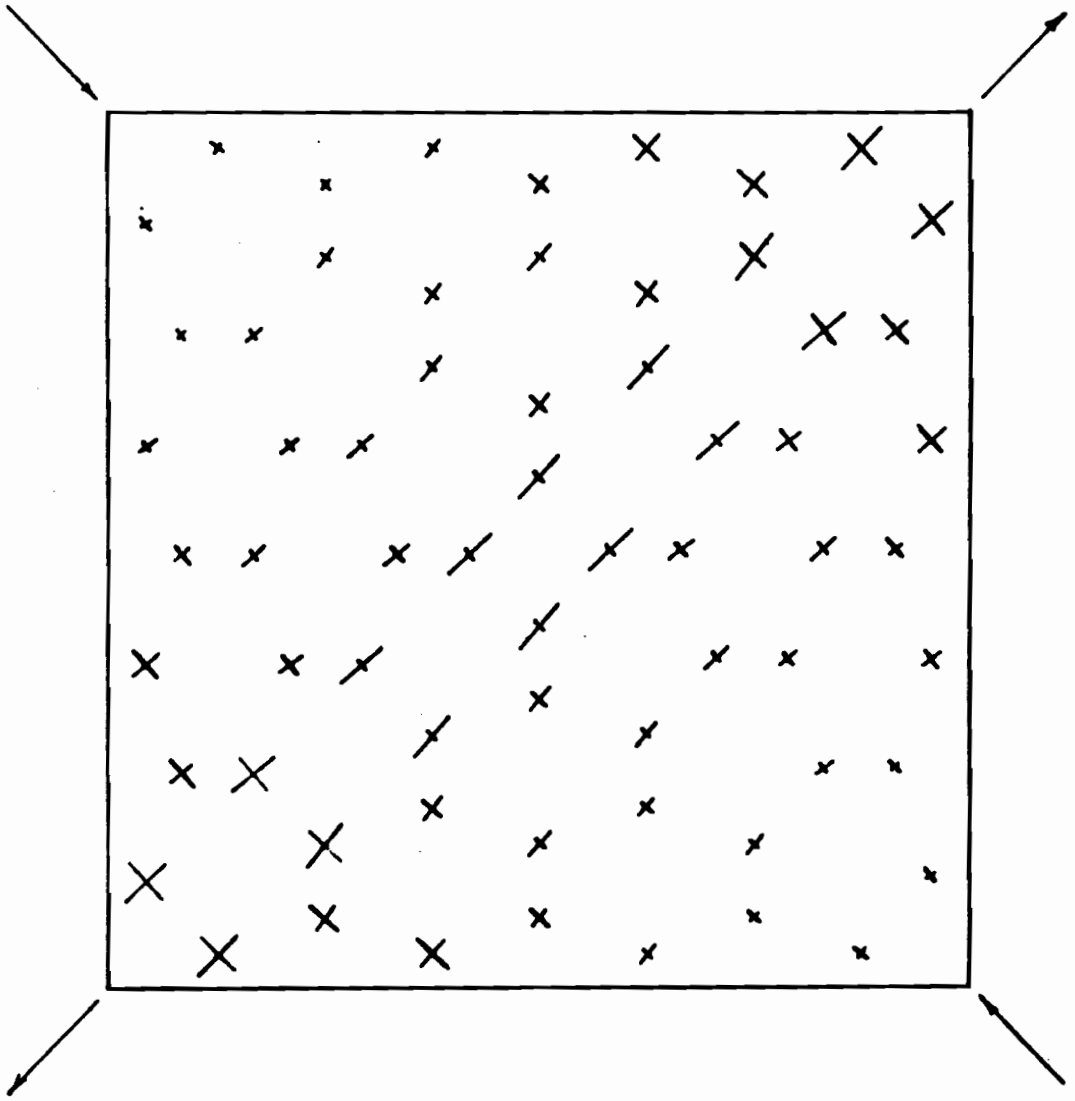

b = 305
t = 0.97
$A_f = 0.8A_w$
$\beta = 0.09$

Fig. 28 PRINCIPAL STRESSES AT FIRST YIELD, SQUARE PLATE, TG14

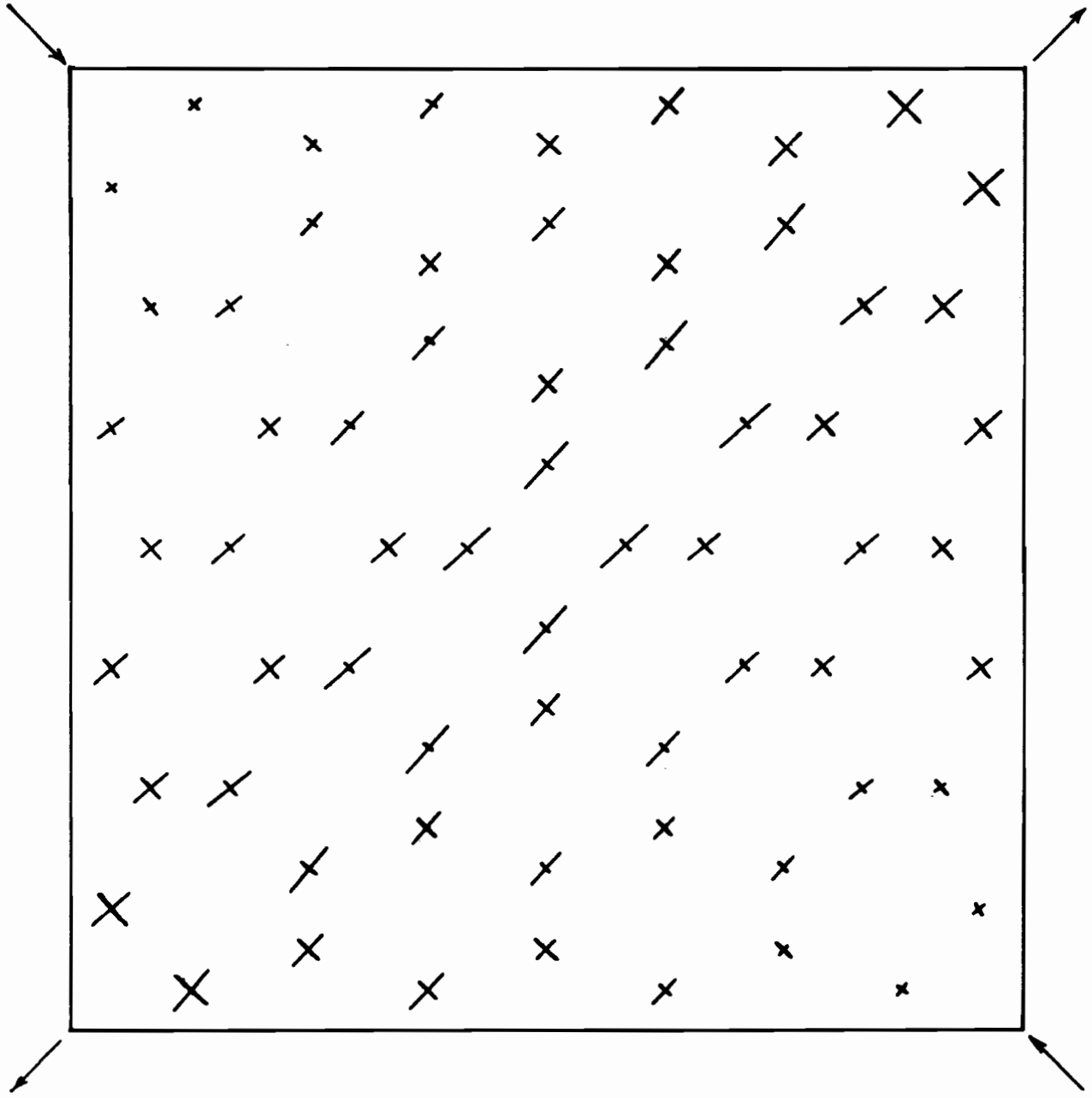

$b = 305$
$t = 0.97$
$A_f = 4A_w$
$\beta = 2$

Fig. 29 PRINCIPAL STRESSES AT FIRST YIELD, SQUARE PLATE, TG19

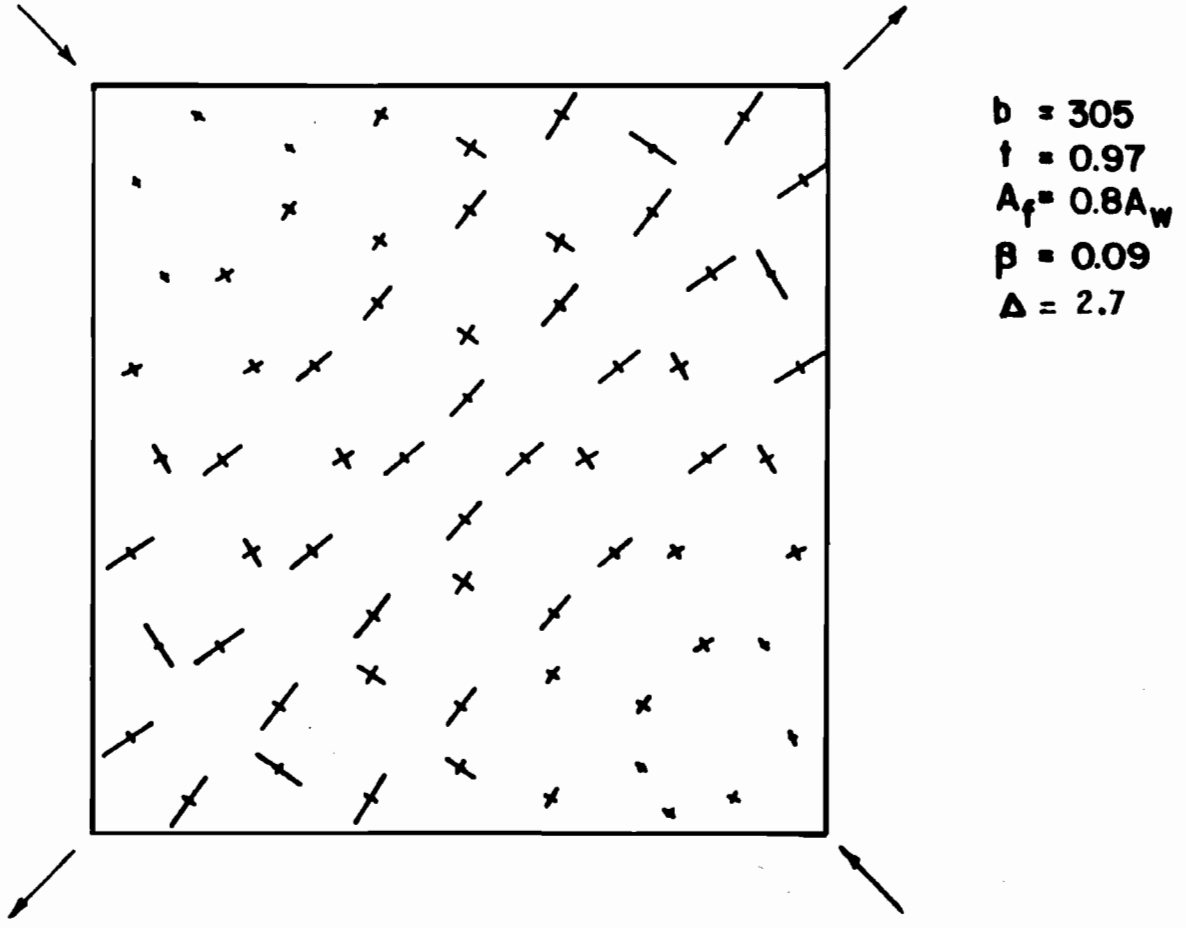

Fig. 30 **PRINCIPAL STRESSES AFTER FIRST YIELD, SQUARE PLATE, TG14**

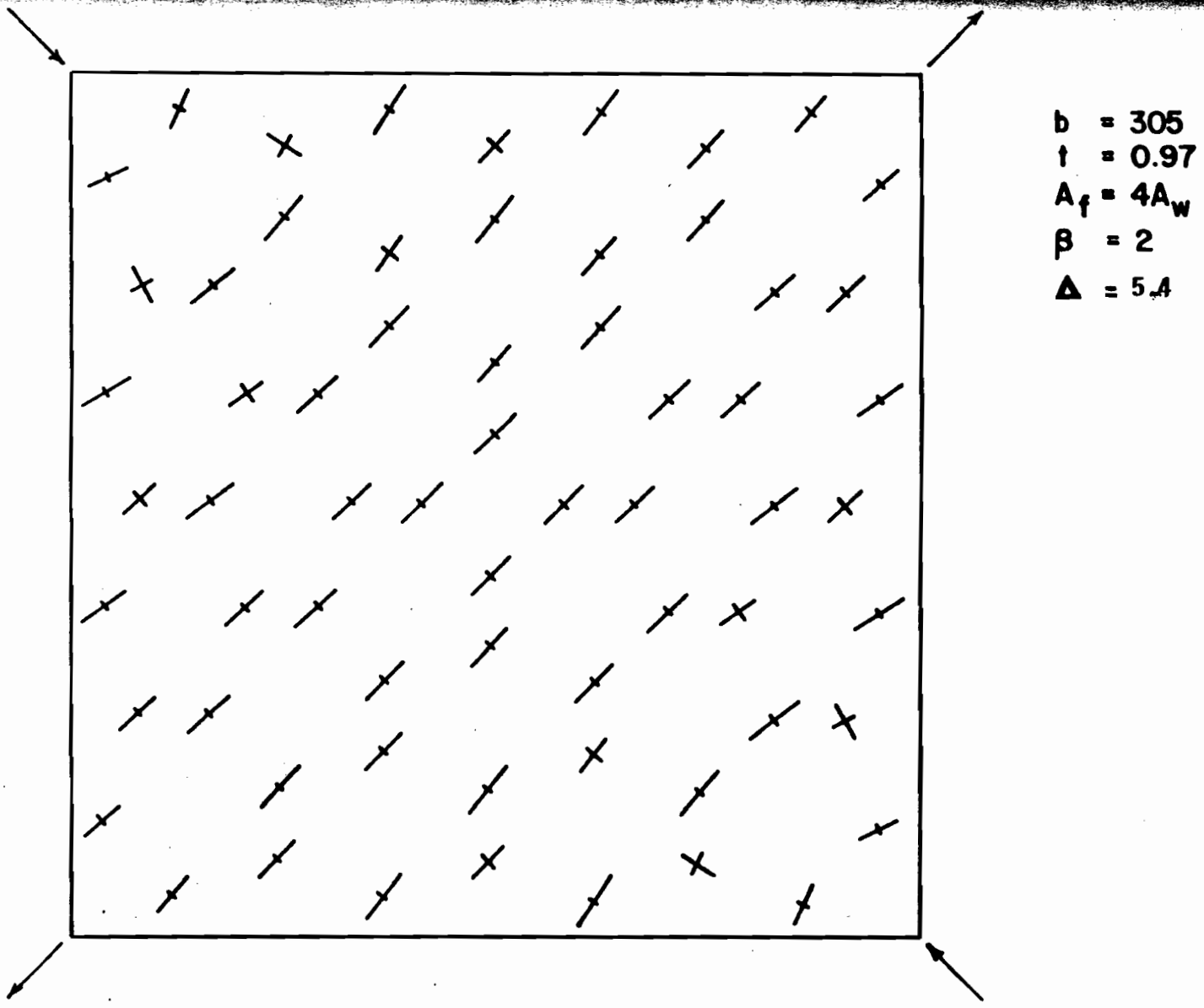

Fig. 31 PRINCIPAL STRESSES AFTER FIRST YIELD, SQUARE PLATE, TGI9

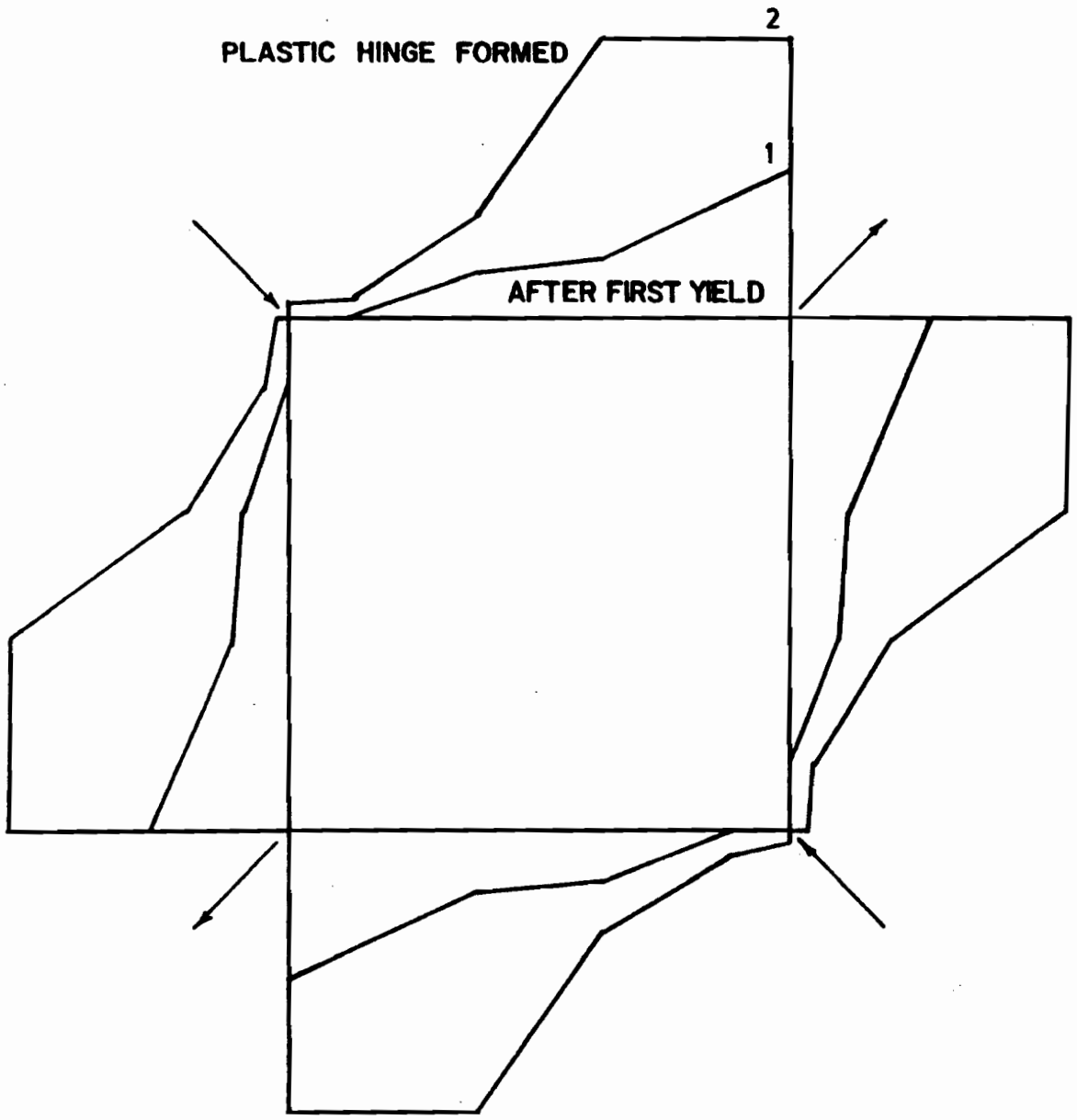

Fig. 32 **NORMAL FORCES AT BOUNDARIES, TG14**

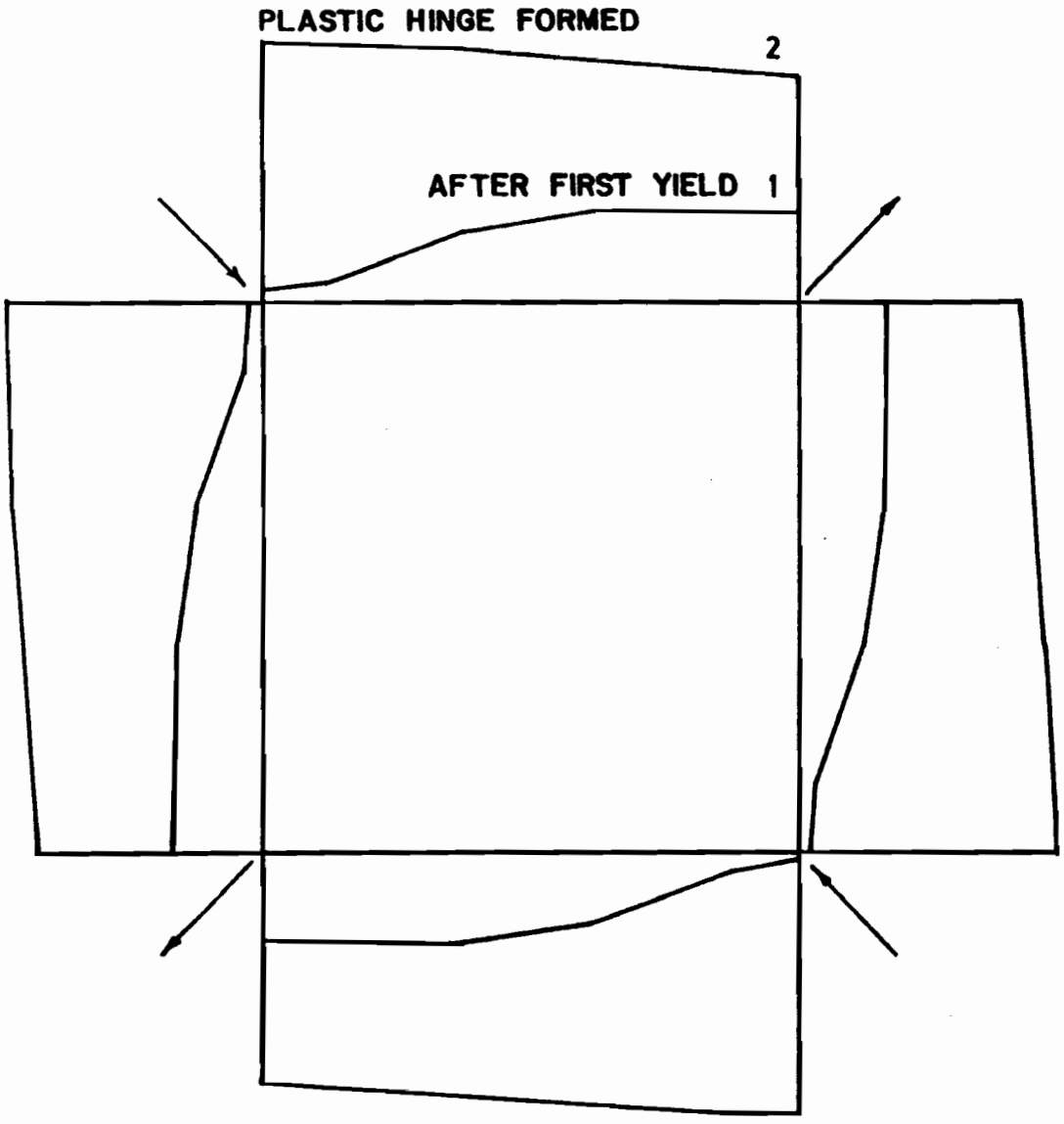

$b = 305$
$t = 0.97$
$A_f = 0.8A_w$
$\beta = 2$
$1 \Rightarrow \Delta = 2$
$2 \Rightarrow \Delta = 25$

Fig. 33 NORMAL FORCES AT BOUNDARIES, TG19

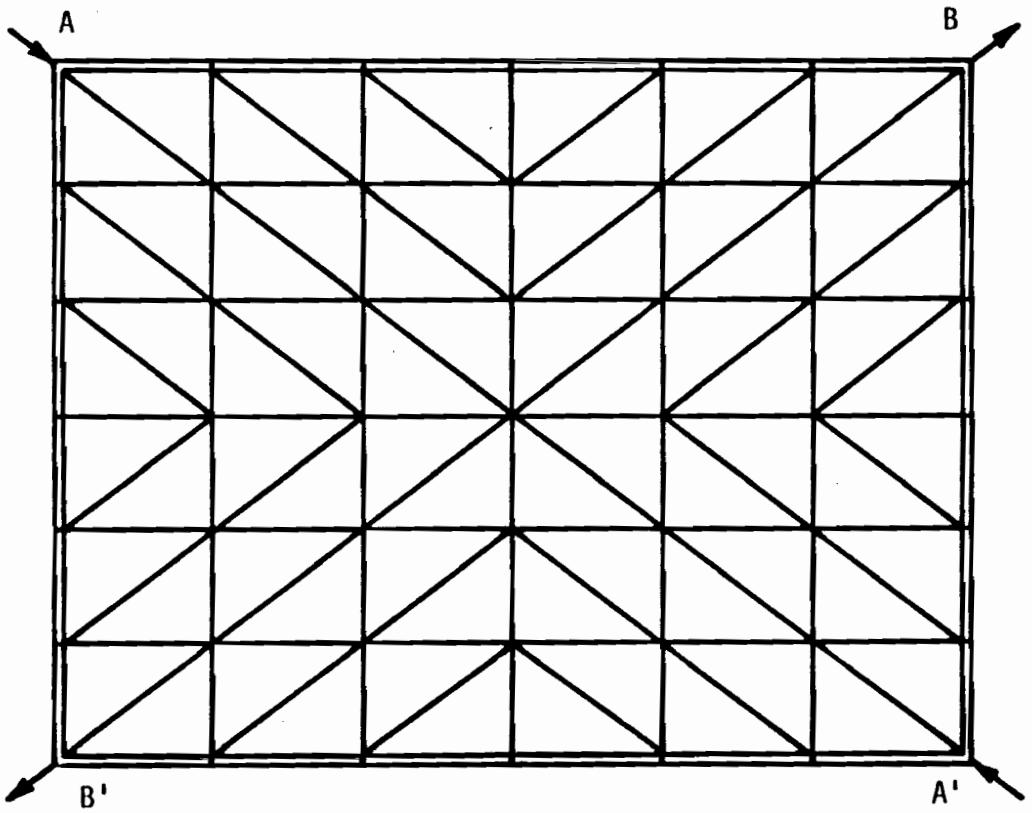

Fig. 34 **FINITE ELEMENT GRID FOR RECTANGULAR PANELS**

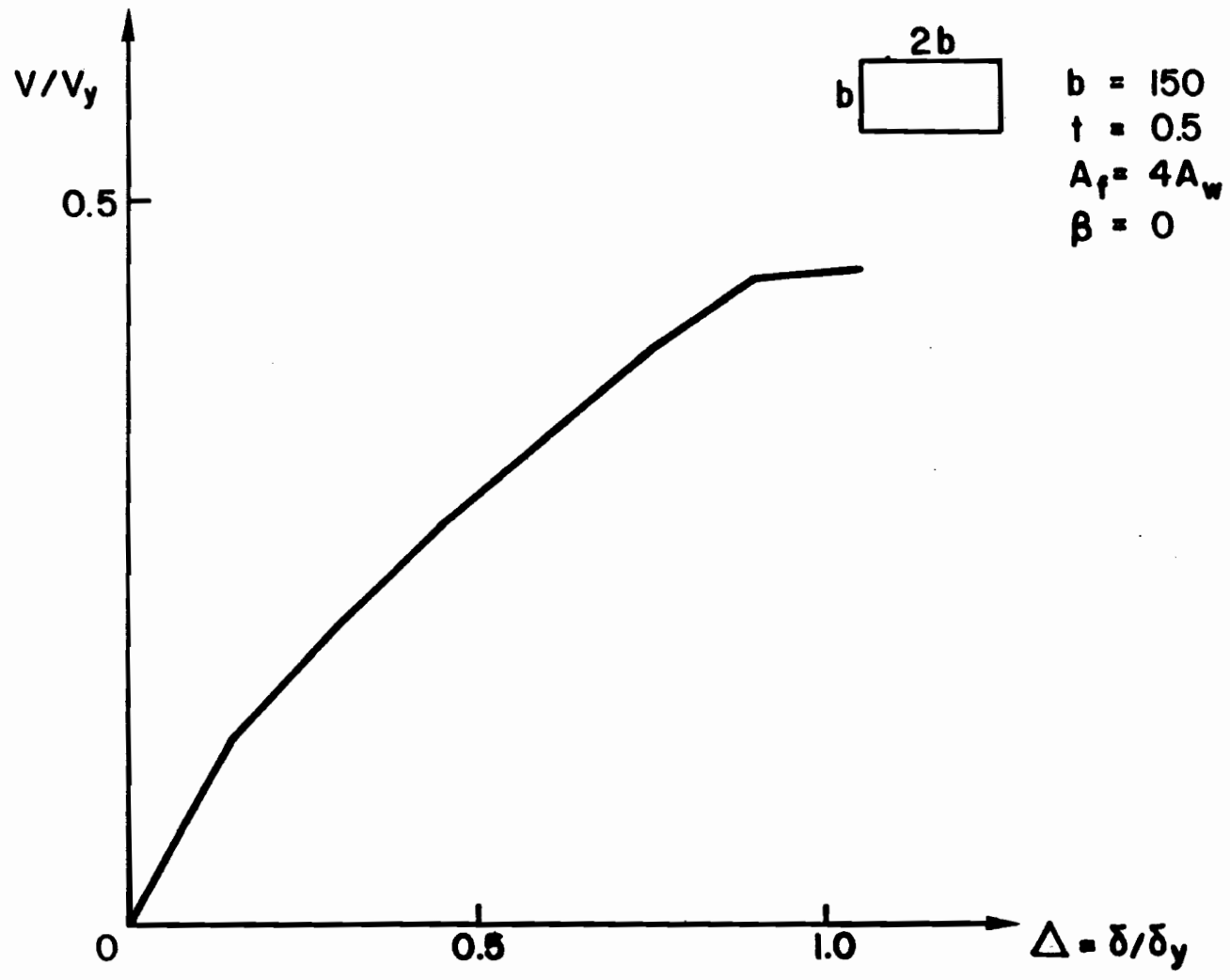

Fig. 35 SHEAR FORCE V DISPLACEMENT

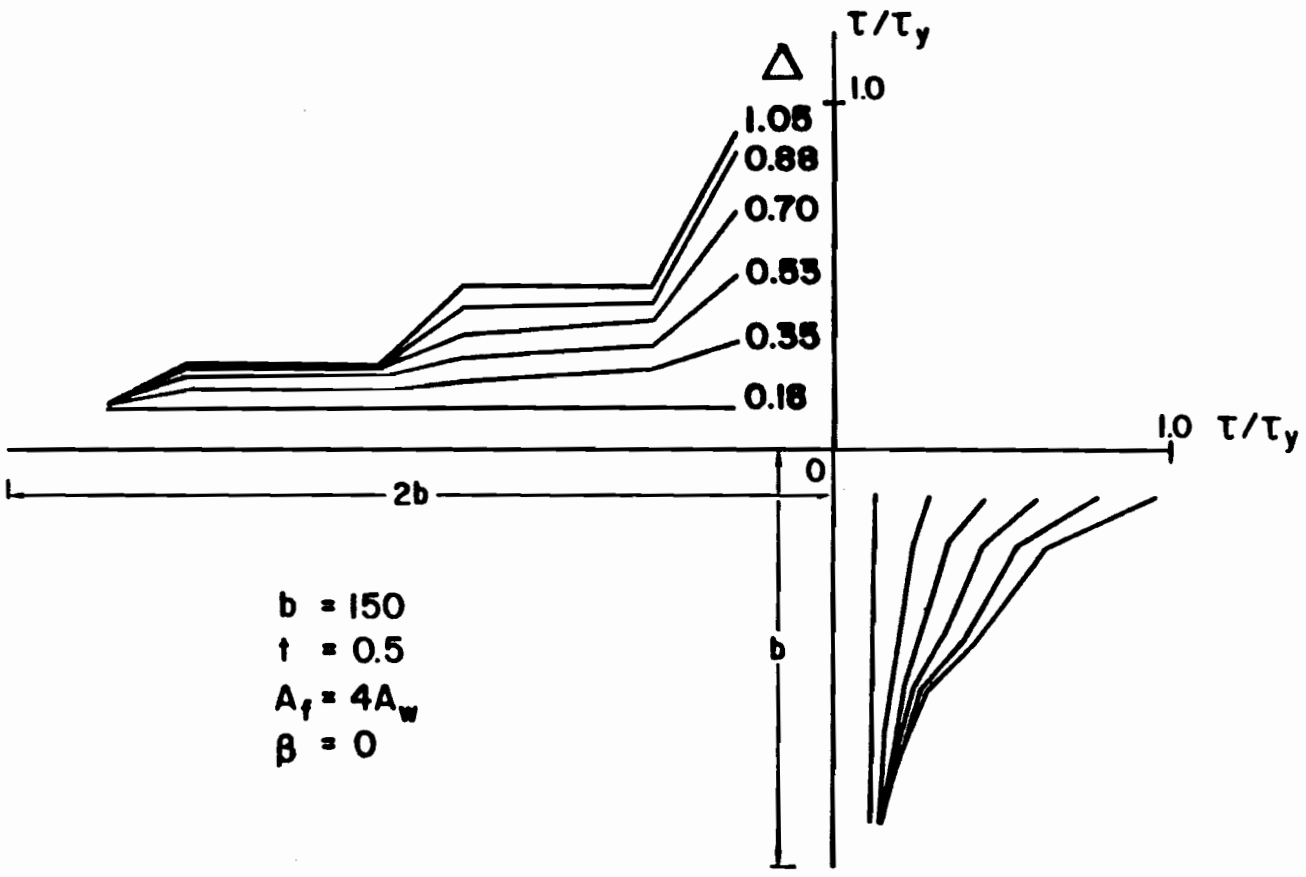

Fig. 36 **SHEAR STRESS ALONG BOUNDARIES FOR VARYING DISPLACEMENT, RECTANGULAR PANEL**

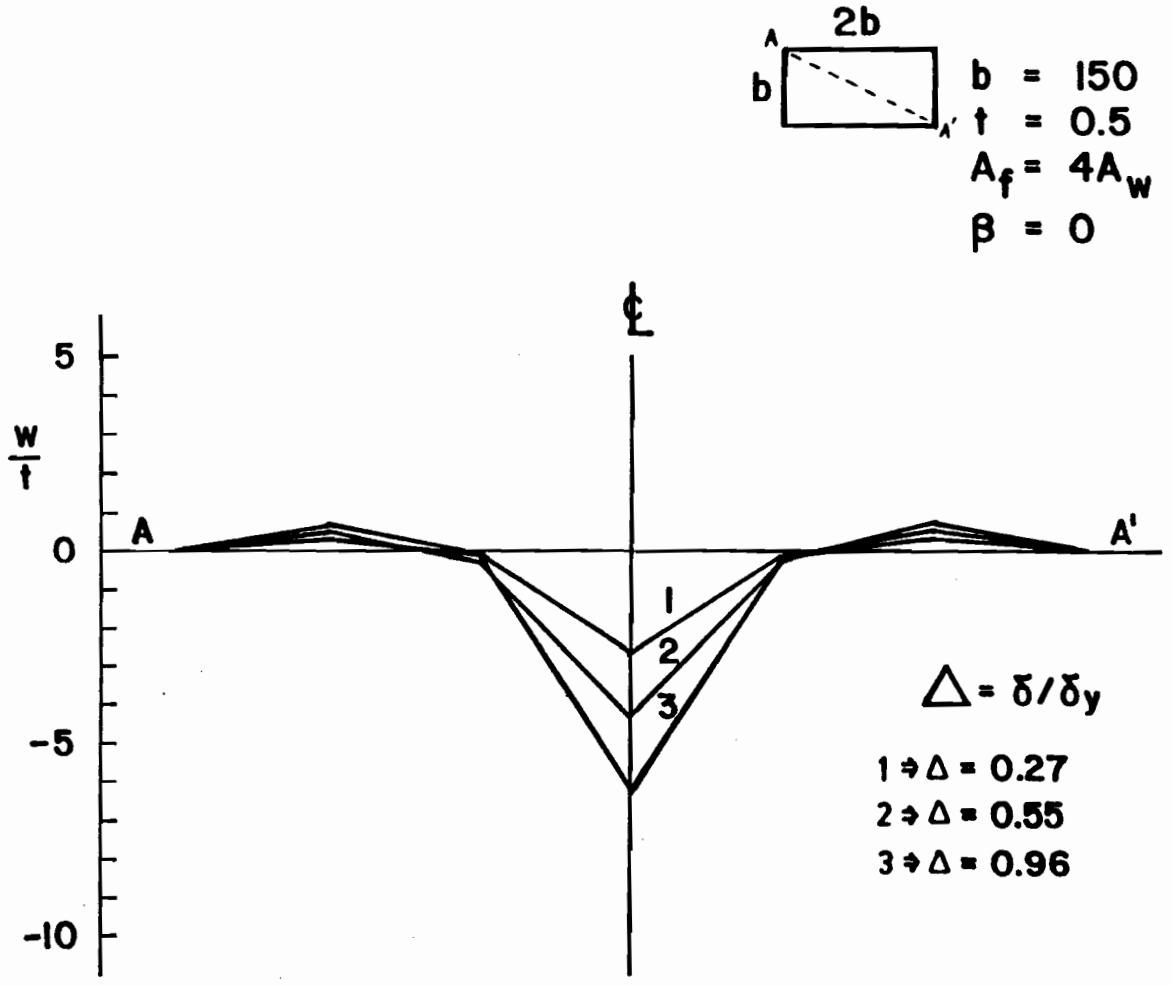

Fig. 37 **DEFLECTION ALONG COMPRESSION DIAGONAL**

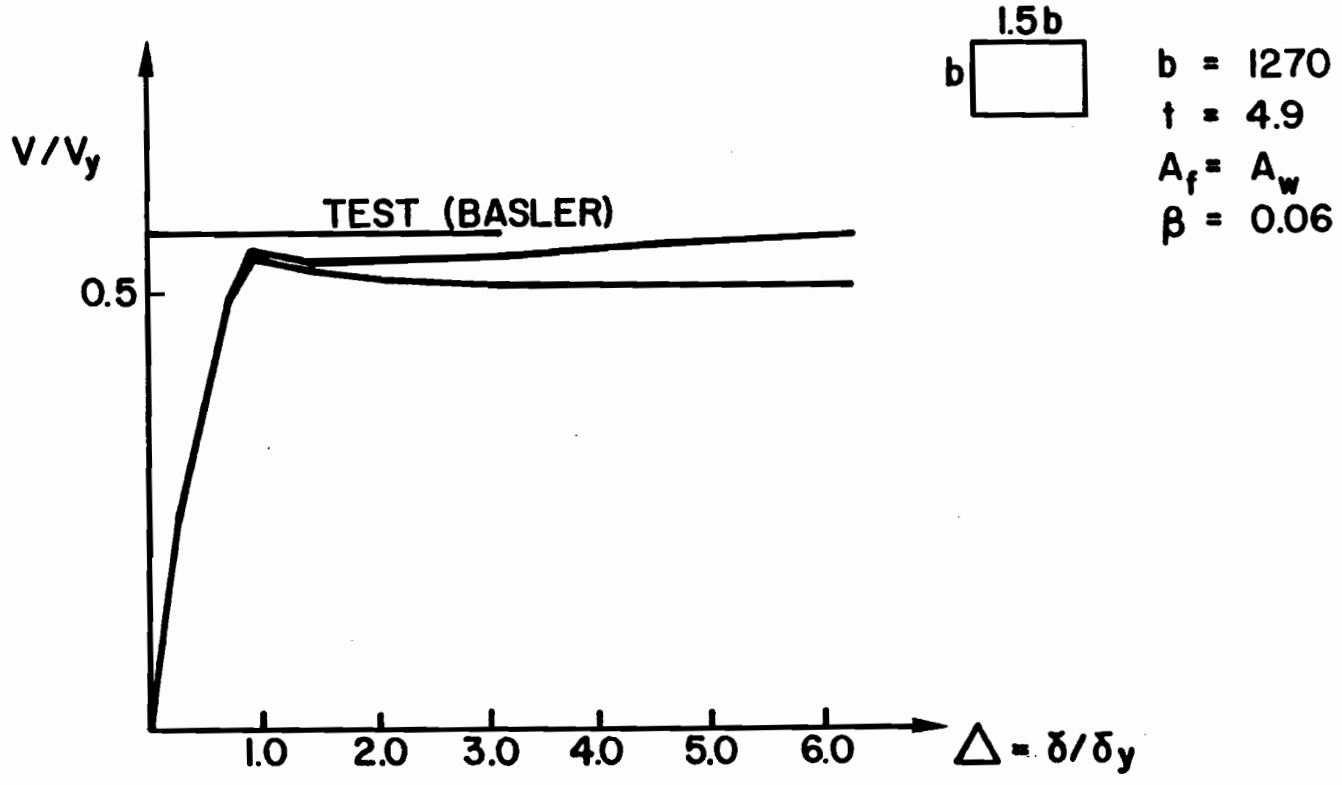

Fig. 38 SHEAR FORCE V DISPLACEMENT, G6T1

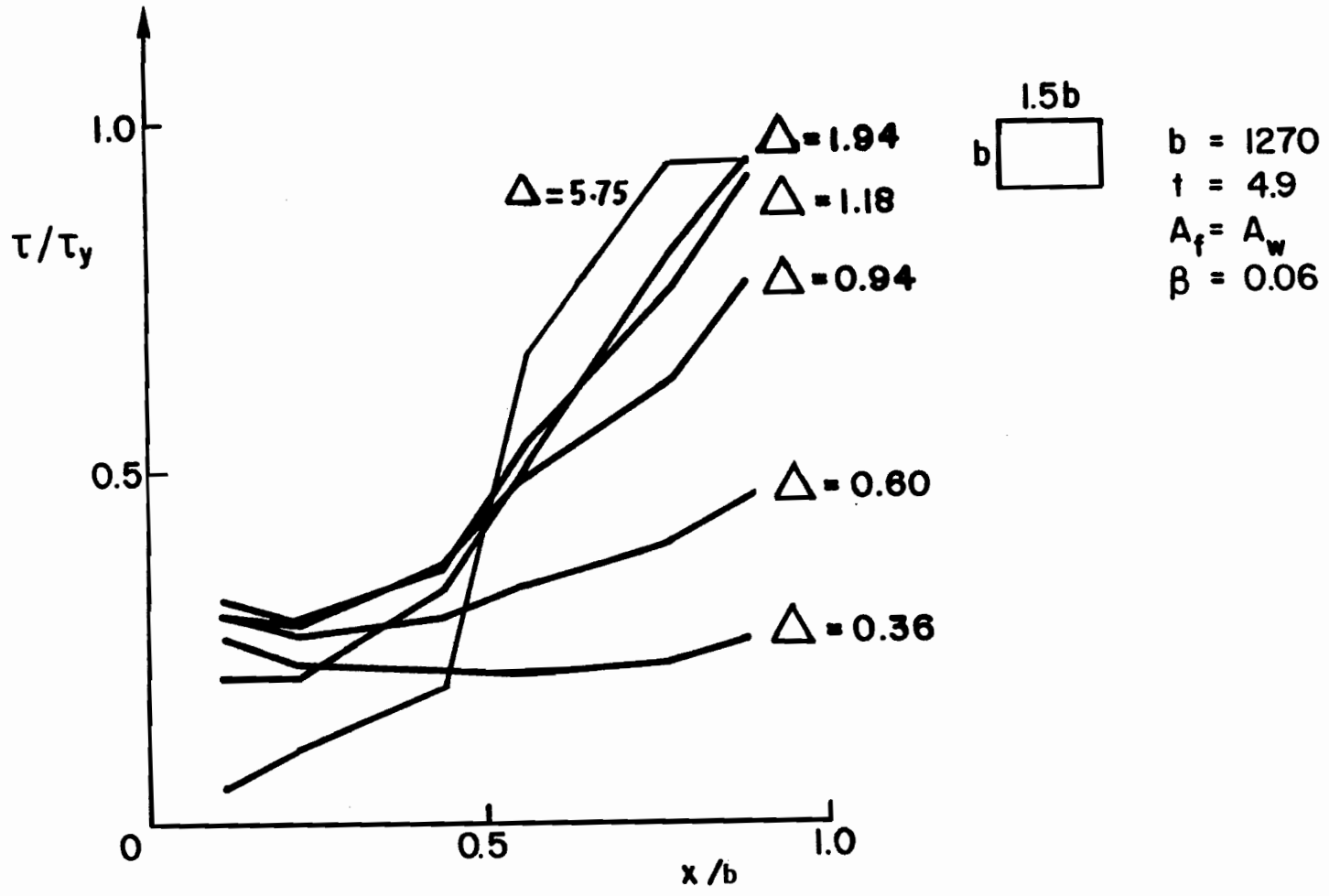

Fig. 39 SHEAR STRESS ALONG BOUNDARY WITH VARYING DISPLACEMENT, G6T1

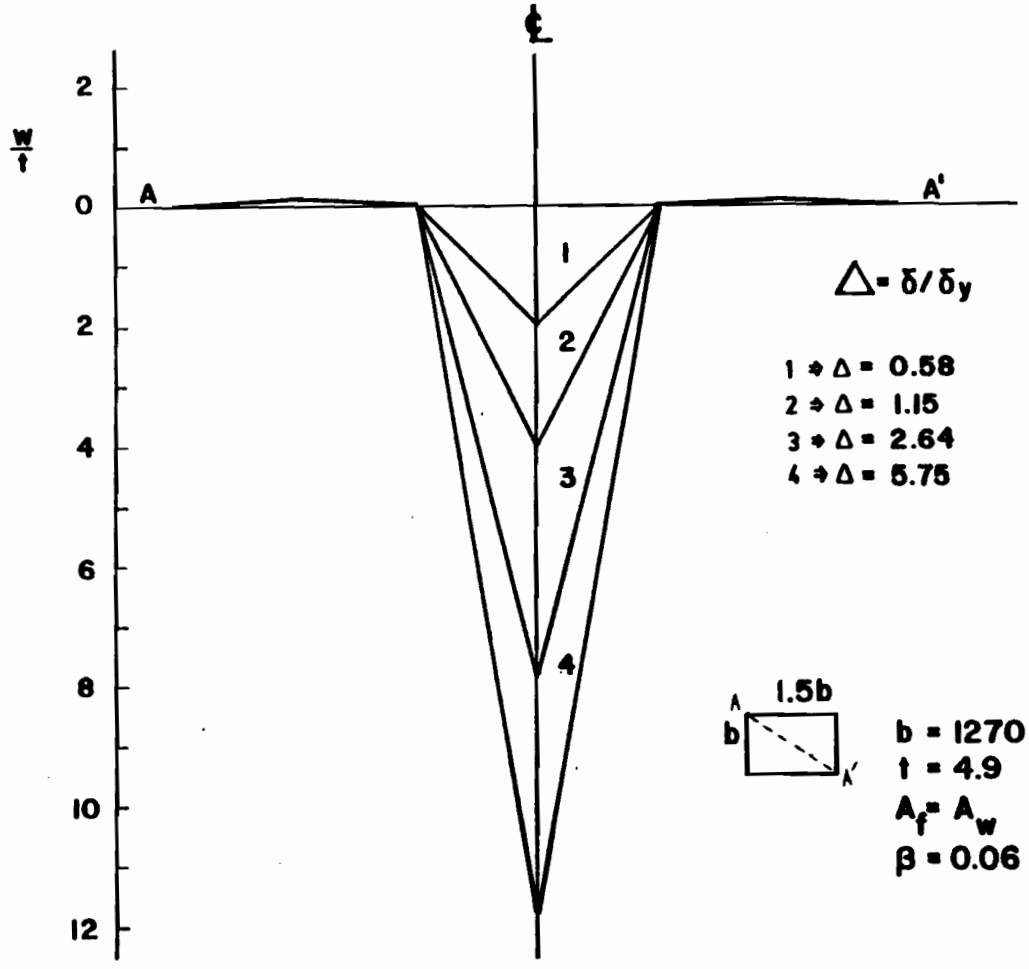

Fig. 40 **DEFLECTION ALONG COMPRESSION DIAGONAL, G6T1**

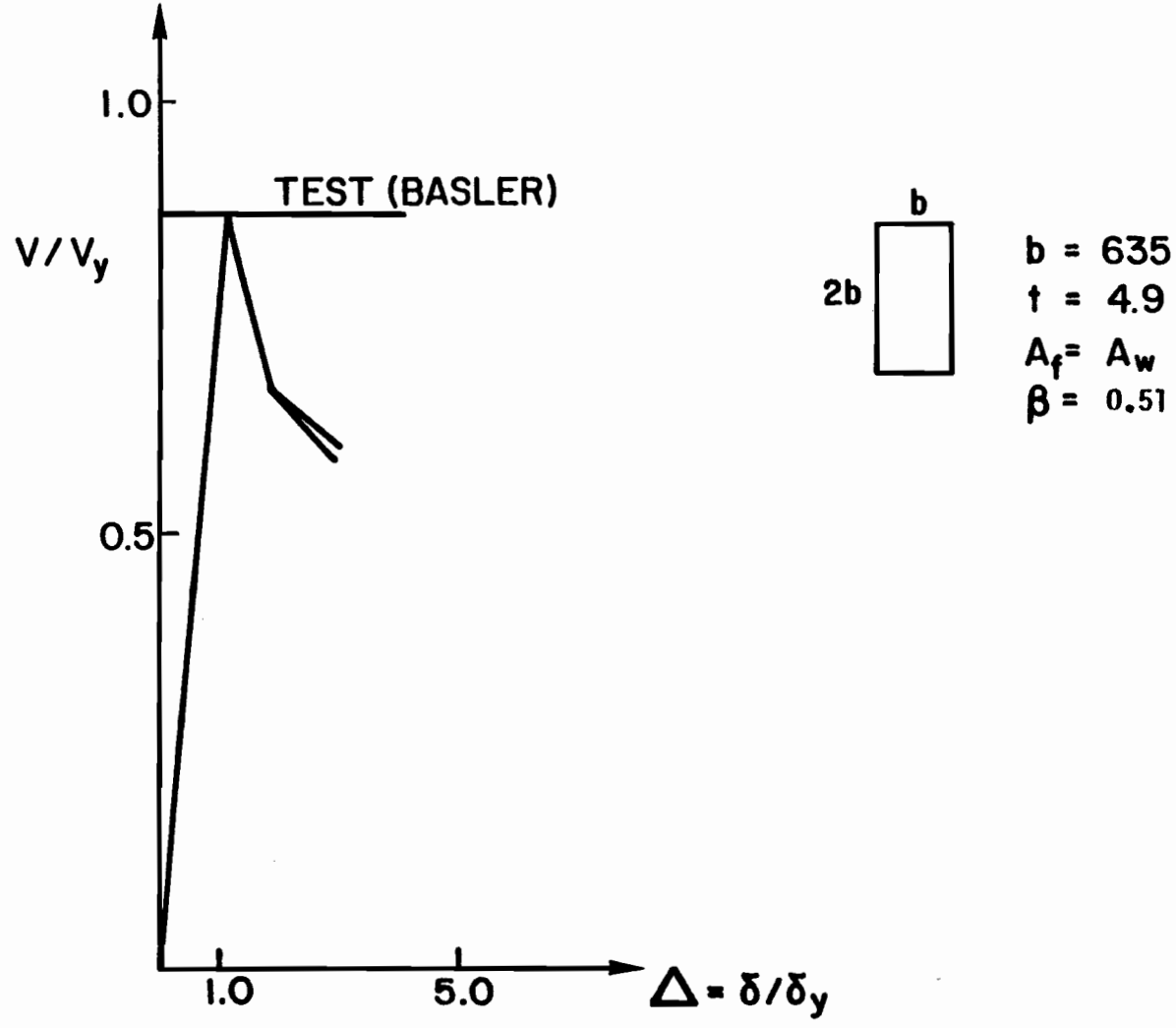

Fig. 41 SHEAR FORCE V DISPLACEMENT, G6T3

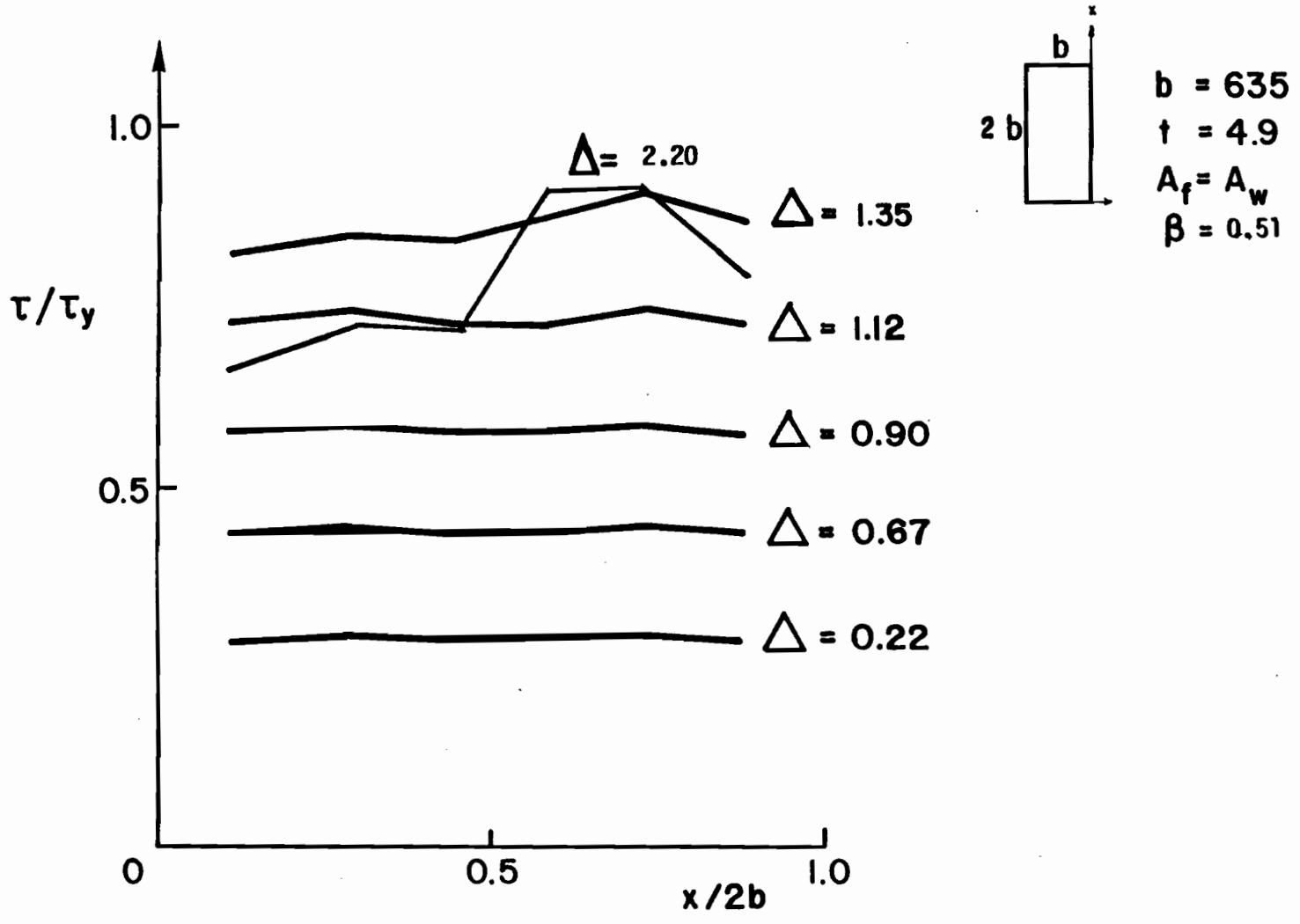

Fig. 42 SHEAR STRESS DISTRIBUTION FOR VARYING DISPLACEMENT, G6T3

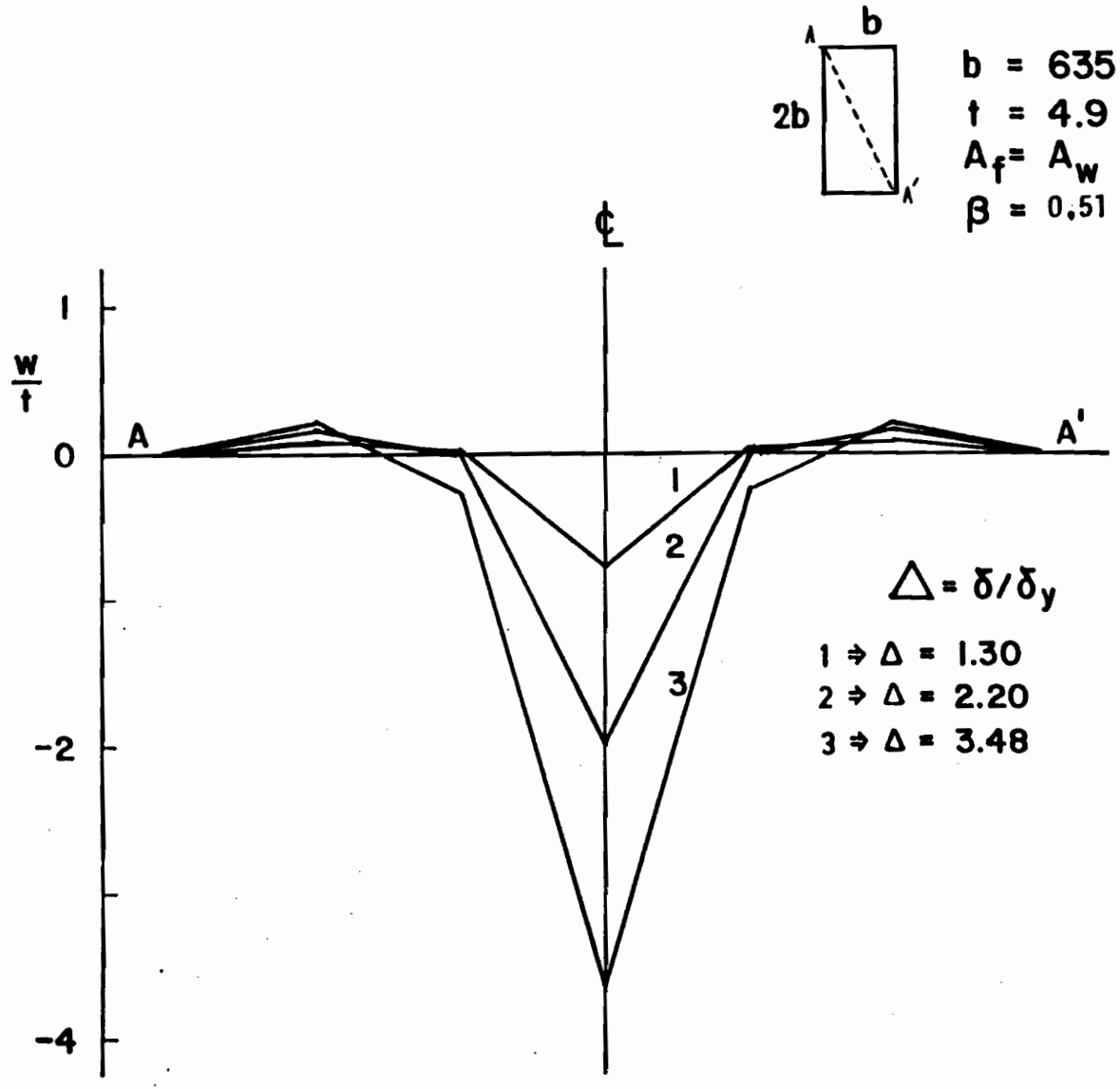

Fig. 43 DEFLECTION ALONG COMPRESSION DIAGONAL, G6T3

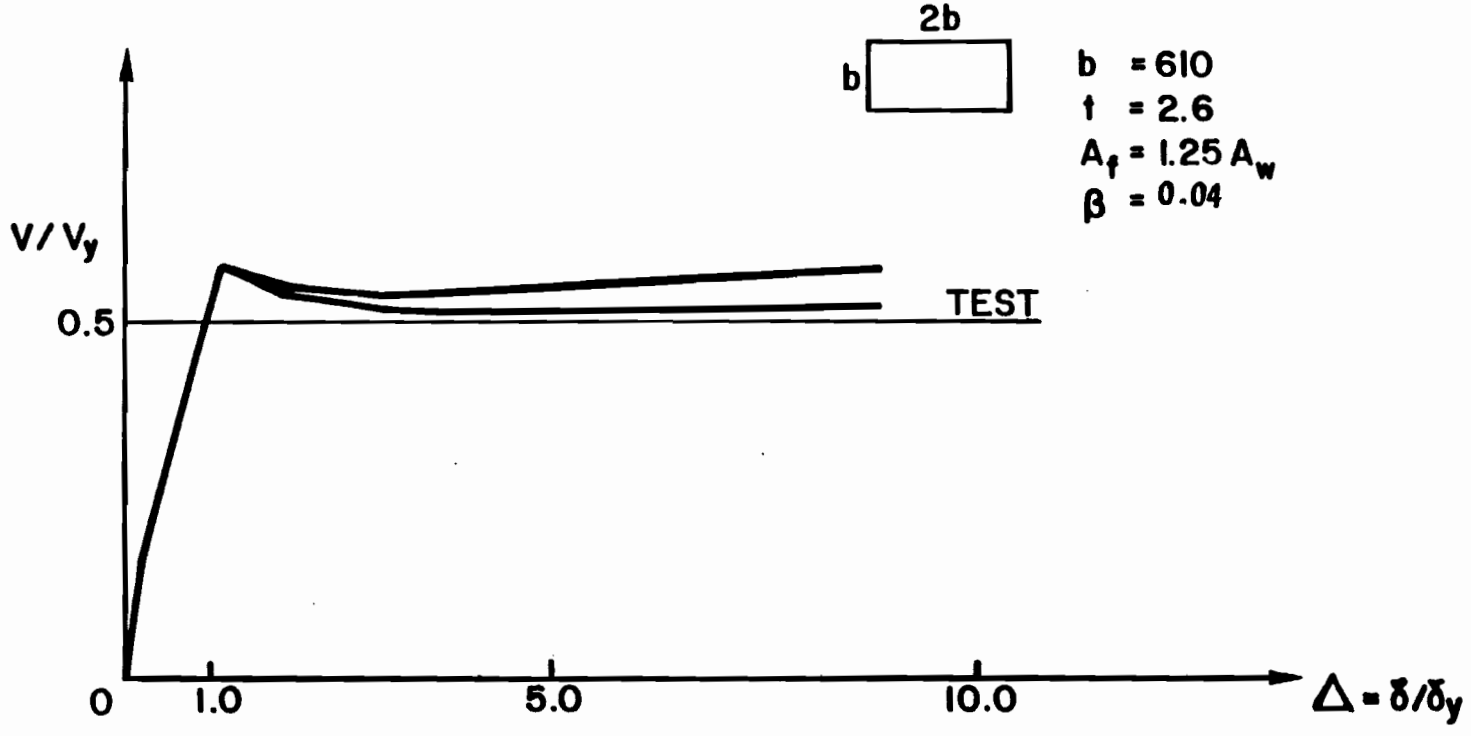

Fig. 44 SHEAR FORCE V DISPLACEMENT, TG9

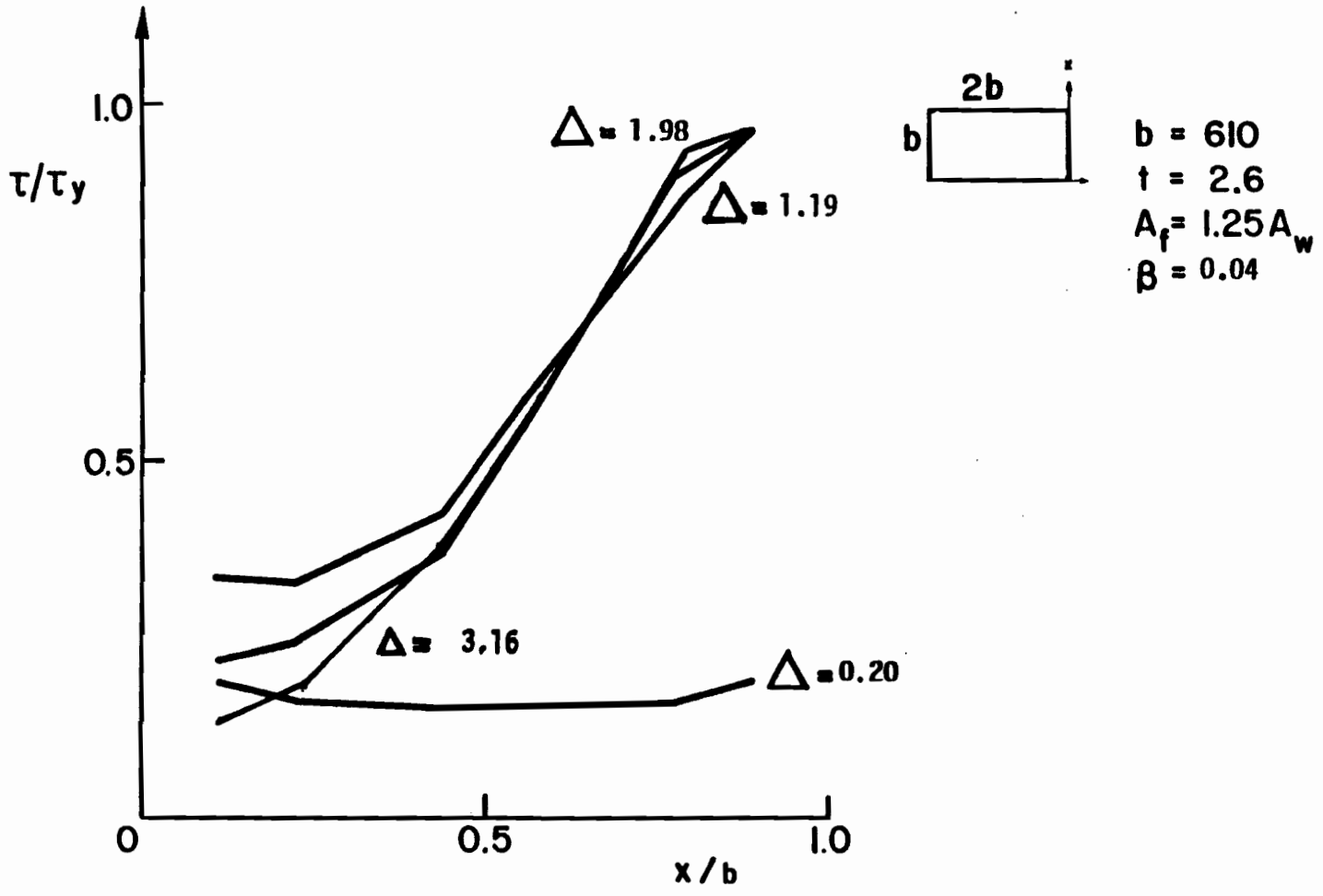

Fig. 45 SHEAR STRESS ALONG BOUNDARY FOR VARYING DISPLACEMENT, TG9

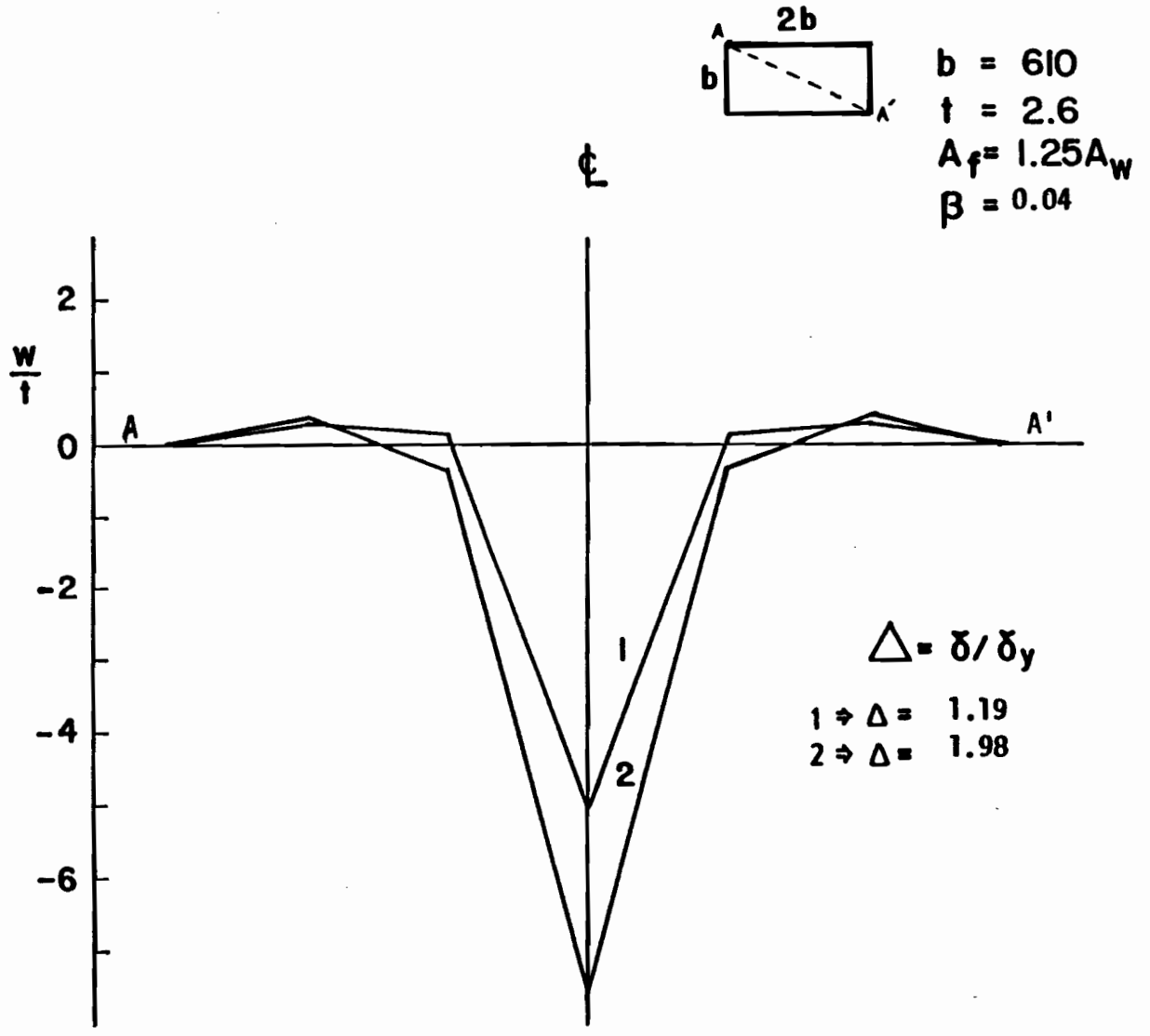

Fig. 46 **DEFLECTION ALONG COMPRESSION DIAGONAL, TG9**

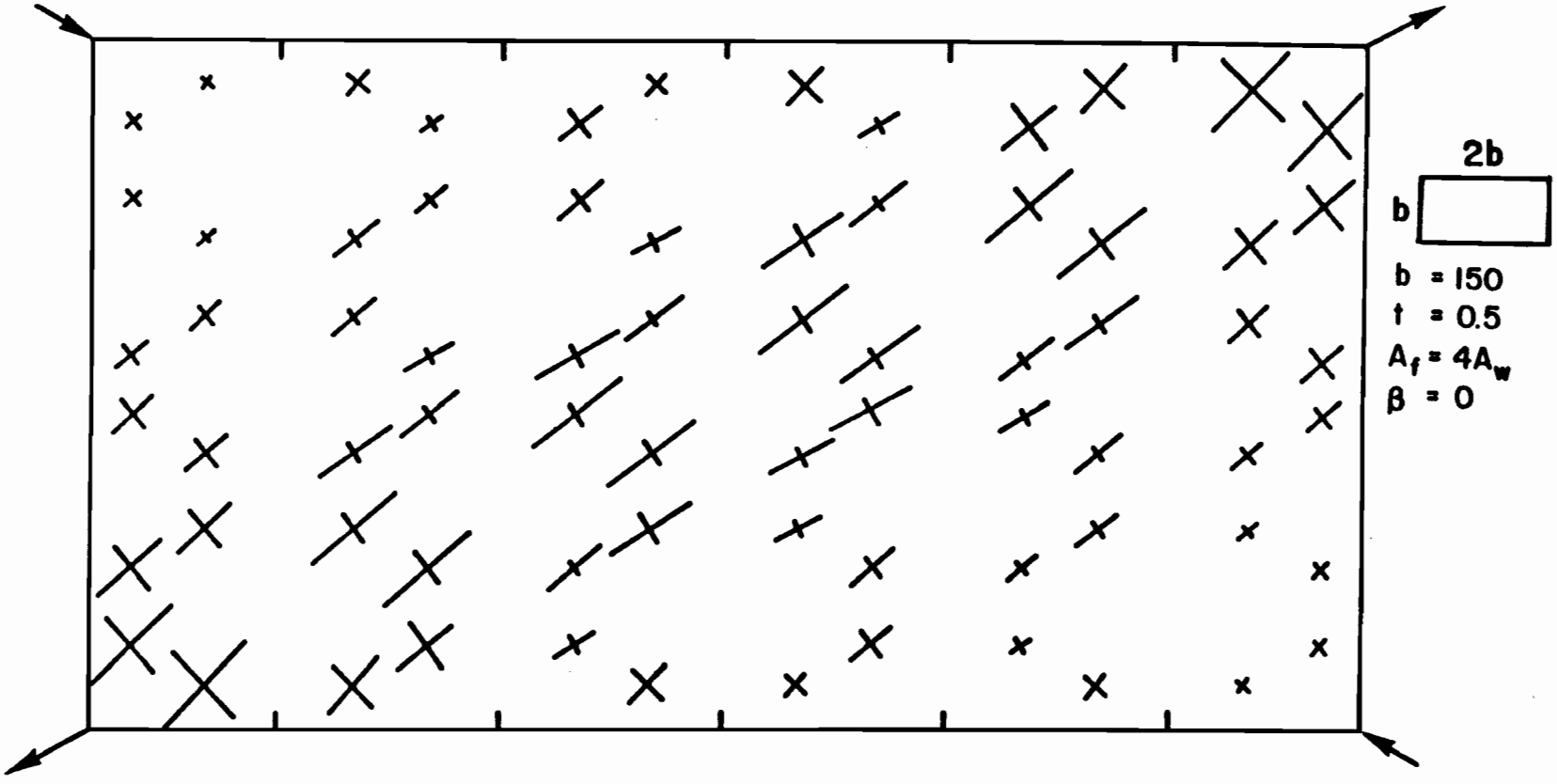

Fig. 47 PRINCIPAL STRESS DIRECTIONS
RECTANGULAR PLATE

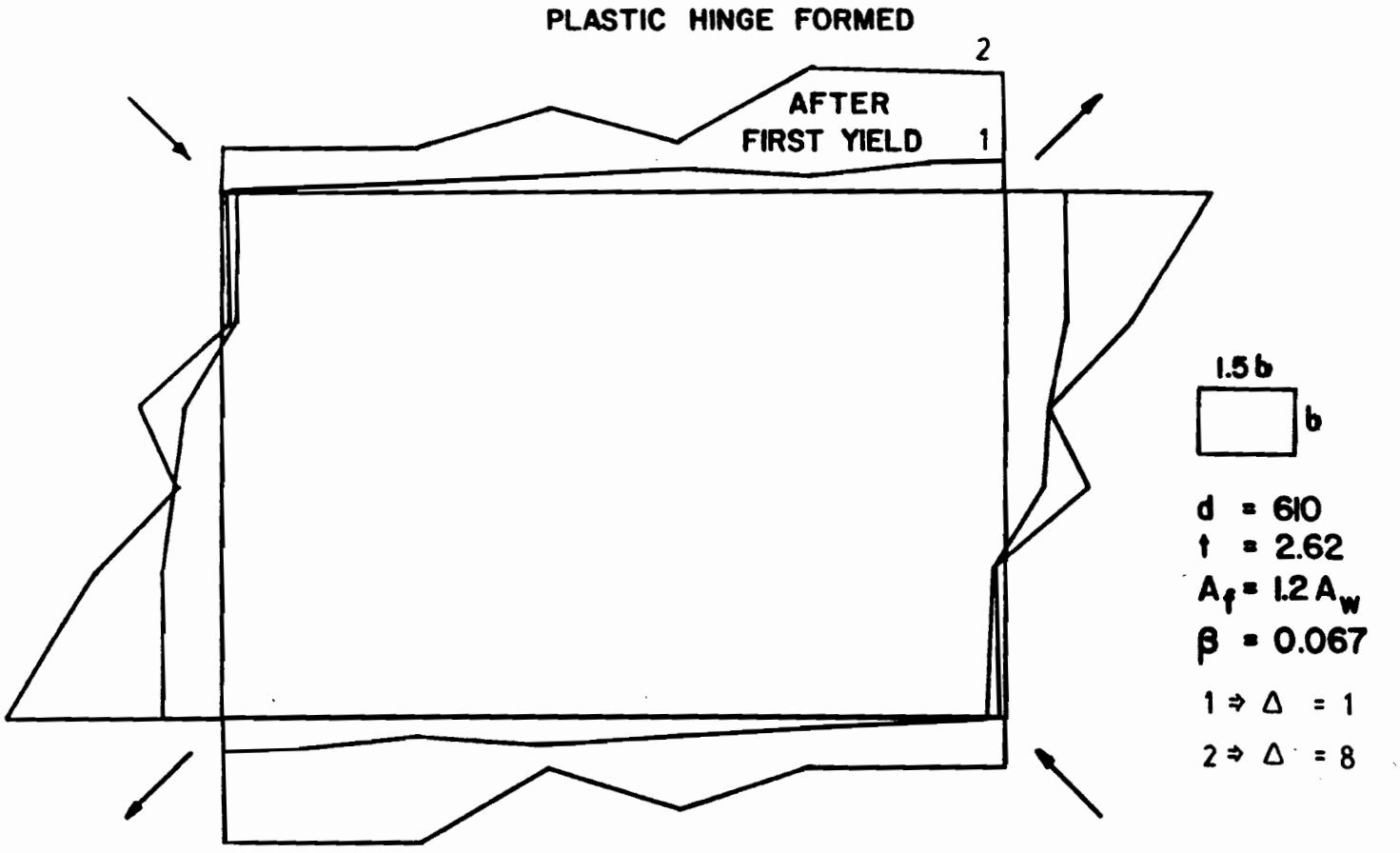

Fig. 48 **NORMAL FORCE AT BOUNDARIES , TG5**

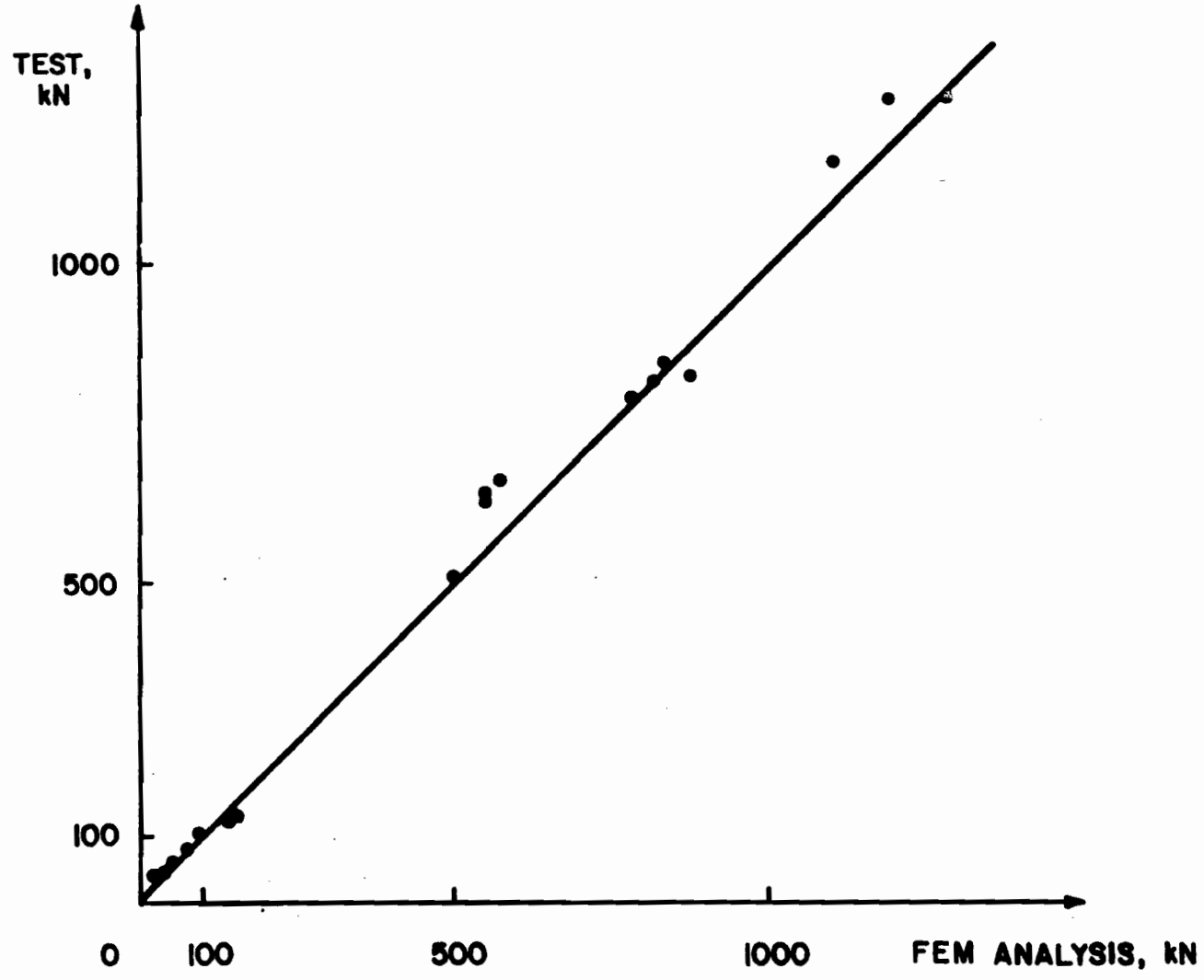

Fig. 49 COMPARISON BETWEEN TEST RESULTS AND FEM ANALYSIS

CHAPTER 4

PROPOSED MODEL FOR ULTIMATE SHEAR LOADING

4.1- SQUARE PANEL

4.1.1- Description

The proposed model is developed for a square panel. The shear capacity is divided into that contributed by the web and that contributed by the flanges.

For the capacity of the web, the model is developed for a panel with stiffeners along all four edges; these boundary stiffeners will be referred to as flanges. The flanges are integrally attached to the web of the panel, but are initially assumed to posses no bending or torsional rigidity. If this panel is subjected to shear force, it is evident that there can be no normal stress at right angles to the boundaries. The results of the F.E. analysis (Chapter 3) for a panel with flanges having axial rigidity only, show that the principal stresses are equal at the boundaries, and the web remains elastic up to first shear yield in the corners, the distribution of the shear stress at the boundaries may be approximated by a parabola.

After first yield the capacity of the flange is analysed independently of the web. Because the length of the yield zone between the web and the flange increases with increasing loading, there is no available shear resistance

between the web and the flange. Any diagonal tension can only be reacted by the flange, causing the flange to bend without assistance from the web. The results of the F.E. analysis show the contribution of the flanges are negligible up to first yield in the web, after which the flange bends and begins to contribute to the shear capacity of the panel.

4.1.2- Webs

The model proposed resembles two sets of diagonal strips, one in tension and one in compression; limiting to τ_{cr} at the longest compression diagonal and to τ_y at the longest tension diagonal. It's assumed that the buckling stress at the boundaries varies in parabolic form, the shear stress at a point, s, on the edge, OX, is:

$$\tau_s = \tau_{cr} + (\tau_y - \tau_{cr})(x/d)^2 \qquad \text{eq. 4.1}$$

in which x = distance from the corner; τ_{cr} = theoretical critical shear stress which occurs at x = zero; and τ_y = yielding shear stress which occurs at x = d.

The principal stress along any line running at 45° remains constant along that line, with a maximum value of $\sigma_c = \sigma_t = \tau_y$. At any point in the web, for values of $(x + y) < d$, $x < y$, the stresses are given by:

$$\sigma_c = \tau_{cr} + (\tau_y - \tau_{cr}) ((x-y)/d)^2 \qquad \text{eq. 4.2}$$

$$\sigma_t = \tau_{cr} + (\tau_y - \tau_{cr}) ((x+y)/d)^2 \qquad \text{eq. 4.3}$$

$$\tau_{xy} = \tau_{cr} + (1/2)(\tau_y - \tau_{cr})\left((x-y)^2 + (x+y)^2\right)/d^2 \quad \text{eq. 4.4}$$

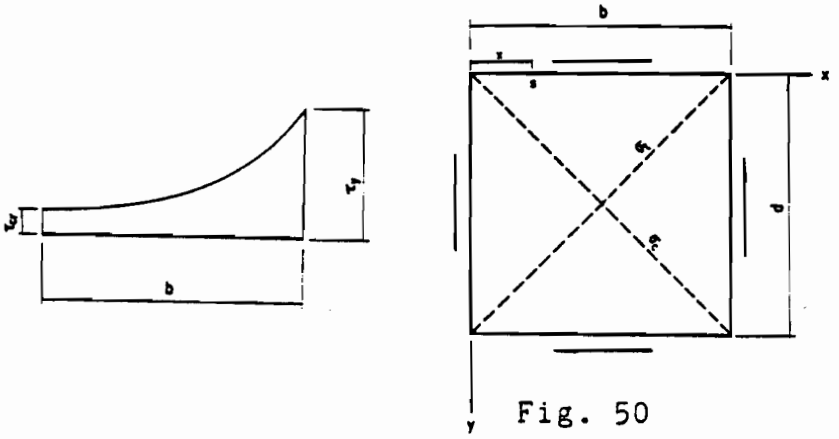

Fig. 50

The shear force V on a boundary is the area under the shear stress curve times the thickness.

$$V = t \int_0^d \tau_s \, dx \qquad \text{eq. 4.5}$$

The equations of equilibrium for plane stress at a point are:

$$\frac{\partial \sigma_x}{\partial x} + \frac{\partial \tau_{xy}}{\partial y} = 0$$

$$\frac{\partial \sigma_y}{\partial y} + \frac{\partial \tau_{xy}}{\partial x} = 0 \qquad \text{eq. 4.6}$$

That the stress system satisfies the requirement is proved in APPENDIX 1.

The critical shear stress depends upon the boundary conditions of the isolated panel, but the true boundary conditions for a girder web are difficult to establish

accurately because the degree of restraint imposed by the flanges and by the adjacent web panels cannot be evaluated. It can be assumed conservatively that all the boundaries of the web panel are simply supported, so that the critical shear stress is given by:

$$\tau_{cr} = K \pi^2 E t^2/12(1 - \nu^2) d^2 \qquad \text{eq. 4.7}$$

where the buckling coefficient K is given by:

$$K = 5.34 \left(1 + 0.75 (d/b)^2 \right) \qquad \text{when } b > d$$

Up to first yield, eq. 4.1 represents the variation of the shear stress along the boundaries. The shear forces in the plate at first yield in the web is obtained by integrating the shear stress distribution along the edge, giving:

$$V_w = (1/3)(2 \tau_{cr} + \tau_y) d t \qquad \text{eq. 4.8}$$

For more rigid flanges the ultimate shear force is equal to the shear force up to first yielding plus the contribution of the flanges in shear.

The failure load can be determined from a consideration of the mechanism developed in the frame panel.

In this model up to first yielding in shear there is no normal force at the boundary. As the load increases, σ_t will increase and σ_c will reduce in such way as to conserve the value of shear stress τ_y at the tension corner, as the

normal force increases.

The tension stress in the longer diagonal increases up to the value of σ_y, the final condition approaching a series of yielded diagonals strips, the maximum value of the normal force developed at the boundary is $t\,\sigma_y/2$.

4.1.3- Flanges

A finite element analysis was conducted, for a panel with a high slenderness ratio, shown in Fig. 51. The two tension corners are free to move; one compression corner is fixed in the X and Y directions. The load is applied at the other compression corner in X and Y direction.

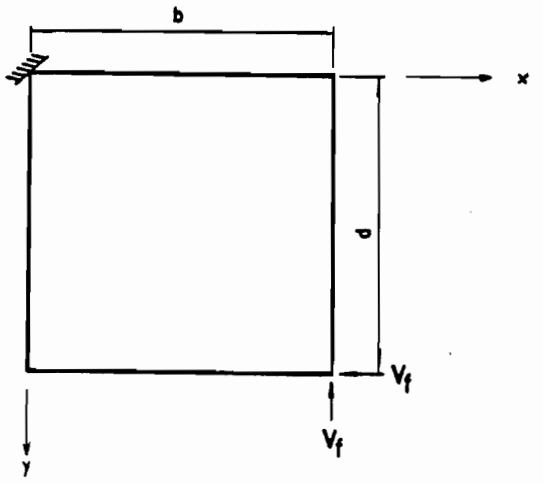

Fig. 51

After first yielding in shear at the tension corner, as the load increases the yielded zone spreads, and normal forces are created on the flanges. Failure occurs when hinges have formed in the flanges which together with the

yielded zone A A' A'', B B' B'' form a plastic mechanism,

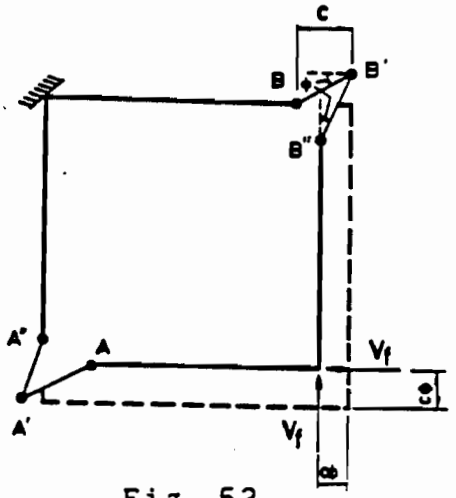

Fig. 52

Consider a rotation ϕ to occur at the plastic hinges producing the mechanism shows in Fig 52, the work done in the plastic deformation of the flange and web is:

$$2\, V_f\, c\, \phi = 8\, M_p\, \phi + 4\, (\sigma_y/2)\, c\, t\, c\, \phi/2$$

$$V_f = 4\, M_p/c + c\, t\, \sigma_y/2 \qquad \text{eq. 4.9}$$

The load is applied at the compression corner in Fig. 51 in the Y direction only, and is assumed to be reacted by a uniformly distributed load $\sigma_y\, t/2$ normal to the flange exerted by the web. Since the plastic hinge will occur at the point of maximum bending moment where the shear is zero, the position of the internal hinge A is obtained by considering the equilibrium of the beam section A A'. Taking moments about A', one obtains.

$$(ct\ \sigma_y/2)\ c/2 = 2\, M_p \quad \Rightarrow \quad 4M_p/c = ct\ \sigma_y/2$$

$$c = \sqrt{(8\, M_p / (\sigma_y\, t)} \qquad \text{eq. 4.10}$$

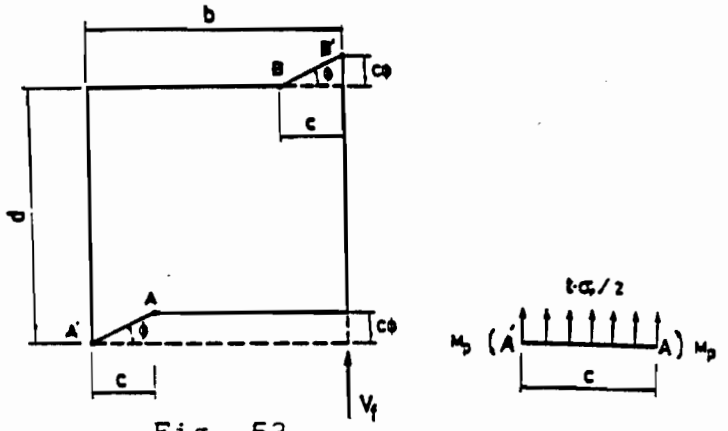

Fig. 53

The failure load will be equal to the force at first yield plus the contribution of the flange when the normal forces are developed.

$$V_u = V_w + V_f \qquad \text{eq. 4.11}$$

In the case of a girder, the internal hinges A'' and B'' will not be formed because we have a continous web, and the failure load will be determined from a consideration of the mechanism developed in Fig. 53. Consider a rotation $\emptyset$ at the plastic hinges, the work is done only on the sections A A' and B B'. For equal flanges the distance c for upper and lower flanges will be equal, and the work done by the axial force in the flanges will be zero.

The virtual work done in the mechanism is:

$$V_f\, c\, \emptyset = 4\, M_p\, \emptyset + (\sigma_y/2)(c\, t)\, c\, \emptyset$$

$$V_f = 4\, M_p / c + (\sigma_y/2)(c\, t) \qquad \text{eq. 4.12}$$

Equation 4.12 is the same as equation 4.9. The first term of this equation, on the right hand side, represents

the frame resistance in shear, the second term represents the contribution of the flanges to increasing the web capacity. By using equation 4.10 these two terms are shown to be equal. Putting eq. 4.8 and eq. 4.12 into eq. 4.11 gives:

$$V_u = (1/3)(2 \tau_{cr} + \tau_y) d t + \sigma_y c t \qquad \text{eq. 4.13}$$

Using the value of c from eq. 4.10 in eq. 4.13 the ultimate shear force becomes:

$$V_u = (1/3)(2 \tau_{cr} + \tau_y) d t + \sqrt{8 M_p \sigma_y t} \qquad \text{eq. 4.14}$$

It should be noted that the value of the plastic moment in the flange will be reduced by the presence of the axial force P'. The value of the effective moment M' is given by:

$$M' = M_p (1 - (P'/ P)^2) \qquad \text{eq. 4.15}$$

where P is the axial force to yield the flange, equal to $A_f \sigma_y$.

4.1.4- Extreme Cases

From eq. 4.13, it is seen that the shear capacity is composed of two components. The first component represents the capacity of the web up to first yield without any contribution from the flange; the second component represents the additional shear capacity of the flange bending rigidity.

In the case of a girder with very weak flanges, taking account of the reduced moment resistance due to the axial force in the flange, the value of the flange strength M_p becomes small and the value of c becomes very small; the second term of eq. 4.13 becomes negligible so that:

$$V_u = (1/3)(\tau_{cr} + \tau_y) \, d \, t \qquad \text{eq. 4.16}$$

When the flanges are very strong, the distance of the plastic hinge from the end of the panel c increases, as shown by eq. 4.10. When c becomes equal to the width b, the hinges form at the four corners of the panel to form a " picture frame " mechanism, as shown in Fig. 54.

By substituting the value of c = b = d into eq. 4.10 we get:

$$M_p = d^2 \, \sigma_y \, t \, / \, 8 \qquad \text{eq. 4.17}$$

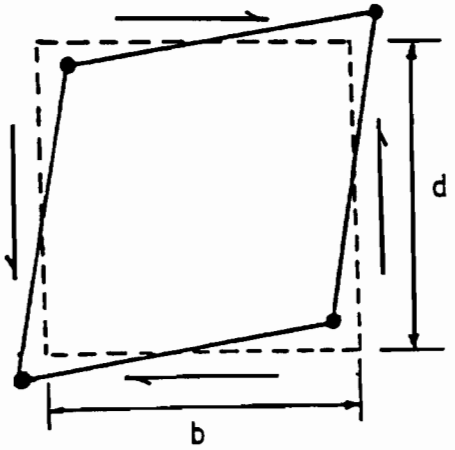

Fig. 54

When determining the ultimate shear load for any girder, the flange strength should be evaluated to see

whether it exceeds the limiting value given by eq. 4.17. If this is so (it will not often be the case for girders of civil engineering proportions), the expression for shear capacity is:

$$V_u = ((1/3)(2 \tau_{cr} + \tau_y) + \sigma_y) d t \qquad \text{eq. 4.18}$$

The adoption of the Tresca yield criterion, $\tau_y = \sigma_y / 2$, for panels in shear leads to simple analysis, and give better results than using the Von Mises criterion, $\tau_y = \sigma_y/\sqrt{3}$, because in the finite element analysis the membrane shear yielding according to the Ilyushin criterion is less than the true shear yield, due to the additional stresses developed by the bending moments. If we assume Tresca yield criterion the expression for shear capacity is :

$$V_u = (1/3)(2 \tau_{cr} + 7 \tau_y) d t \qquad \text{eq. 4.19}$$

4.1.5- Comparisons of predicted shear strength

Table 7 gives the properties of the plate girder panels. Table 8 gives comparisons of predicted shear strengths according to the present model with results of tests from a number of sources. Table 9 gives comparisons of predicted shear strengths according to Hoglund, Rockey and the proposed design procedure with results of tests from a number of sources. Table 10 summarized the comparison of test results.

TABLE 7- Properties of square panels

Ref.	Girder	t mm	d mm	A_w	t_f mm	b_f mm	A_f/A_w	β
4	TG1	2.72	609.8	1658.0	4.70	101.6	0.29	0.018
4	TG2	2.72	609.8	1658.0	6.55	101.6	0.40	0.034
4	TG14	.965	304.8	294.0	3.12	76.2	0.81	0.093
4	TG15	.965	304.8	294.0	5.00	76.2	1.30	0.224
4	TG16	.965	304.8	294.0	6.45	76.2	1.67	0.451
4	TG17	.965	304.8	294.0	9.32	76.2	2.41	0.850
4	TG18	.965	304.8	294.0	12.95	76.2	3.36	1.593
4	TG19	.965	304.8	294.0	15.52	76.2	4.02	2.004
4	TG20	2.03	304.8	619.0	3.25	76.2	0.40	0.046
4	TG21	2.03	304.8	619.0	4.88	76.2	0.60	0.097
4	TG22	2.03	304.8	619.0	6.48	76.2	0.80	0.207
4	TG23	2.03	304.8	619.0	9.22	76.2	1.14	0.419
4	TG24	2.03	304.8	619.0	12.95	76.2	1.59	0.724
4	TG25	2.03	304.8	619.0	15.54	76.2	1.91	0.914
4	G7T1 G7T2	4.98	1270.0	6325.0	19.50	310.0	0.96	0.120
24	TG1 TG1'	2.50	1000.0	2500.0	5.06	160.0	0.32	0.019
24	TG2 TG2'	2.50	1000.0	2500.0	10.00	200.0	0.80	0.090
24	TG3 TG3'	2.50	1000.0	2500.0	16.43	200.0	1.31	0.241
24	TG4 TG4'	2.50	1000.0	2500.0	20.16	200.0	1.61	0.366
24	TG5 TG5'	2.50	1000.0	2500.0	29.73	200.0	3.00	0.790
27	PC3	1.0	800.0	800.0	10.0	250.0	3.12	0.431

TABLE 8- Comparison between test results and P.D.P.

Girder	d/t	Yield Stress σ_y MPa	Yield Stress σ_{yf} MPa	V P.D.P. kN	V Exp. kN
TG1	224	253	253	120.0	120.0
TG2	224	238	238	130.0	126.0
TG14	316	219	309	24.0	25.0
TG15	316	219	289	29.0	29.0
TG16	316	219	349	35.0	31.0
TG17	316	219	315	43.0	39.0
TG18	316	219	306	54.0	51.0
TG19	316	219	268	59.0	55.0
TG20	150	229	309	65.0	51.0*
TG21	150	229	289	73.0	71.0
TG22	150	229	349	84.0	79.0
TG23	150	229	315	96.0	81.0
TG24	150	229	306	114.0	96.0
TG25	150	229	268	121.0	104.0
G7T1	255	253	259	645.0	623.0
G7T2				645.0	645.0
TG1	400	200	280	131.0	152.0
TG1'				131.0	116.0
TG2	400	200	280	174.0	160.0
TG2'				174.0	139.0
TG3	400	200	280	223.0	190.0
TG3'				223.0	190.0
TG4	400	200	280	251.0	219.0
TG4'				251.0	207.0
TG5	400	200	280	323.0	309.0
TG5'				323.0	300.0
PC3	800	216	262	82.0	79.0

* Premature failure, flange collapse due to bending stress higher than yielding stress in the flange.

TABLE 9- Comparison between test results and shear strength according to Hoglund, Rockey and P.D.P.

Girder	V Hoglund kN	V Rockey kN	V P.D.P. kN	V Exp. kN
TG1	140.0	143.0	120.0	120.0
TG2	138.0	142.0	130.0	126.0
TG14	21.0	23.0	24.0	25.0
TG15	24.0	26.0	29.0	29.0
TG16	29.0	30.0	35.0	31.0
TG17	37.0	36.0	43.0	39.0
TG18	46.0	44.0	54.0	51.0
TG19	50.0	48.0	59.0	55.0
TG20	64.0	68.0	65.0	51.0*
TG21	67.0	71.0	73.0	71.0
TG22	74.0	76.0	84.0	79.0
TG23	83.0	81.0	96.0	81.0
TG24	99.0	90.0	114.0	96.0
TG25	106.0	94.0	121.0	104.0
G7T1	575.0	605.0	645.0	623.0
G7T2	575.0	605.0	645.0	645.0
TG1	119.0	142.0	131.0	152.0
TG1'	119.0	142.0	131.0	116.0
TG2	136.0	166.0	174.0	160.0
TG2'	136.0	166.0	174.0	139.0
TG3	168.0	196.0	223.0	190.0
TG3'	168.0	196.0	223.0	190.0
TG4	191.0	214.0	251.0	219.0
TG4'	191.0	214.0	251.0	207.0
TG5	256.0	265.0	323.0	309.0
TG5'	256.0	265.0	323.0	300.0
PC3	49.0	73.0	82.0	79.0

*Premature failure, flange collapse due to bending stress higher than yielding stress in the flange.

TABLE 10- Ratio of predicted to experimental capacity

Investigator	Mean of V_u/V_{ex}	Standard Deviation	Range Of V_u / V_{ex}
Hoglund	0.91	0.17	0.62-1.17
Rockey	0.97	0.11	0.82-1.22
P.D.P.	1.08	0.11	0.86-1.25

4.2- RECTANGULAR PANEL

4.2.1- Description

This approximate model of the stress distribution in the panel is developed for a rectangular panel with aspect ratio b/d=i, where d is the beam depth, with flanges along all four edges. The flanges are integrally attached to the web of the panel, but are initially assumed to possess no bending or torsional rigidity.

4.2.2- Webs

Along the shorter length d, the shear stress varies parabolically from τ_{cr} to τ_y. The shear stress along the longer boundary is divided into three zones;

1- A length of 2(b-d)/3 from the compression corners in which $\tau = \tau_{cr}$.

2- A length d in which τ varies parabolicaly from τ_{cr} to τ_y.

3- A length (b-d)/3 in which $\tau = \tau_y$.

The total shear force along the length of the panel, b, is equal to i V, where V is the total shear force along the shorter length of the panel. Fig. 55 shows how the three zones along the width b will be formed for the assumed shear stress distribution along the boundary when yield first occurs.

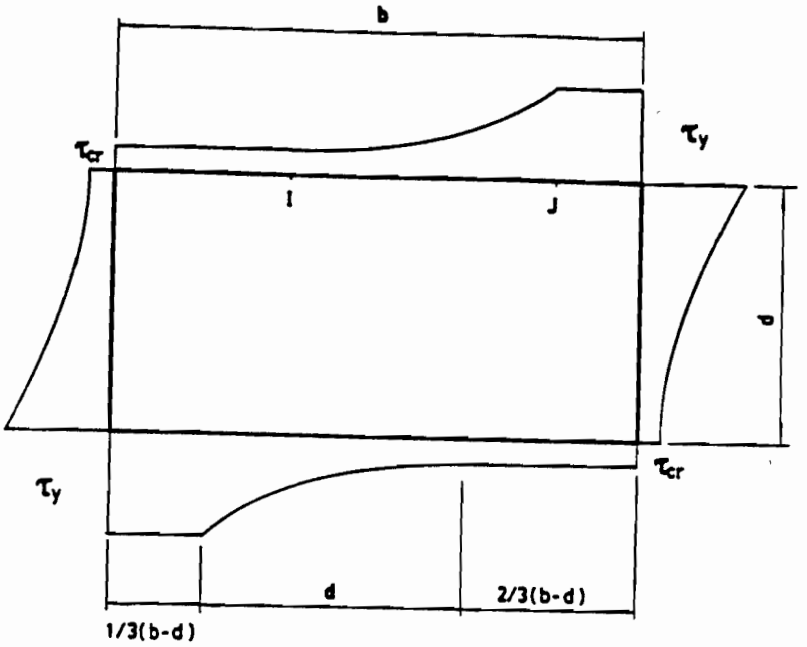

Fig. 55

Taking the origin of the coordinates at point I, the shear stress at a point s, on the edge between I and J, is:

$$\tau s = \tau cr + (\tau y - \tau cr) (x/d)^2 \qquad \text{eq. 4.1}$$

The shear force at the boundary for the width b is the area under the shear stress curve times the thickness.

$$V = (2/3)(i-1)\ d\ t\ \tau cr + t \int_{(2/3)(i-1)d}^{(1/3)(2i+1)d} \tau s\ dx + (1/3)(i-1)\ d\ t\ \tau y$$

$$V = ((2\ \tau cr + \tau y\ )/3)\ (i-1)\ d\ t + t \int_{(2/3)(i-1)d}^{(1/3)(2i+1)d} \tau s\ dx \qquad \text{eq. 4.20}$$

The shear force at the boundary for depth d is the area under the shear stress curve times the thickness.

$$V = t \int_0^d \tau s\ dx$$

All the boundaries of the web panel are assumed to be simply supported, thus the critical shear stress is given by:

$$\tau_{cr} = K \pi^2 E t^2 / (12(1 - \nu^2) d^2) \qquad \text{eq. 4.7}$$

where the buckling coefficient K is obtained as:

$$K = 5.34 (1 + 0.75 (d/b)^2) \qquad \text{when } b > d$$

4.2.3- Flanges

Up to first yield eq. 4.1 represents the variation of the shear stress along the boundaries, the integration of eq. 4.1 gives the total capacity in shear for a panel having low flange rigidity. After yield for higher flange rigidities the width of the yield zone and the normal force both increase. Failure is accompanied by the creation of plastic moment in the flanges.

The ultimate shear force is equal to the shear force up to first yielding, plus the contribution of the flanges when plasticmoments are creative in the flanges.

For rectangular panels the finite element analysis has shown that the inclination of the principal stress is not constant. The principal tensile stress varies from 45° at the boundary to the angle of the panel diagonal in the middle. To facilate the work, assume a constant membrane tension inclination equal to the angle of the panel diagonal, θ_d.

The value of the normal force at the boundaries has a higher value in the X direction along the depth d and a lower value in the Y direction along the width b, the ratio of the normal forces is:

$$\frac{\sigma_x}{\sigma_y} = (1 + \cos 2\theta_d)/(1 - \cos 2\theta_d) = \cot an^2 \theta_d = (b/d)^2 = i^2 \quad \text{eq. 4.21}$$

Assume a uniform load t $\sigma_y/2$ distributed for some length along the depth d. The magnitude of the normal force along the width b is than equal to t σ_y / (2 i^2), which agrees with the finite element results.

Since the plastic hinge occurs at the point of maximum bending moment where the shear force across the flange is equal to zero, the position of the internal hinge is obtained by considering the equilibrium of the beam section A A'. Taking moments abouts A', one obtains:

$$(\sigma_y/(2\, i^2))\ t\ c/2 = 2\ Mp \Rightarrow\ c = i\sqrt{8\ Mp/\ \sigma_y\ t} \quad \text{eq. 4.22}$$

The failure load will be equal to the force at first yielding in shear in the web plus the contribution of the flanges when the normal force are developed:

$$Vu = Vw + Vf$$

$$Vf = c\ t\ \sigma_y/(i)^2$$

$$V_w = (1/3)(2\ \tau_{cr} + \tau_y)\ d\ t$$

$$Vu = (1/3)(2\ \tau_{cr} + \tau_y)\ d\ t + c\ t\ \sigma_y/(i)^2 \quad \text{eq. 4.23}$$

Put the value of c from eq. 4.22 into eq. 4.23 we get

$$V_u = (1/3)(2\,\tau_{cr} + \tau_y) d\,t + 1/i\,\sqrt{8\,M_p\,\sigma_y\,t} \qquad \text{eq.4.24}$$

The aspect ratio i reduces the second term on the right hand side. This is the only the difference between eq. 4.14 which represent the ultimate force for square panel and eq. 4.24 which represent the ultimate force in a rectangular panel. Eq. 4.24 could be used as a general equation, including the square panel. It should be noted when the aspect ratio b/d of the panel is less than 1 the equation of the square panel 4.14 is used to get the ultimate shear force, because the normal force can not increase to more than $t\,\sigma_y/2$.

4.2.4- Extreme Cases

In the case of a girder with light flanges, the value of the flange strength, Mp, is small and the distance of the plastic hinge from the end of the panel c becomes very small; so the ultimate shear force will equal to:

$$V_u = (1/3)(\tau_{cr} + \tau_y)\, d\, t \qquad \text{eq. 4.25}$$

When the flanges are heavy, the distance of the plastic hinge from the end of the panel c increases, when c becomes equal to the width b, the hinges form at four corners of the panel. By substituting the value c = b into eq. 4.22 we get:

$$M_p = d^2 \sigma_y\, t\, /\, (8\, i^2) \qquad \text{eq. 4.26}$$

When determining the ultimate shear load for any girder, the flange strength should be evaluated to see whether it exceeds the limiting value of eq. 4.26 . The expression for shear capacity is:

$$V_u = ((1/3)(2\tau_{cr} + \tau_y) + \sigma_y / i^2)\, d\, t \qquad \text{eq. 4.27}$$

4.2.5- Comparisons Between Test Results And Proposed Design Procedure

Table 12 gives comparisons of predicted shear strengths according to the proposed design procedure with the results of tests from a number of sources. Table 11 gives the properties of the plate girders. Table 13 gives comparisons of predicted shear strengths according to Hoglund, Rockey and the proposed design procedure with the results of tests from a number of sources. Table 14 summarized the comparison of test results.

Fig. 56 shows the comparison between the experimental results and those predicted by the present model for square and rectangular panels.

TABLE 11- Properties of rectangular panels

Ref.	Girder	t mm	d mm	A_w	t_f mm	b_f mm	A_f/A_w	b/d	β
4	G6T3	4.9	1270	6223	19.8	308	0.98	0.5	0.504
4	G6T2	4.9	1270	6223	19.8	308	0.98	0.75	0.224
4	G6T1	4.9	1270	6223	19.8	308	0.98	1.5	0.056
4	TG5	2.62	610	1598	9.5	203	1.22	1.5	0.067
4	TG9	2.62	610	1598	9.9	203	1.25	2.0	0.041
24	F10-P1	6.65	1270	8446	32.0	395	1.5	1.5	0.107
24	F10-P2	6.53	1270	8293	25.4	408	1.25	1.5	0.066
26	G1-1	6.6	1200	7920	23.0	250	0.73	3.0	0.013
26	G1-2	6.6	1200	7920	36.0	250	1.14	1.5	0.118
26	G2-1	6.6	950	6270	19.0	250	1.32	3.0	0.014
26	G2-2	6.6	950	6270	32.0	250	1.28	1.5	0.096
26	G1	8.0	440	3520	30.0	160	1.36	2.61	0.104
26	G2	8.0	440	3520	30.0	200	1.70	2.61	0.130
26	G3	8.0	560	4480	30.0	250	1.67	2.63	0.099
26	G4	8.0	560	4480	30.0	250	1.67	3.57	0.054
26	G5	8.0	560	4480	30.0	250	1.67	2.68	0.095
26	G6	8.0	560	4480	30.0	250	1.67	1.25	0.439
26	G7	8.0	560	4480	30.0	250	1.67	2.68	0.095
26	G9	8.0	720	5760	30.0	250	1.30	2.78	0.054
27	PA3	.96	800	800	12.0	249	3.75	0.75	0.792

TABLE 12- Comparison between test results and P.D.P.

Girder	d/t	Yield Stress σ_y MPa	σ_{yf} MPa	V P.D.P. kN	V EXP. kN
G6T3	255	253	261	821.0	787.0
G6T2	255	253	261	687.0	667.0
G6T1	255	253	261	518.0	516.0
TG5	316	291	291	160.0	130.0
TG9	316	266	266	133.0	123.0
F10-P1	193	236	188	837.0	819.0
F10-P2	196	267	199	817.0	846.0
G1-1	184	486	499	924.0	971.0
G1-2	184	486	474	1478.0	1265.0
G2-1	144	486	519	807.0	961.0
G2-2	144	486	485	1335.0	1226.0
G1*	55	430	411	757.0**	804.0
G2*	55	430	411	920.0	824.0
G3*	70	430	411	963.0**	971.0
G4*	70	430	411	944.0**	952.0
G5*	70	430	411	1125.0	1050.0
G6*	70	430	411	1550.0	1177.0
G7*	70	430	411	1125.0	1050.0
G9	90	430	411	1077.0	1158.0
PA3	832	216	206	85.0	86.0

* The theoretical critical shear stress is higher than yield shear stress so the value of yield shear stress is used in the equation.

** Flange collapsed because the bending stress exceeded the yield stress in the flange.

TABLE 13- Comparison between test results and shear strength according to Hoglund, Rockey and P.D.P.

Girder	V Hoglund kN	V Rockey kN	V P.D.P. kN	V EXP. kN
G6T3	819.0	878.0	821.0	787.0
G6T2	654.0	712.0	687.0	667.0
G6T1	492.0	460.0	518.0	516.0
TG5	153.0	142.0	160.0	130.0
TG9	135.0	111.0	133.0	123.0
F10-P1	829.0	757.0	837.0	819.0
F10-P2	825.0	752.0	817.0	846.0
G1-1	1046.0	710.0	924.0	971.0
G1-2	1367.0	1289.0	1478.0	1265.0
G2-1	996.0	680.0	807.0	961.0
G2-2	1290.0	1181.0	1335.0	1226.0
G1*	914.0	757.0	757.0	804.0**
G2*	947.0	920.0	920.0	824.0
G3*	1070.0	1123.0	963.0	971.0**
G4*	1082.0	1099.0	944.0	952.0**
G5*	1133.0	1150.0	1125.0	1050.0
G6*	1352.0	1550.0	1550.0	1177.0
G7*	1133.0	1150.0	1125.0	1050.0
G9	1217.0	1093.0	1077.0	1158.0
PA3	61.0	83.0	85.0	86.0

* The theoretical critical shear stress is higher than yield shear stress so the value of yield shear stress is used in the equation.

** Flange collapsed because the bending stress exceeded the yield stress in the flange.

TABLE 14- Ratio of predicted to experimental capacity for rectangular panels

Investigator	Mean of V_u / V_{ex}	Standard Deviation	Range Of V_u / V_{ex}
Hoglund	1.03	0.12	0.71-1.15
Rockey	1.00	0.16	0.71-1.32
P.D.P.	1.02	0.11	0.82-1.32

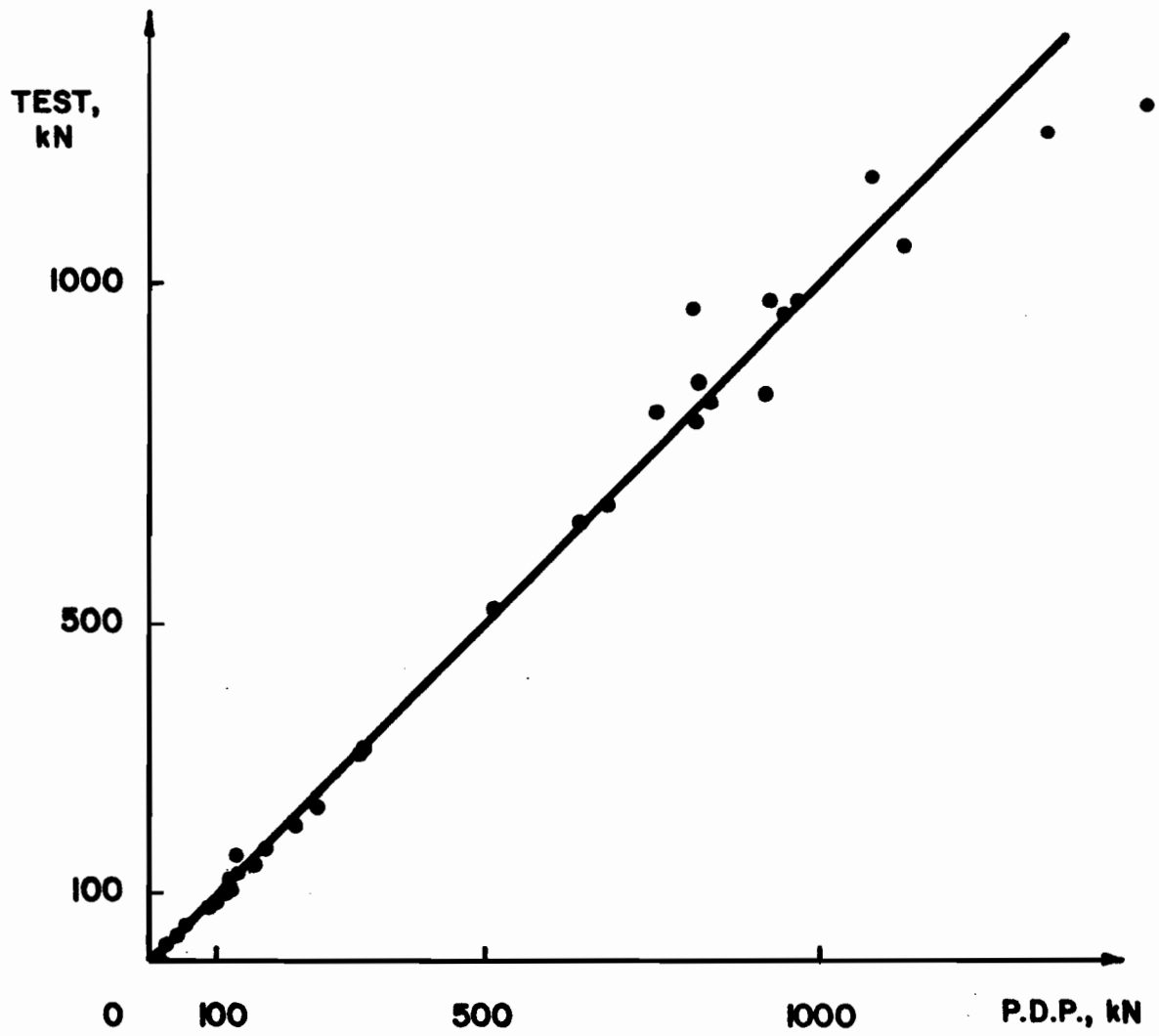

Fig. 56 **COMPARISON BETWEEN TEST RESULTS AND PROPOSED DESIGN PROCEDURE**

4.3- PANEL SUBJECTED TO COMBINED BENDING MOMENT AND SHEARING FORCE.

In a fabricated plate girder, the primary function of the top and bottom flange plates is to resist the axial tensile and compressive forces arising from the bending action, whilst the web plate resists the shear force.

When a girder with heavy flange is subjected to a bending moment in addition to shear, the pure shear capacity will be reduced by the presence of bending moment. On the other hand, the axial force $P' = M / d$ in the flanges reduces the moment capacity in the flanges hinges to $M' = M_p (1 - (P'/ P)^2)$ and M' should used in place of M_p in eq. 4.14 or 4.24.

For a girder with a light flange stiffened transversely with a $d/t > 200$ typical of those used in civil engineering ($A_f < A_w$), at first yield in shear there is no normal force at the flange from the web, and because the web is buckled any bending moment contributed by the web may be neglected. The flange failure mode normally occurs when the value of the applied bending moment is approximately equal to the plastic moment resistance provided by the flange plates only:

$$M = A_f \sigma_{yf} d$$

For a girder carrying a single concentrated load, S, in the middle, simply supported over a span length L, the panel

is subjected to bending moment and shear. The ultimate load capacity, S, for failure due to bending is then:

$$S = 4 A_f \sigma_{yf} d / L$$

4.4- LONG THIN PLATE GIRDERS WITHOUT WEB STIFFENERS

The simply supported girder is a common element in construction. When the load is sufficiently distributed along the girder no other vertical web stiffeners than at the supports are needed. When the girder is subjected to a few concentrated loads vertical web stiffeners are required to prevent web crippling.

Even in the case of a long web plate without transverse stiffeners there is on additional post-buckling capacity due to redistribution of the stresses.

Hoglund [25] replaced the web by a system of intersecting bars whose inclination is changed when the load is increased. The compressed bars carry a constant stress equal to the critical shear buckling stress, $\sigma_c = \tau_{cr}$, while the stress in the tension bars increases as their inclination decreases. The ultimate shear force is reached when yielding according to the Von Mises criterion occurs. Hoglund developed an empirical formula to give the ultimate load.

The ultimate mean shear stress for the three girders tested by Hoglund agrees very well with the formula

developed in this study up to first yield with no contribution from the flange. Tables 15 and 16 gives the properties of the plate girders and the comparison of the predicted mean shear stress according to the present model with the results of the tests.

TABLE 15

Ref.	Girder	t mm	d mm	Aw	tf mm	bf mm	Af/Aw	d/t
25	B1	2.86	600	1716	9.9	226	1.30	210
25	B4	2.0	600	1200	6.1	151	0.77	300
25	K1	2.86	600	1716	9.9	226	1.30	210

TABLE 16

Ref.	Girder	L mm	Yield stress σ_y MPa	σ_{yf} MPa	P.D.P. τ MPa	Tests τ MPa
25	B1	9000	418.5	294.4	85.1	85.3
25	B4	9000	280.0	304.0	54.2	52.9
25	K1	6000	418.5	294.4	85.1	92.4

CHAPTER V

SUGGESTIONS FOR FUTURE RESEARCH

5.1- TRANSVERSE WEB STIFFENERS

The stiffeners must sustain axial forces developed from the web membrane action plus the effect of frame action, the stiffeners must remain straight and not deflect out of the web plane during the web buckling and post-buckling stages, up to reaching the ultimate load.

The experimental study conducted by Rockey et al. 1981 [28], and a similar study by Mele and Puthali 1979[28], has shown that a portion of the web plate acts with the stiffener in resisting the axial loading. Four factors must be considered in stiffeners design:

- The amount of web acting with the stiffener.

- The moment arising due to the eccentricity of the applied load P from the centroidal axis of the stiffener.

- The Euler buckling load of stiffeners.

- The connection welds between the stiffeners the web and the two flanges.

5.2- LONGITUDINAL WEB STIFFENERS

The webs of plate girders may be reinforced by longitudinal, in addition to transverse, stiffeners, to increase their bending and shear capacity.

The longitudinal stiffeners increase the buckling resistance of the web in shear, because the sub-dividing of the web increases the buckling stress in the smaller sub-panels.

Several researchers have studied longitudinal web stiffeners [28], notably Owen et al. 1970, Massonet 1960, Meszaros and Djubek 1966, Rockey 1977, but up to now no universal satisfactory method has been developed.

When the longitudinal stiffened web is subjected to axial force due to bending moments in addition to shear, two main problems need to be studied.

- The number of the stiffeners across the depth and how each longitudinal stiffener acts.

- The deployment of the longitudinal stiffeners in the compression zone, to increases the yielding length at the boundary.

5.3- OPENINGS IN THE WEB

Designers frequently find it necesary to introduce openings in the webs in order to provide services.

The cutting of a large opening in the web of a plate girder can have a significant effect on the behaviour of the plate girder under load, the stress distribution in the web, the ultimate strength and the deflection.

In general, webs in built-up girders are made up of relatively thin plates having web-slenderness values, d/t, in excess of 200 subjected predominatly to shear loading.

Several researchers have proposed methods including Hoglund 1971 [30], European Convention for Constructional Steelwork (ECCS) 1976 [28], Redwood and Shrivastava 1980 [29], Narayanan and Adorisio 1983 [28].

Redwood developed a mathematical model for the design of thick webs, however, these methods are not valid for thin webs. For thin webs, Narayanan and Rockey studied several tests and developed a method to predict the ultimate load, but these methods are based on the theories developed by Rockey et al. for plate girders without openings, with some modification including the opening in the web.

Up to now no satisfactory method has been found for the ultimate value of shear plates with openings. There are four effects associated with web opening which need to be investigated:

1- Hole size relative to the web size.

2- Location of the opening in the web.

3- The shape of the opening(rectangular, circular,..etc).

4- The presence of any reinforcement around the opening.

CHAPTER VI

CONCLUSION

-Finite Element Method

The finite element method has been used for the large deflection elastic-plastic analysis of plates under shear loading, in the post-buckled regime.

Before buckling the shear stress is uniformly distributed along the boundary. After buckling the shear stress distribution becomes non-uniform with a maximum value at the tension corner. Up to the shear force which causes first yielding at the junction between the web and the flange at the tension corner, there is no normal force at the boundaries. For panels with very strong flanges and thin webs, as the load increases a normal force is developed at the boundaries reacted by the flanges. The principal tension stress increases and the principal compression stress decreases in a such way as to conserve shear yield along the boundary near the tension corner. The maximum value of the stress normal to the boundary is $\sigma_y/2$.

It has been shown that the shear capacity of a web, having flanges with small bending rigidity along the boundaries, is reached at first yielding of the web in shear in the tension corner, with no stress normal to the boundary.

With stronger stiffeners, after first yield, the

capacity of the web increases as a result of the resistance to normal force at the boundary due to the bending rigidity of the flange. Furthermore, the capacity of the frame itself in shear is added to the total capacity of the panel. In this case as the displacements increase, the number of half-waves increases from 3 to 5 or more, and some diagonal tension is developed.

In most girders used in civil engineering the flanges are light (flange area < web area) and no useful diagonal tension is developed before the maximum capacity is reached.

When the d/t ratio of the panel is small enough that the shear force to cause yielding exceeds that to cause elastic buckling, no bending is developed in the flanges. The first yield may take place in the middle of the panel area, due to a combination of membrane stresses and bending stresses (this may explain the difference between some author's test observations).

For rectangular panels all the above considerations are equally valid. The magnitude of the normal force at the boundary after first yield is a function of the aspect ratio b/d, and any contribution from the flanges to the shear capacity reduces rapidly with the increase of the aspect ratio of the panel.

With light flanges the inclination of the stress stays

at 45° along the boundaries at first yield. With heavy flanges some diagonal tension develops after first yield and the capacity of the web increases. The inclination of the stress near the centre of the panel is equal to the angle of the panel diagonal.

-Proposed Design Procedure

The proposed model to predict the ultimate load capacity of shear webs in a plate girder treats the shear strength of the web and the bending strength of the flanges independently.

The proposed equation is simple, applies to square and rectangular panels, gives satisfactory results compared with many tests, and avoids the need for iteration used in other methods.

The model illustrates that for girders of typical engineering proportions the contributions by the flange to the ultimate capacity is less than 10 %.

REFERENCES

1. WASTLUND, D. and BERGMANN, S. G. A., " Buckling of Webs in Deep Steel I Girder, " IABSE, Vol. 8, p. 291 - 310, 1947.
2. BASLER, K., " Strength of Plate Girders in Shear, " ASCE, Proc. No 2967, Part 1. ST. 7, p. 151-180, Oct. 1969.
3. ROCKEY, K. C. and SKALOUD, M., " Influence of Flange Stiffeners Upon the Load Carrying Capacity of Webs in Shear, " Proc. 8 th Congress, IABSE, New York, Sept. 1968.
4. ROCKEY, K. C. and SKALOUD, M., " The Ultimate Load Behaviour of Plate Girders Loaded in Shear , " The Structural Engineer, Vol. 50, No 1, p. 29-47, Jan. 1972.
5. PORTER, D. M., ROCKEY, K. C. and EVANS,H. R., " The Collapse Behaviour of Plate Girders Loaded in Shear, " The Structural Engineer, Vol. 53, No 8, P. 312-325, Aug. 1975.
6. FUJII, T., " On an Improved Theory for Dr. Basler's Theory, " 8 th Congress, IABSE, New York, Sept. 1968.
7. MARSH, C., " Theoretical Model for Collapse of Shear Webs, " Journal of the Engineering Mechanics Division, ASCE, Vol. 108, No. EM5, p. 819-832, Oct. 1982.
8. MARSH, C., " Photoelastic Study of Postbuckled Shear Web, " Canadian Journal of Civil Engineering, Vol. 12, No. 2, p. 415-417, 1985.
9. DJUBEK, J., " Deformation of Rectangular Slender Web Plates With Boundary Members Flexible in the Web Plate

Plane, " The Aeronautical Quarterly, Vol. xvii, p. 371-394, Nov. 1966.

10. LEVY, S., FIENUP, K., and WOOLY, R., " Analysis of Square Shear Web Above Buckling Load, " NACA Technical Note, No. 962, Washington, Feb. 1945.

11. LEVY, S., WOOLEY, R. and CORRICK, J., " Analysis of Deep Rectangular Shear Web Above Buckling Load, " NACA Technical Note, No. 1009, Washington, Mar. 1946.

12. LEVY, S., " Bending of Rectangular Plates With Large Deflection, " NACA Technical Note, No. 846, Washington, May. 1942.

13. OSTAPENKO, A., YEN, B. AND BEEDLE, L., " Research on Plate Girders at Leigh University, " Proc. 8 th, Congress, IABSE, New York, Sept. 1968.

14. BATHE, K. and BOLOURCH S., " Large Displacement Analysis of Three-Dimensional Beam Structures, " International Journal for Numerical Methods in Engineering, Vol. 14, p. 961-986, 1979.

15. BATHE, K. and BOLOURCHI S., " A Geometric and Material Nonlinear Plate and Shell Element, " Computers and Structures, Vol. 11, p. 23-48, 1981.

16. BATHE, K. and HO, L., " A Simple and Effective Element for Analysis of General Shell Structures, " Computers and Structures, Vol. 13, p. 673-681, 1981.

17. BATHE, K. and DVORKIN, E., " On the Automatic Solution of Nonlinear Finite Element Equations, " Computers and Structures, Vol. 17, No. 5-6, p. 871-879, 1983.

18. JOHNSTON, B., " Guide to Stability Design Criteria for Metal Structures, " John Willey and Sons, 3rd edition.

19. TIMOSHENKO, S. and GERE, J., " Theory of Elastic Stability, " McGraw-Hill Book Company, 2nd edition.

20. BATHE, K., " Finite Element Procedures in Engineering Analysis, " Prentice-Hall, 1982.

21. FUNG, Y. C., " Foundations of Solids Mechanics, " Prentice-Hall, 1965.

22. CRISFIELD, M. A., " Large-Deflection Elasto-Plastic Buckling Analysis of Plates Using Finite Elements, " Transport and Road Research Lab., London, Report LR 593.

23. CALLADINE, C. R. " A Plastic Theory for Collapse of Plate Girders Under Combined Shearing Force and Bending Moment, " The Structural Engineer,Vol. 51, No. 4, p. 147-154, April 1973.

24. SADAO, K., " Ultimate Strength of Stiffened Plate Girders Subjected to Shear, " Proc. IABSE Colloquium, London, 1971.

25. HOGLUND, T. , " Simply Supported Long Thin Plate Girders Without Web Stiffeners Subjected to Distributed Transverse Load, " Proc. IABSE Colloquium, London, 1971.

26. FUJII, T., " A Comparison Between the Theoretical Values and the Experimental Results for the Ultimate Shear Strength of Plate Girders, " Proc. IABSE Colloquium, London, 1971.

27. TANG, K. H. and EVANS, H. R., " Transverse Stiffeners for Plate Girder Webs an Experimental Study, " J.

Construct. Steel Research 4, Elsevier Applied Science Publishers, England, p. 253-280, 1984.

28. NARAYANAN, R., " Plated Structures Stability and Strength, " Applied Science Publishers, 1983.

29. REDWOOD, R. G., and SHRIVASTAVA, S. C., " Design Recommendations for Steel Beams With Web Holes, " Canadian Journal of Civil Engineering, 7(4), p. 642-650, 1980.

30. HOGLUND, T., " Strength of Thin Plate Girders With Circular or Rectangular Web Holes Without Web Stiffeners, " Proc. IABSE Colloquium, London, 1971.

APPENDIX 1

The panel is square b = d, with uniform edge flanges. By symetry, each edge carries the same shear force, V;

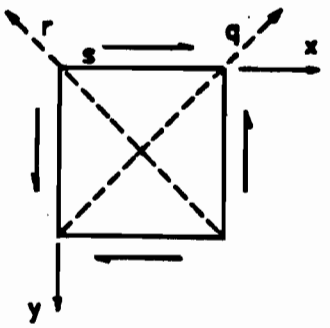

Fig. A.1

and the same shear stress distribution.

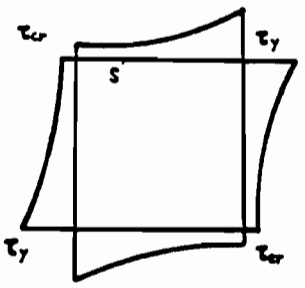

Fig. A.2

the shear stress at a point s on the boundary A B, is

$$\tau_s = \tau_{cr} + (\tau_y - \tau_{cr}) (x/d)^2 \qquad \text{eq. 4.1}$$

The shear force on a boundary is the area under the shear stress curve times the thickness.

PROUVE

The equation of equilibrium for plane stress at a point are:

$$\frac{\partial \sigma x}{\partial x} + \frac{\partial \tau xy}{\partial y} = 0$$

eq. 4.6

$$\frac{\partial \sigma y}{\partial y} + \frac{\partial \tau xy}{\partial x} = 0$$

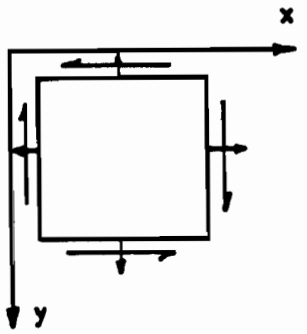

Fig. A.3

The positive sign convention is shown in Fig. A.3, on the face of the positive direction of Y axis the positive shear stress take the direction of the positive X axis, on the face of the positive direction of X axis the positive shear stress take the direction of the positive Y axis, Fig. A.4 shown the shear stress in the model studied has an opposit signe. The equations of equilibrium become:

$$\frac{\partial \sigma x}{\partial x} - \frac{\partial \tau xy}{\partial y} = 0$$

eq. A.1

$$\frac{\partial \sigma y}{\partial y} - \frac{\partial \tau xy}{\partial x} = 0$$

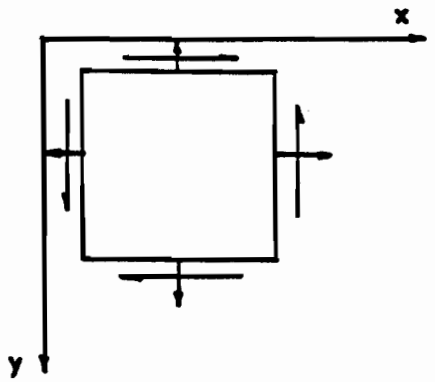

Fig. A.4

eq. 4.4 in CHAPTER 4 give:

$$\tau_{xy} = \tau_{cr} + (\tau_y - \tau_{cr}) ((x-y)^2 + (x+y)^2) (1/2b^2)$$

From Mohr's circle;

$$\sigma x = \sigma y = (\sigma_t - \sigma_c) / 2 \qquad \text{eq. A.2}$$

σ_c and σ_t are equations 4.2 and 4.3 in CHAPTER 4.

$$\sigma_x = (\tau_y - \tau_{cr}) (2 x y / b^2) \qquad \text{eq. A.3}$$

$$\frac{\partial \sigma_x}{\partial x} = (\tau_y - \tau_{cr}) (2 y / b^2) \qquad \text{eq. A.4}$$

$$\frac{\partial \tau_{xy}}{\partial y} = (\tau_y - \tau_{cr}) (2 y / b^2) \qquad \text{eq. A.5}$$

put eq. A.4 and A.5 into eq. A.1 we get zero.

Also same:

$$\sigma_y = (\tau_y - \tau_{cr}) (2 x y / b^2) \qquad \text{eq. A.6}$$

$$\frac{\partial \sigma y}{\partial y} = (\tau y - \tau cr) (2 x / b^2) \qquad \text{eq. A.7}$$

$$\frac{\partial \tau xy}{\partial x} = (\tau y - \tau cr) (2 x / b^2) \qquad \text{eq. A.8}$$

put eq. A.7 and A.8 into eq. A.1 we get zero.